FINAL REPORT

on

NASA RESEARCH GRANT NO. NAG-1-250

for

Period Covering 17 January 1982 through 17 January 1985

"DESIGN OF HELICOPTER ROTOR BLADES FOR
OPTIMUM DYNAMIC CHARACTERISTICS"

by

David A. Peters, Professor and Chairman

and

Timothy Ko, Research Assistant

Department of Mechanical Engineering

Washington University, Campus Box 1185

St. Louis, MO 63130

Alfred Korn, Professor

and

Mark P. Rossow, Professor

Department of Civil Engineering

Southern Illinois University

Edwardsville, IL 62026

January 17, 1985

TABLE OF CONTENTS

1. INTRODUCTION

This document is the final report of a research project concerned with the optimal design of helicopter rotor blades. The report contains three main parts:

1. a discussion of the reasons for which the research was undertaken;

2. a summary of project accomplishments, presented in the form of a list of optimization problems which have been solved and a list and brief description of findings related to optimization of rotor blades;

3. the doctoral thesis of Timothy Ko, which contains many details of the computations performed during the project.

2. IMPORTANCE OF THE RESEARCH

The design of helicopter rotor blades involves not only considerations of strength, survivability, fatigue, and cost, but also requires that blade natural frequencies be significantly separated from the fundamental aerodynamic forcing frequencies (e.g. Ref. 1) . A proper placement of blade frequencies is a difficult task for several reasons. First, there are many forcing frequencies (at all integer-multiples of the rotor RPM) which occur at rather closely-spaced intervals. For example, 5/rev and 6/rev are less than 20% apart. Second, the rotor RPM may vary over a significant range throughout the flight envelope, thus reducing even further the area of acceptable natural frequencies.

1

Third, the natural modes of the rotor blade are often coupled because of pitch angle, blade twist, offset between the mass center and elastic axis, and large aerodynamic damping, These couplings complicate the calculation of natural frequencies. In fact, the dependence on pitch angle makes frequencies a function of loading condition, since loading affects collective pitch. Fourth, the centrifugal stiffness often dominates the lower modes, making it difficult to alter frequencies by simple changes in stiffness.

In the early stages of the development of the helicopter, it was believed that helicopter vibrations could be reduced (and even eliminated) by the correct choice of structural coupling and mass stiffness distributions. However, it is easy to imagine how difficult it is to find just the proper parameters such that the desired natural frequencies can be obtained. The difficulties in placement of natural frequencies have led, in many cases', to preliminary designs which ignore frequency placement. Then, after the structure is "finalized" (either on paper or in a prototype blade), the frequencies are calculated (or measured) and final adjustments made. Reference (2) describes the development of the XH-17 helicopter in which a 300-lb weight was added to each blade in order to change the spanwise and chordwise mass distiribution and thereby move the first flapwise frequency away fromn 3/rev. However, these types of alterations are detrimental to blade wight, aircraft development time, and blade cost. In addition, corrections usually are not satisfactory, and the helicopter is often left with a noticeable vibration problem.

The state-of-the-art in helicopter technology is now to the point, however, that it should be possible to correctly place rotor frequencies during preliminary design stages. There are several reasons for this. First, helicopter rotor blades for both main rotors and tai: rotors are now being fabricated from composite materials (Refs. 3 and 4). This implies that the designer can choose, with limited restrictions, the exact EI distribution desired. Furthermore, the lightness of composite blades for the main rotor usually necessitates the addition of weight to give sufficient autorotational blade inertia. Thus, there is a considerable amount of flexibility as to how this weight may be distributed. Second, the methods of structural optimization and parameter identification are now refined to the point where they can be efficiently applied to the blade structure. Some elementary techniques have already been used for the design of rotor fuselages (Ref. 5). It follows that the time is right for the use of structural optimization in helicopter blade design. Some work on this is already under development, and, although not published, some companies are already experimenting with the optimum way to add weight ot an existing blade in order to improve vibrations.

The purpose of the research project described in this report was to investigate the possibilities (as well as the limitations) of tailoring blade mass and stiffness distributions to give an optimum blade design in terms of weight, inertia, and dynamic characteristics. The work has focused on configurations that are

simple enough to yield clear, fundamental insights into the structural mechanism but which are sufficiently complex to result in a realistic result for an optimum rotor blade.

3.0 SUMMARY OF THE PROJECT

3.1 OPTIMIZATION PROBLEMS WHICH WERE SOLVED

The basic structure optimized was a beam free at one end and supported at the other. Various support conditions and constraints on natural freqencies were used. The behavior of the beam was computed by using a 10-element finite-element model. Quantities associated with the finite-element model, such as the thickness or area moment of inertia of each element, served as design variables in the the optimization procedure. A typical formulation of an optimization problem was

> Find the flange and wall thicknesses of a box-beam cross-section (three variables per finite element) which minimize the weight of the beam, while maintaining the first natural frequency within a "window" (e.g., $2.4 < p_1 < 3.0$ per rev).

All optimization problems were solved with the CONMIN computer program [6]. CONMIN is based on the mathematical nonlinear-programming method of feasible directions.

The list of problems solved follows.

Case 1. Cantilever beam

Rotating: no

Objective function: weight

4

Design variables: area moments of inertia

Boundary condition(s) at root: fixed

Frequency Constraints: first flapping specified through equality
    constraint

Autorotation constraint: no

Stress constraint: no

References: First Semi-Annual Report pp.17-18, Thesis, pp. 18-19

Case 2. Cantilever beam with tip mass

Rotating: no

Objective function: weight

Design variables: cross-sectional areas

Boundary condition(s) at root: fixed

Frequency Constraints: lower bound on first flapping

Autorotation constraint: no

Stress constraint: no

References: First Semi-Annual Report pp.17-19, Thesis, pp. 18-21

Case 3. Wind-turbine blade

Rotating: yes

Objective function: weight

Design variables: area moments of inertia, lumped weights

Boundary condition(s) at root: fixed

Frequency Constraints: windows on first and second flapping

Autorotation constraint: yes

Stress constraint: no

References: First Semi-Annual Report pp.21-24, Thesis, pp. 34-37

Case 4. Hingeless rotor-blade

Rotating: yes

Objective function: weight

Design variables: area moments of inertia, lumped weights

Boundary condition(s) at root: fixed

Frequency Constraints: windows on first and second flapping

Autorotation constraint: yes

Stress constraint: no

References: First Semi-Annual Report pp.23-27, Thesis, pp. 38-41

Case 5. Cantilever beam with two frequency constraints

Rotating: no

Objective function: weight

Design variables: area moments of inertia

Boundary condition(s) at root: fixed

Frequency Constraints: windows on first and second flapping

Autorotation constraint: no

Stress constraint: no

References: Second Semi-Annual Report pp.7-16, Thesis, pp. 23-33

Case 6. Cantilever beam (similar to Case 5, except for three
    rather than two frequency constraints)

Rotating: no

Objective function: weight

Design variables: area moments of inertia

Boundary condition(s) at root: fixed

Frequency Constraints: windows on first, second and third flapping

Autorotation constraint: no

Stress constraint: no

References: Second Semi-Annual Report pp.17-18

Case 7. Cantilever beam (similar to Case 6, except for addition
       of lumped weights as design variables.)

Rotating: no

Objective function: weight

Design variables: area moments of inertia, lumped weights

Boundary condition(s) at root: fixed

Frequency Constraints: windows on first, second and third flapping

Autorotation constraint: no

Stress constraint: no

References: Second Semi-Annual Report pp.17-21

Case 8. Cantilever beam (similar to Case 7, except for addition
       of autorotation constraint)

Rotating: no

Objective function: weight

Design variables: area moments of inertia, lumped weights

Boundary condition(s) at root: fixed

Frequency Constraints: windows on first, second and third flapping

Autorotation constraint: yes (constraint applied to mass moment
       of inertia of whole beam)

Stress constraint: no

References: Second Semi-Annual Report pp.17-22

Case 9. Cantilever beam (similar to Case 8, except beam is
       rotating)

Rotating: yes

Objective function: weight

Design variables: area moments of inertia, lumped weights

Boundary condition(s) at root: fixed

Frequency Constraints: windows on first, second and third flapping

Autorotation constraint: yes (constraint applied to mass moment
     of inertia of whole beam)

Stress constraint: no

References: Second Semi-Annual Report pp.17-24

Case 10. Teetering rotor

Rotating: yes

Objective function: initially the weighted sum of squares of
     differences in frequencies; after a feasible design is
     found, the objective is changed to the weight.

Design variables: flange thicknesses, lumped weights

Boundary condition(s) at root: fixed

Frequency Constraints: windows on first, second and third collective
     flapping

Autorotation constraint: yes

Stress constraint: no

References: Third Semi-Annual Report pp.5-6, Thesis, pp. 42-49

Case 11. Teetering rotor (similar to Case 10, except cyclic
     flapping modes considered, instead of collective modes)

Rotating: yes

Objective function: initially the weighted sum of squares of
     differences in frequencies; after a feasible design is
     found, the objective is changed to the weight.

Design variables: flange thicknesses, lumped weights

Boundary condition(s) at root: pinned

Frequency Constraints: windows on first, second and third cyclic
    flapping

Autorotation constraint: yes

Stress constraint: no

References: Third Semi-Annual Report pp.7, Thesis, pp. 50-51

Case 12. Teetering rotor (similar to Cases 10 and 11, except that
    both cyclic and collective flapping modes are considered)

Rotating: yes

Objective function: initially the weighted sum of squares of
    differences in frequencies; after a feasible design is
    found, the objective is changed to the weight.

Design variables: flange thicknesses, lumped weights

Boundary condition(s) at root: one analysis performed with pinned
    conditions, another analysis perfomed with fixed conditions

Frequency Constraints: windows on first, second and third
    collective flapping and also on first, second and third
    cyclic flapping

Autorotation constraint: yes

Stress constraint: no

References: Third Semi-Annual Report pp.7-9, Thesis, pp. 50-54

Case 13. Teetering rotor (similar to Cases 10-12, except that
    collective and cyclic flapping and inplane and also
    torsional modes considered)

Rotating: yes

Objective function: initially the weighted sum of squares of differences in frequencies; after a feasible design is found, the objective is changed to the weight.

Design variables: flange thicknesses, wall thicknesses of both sides of box cross-section, lumped weights, stiffness of torsional spring at root

Boundary condition(s) at root: a) flapping -- one analysis performed with pinned conditions, another analysis perfomed with fixed conditions; b) inplane -- one analysis performed with pinned conditions, another analysis perfomed with fixed conditions; c) torsion -- fixed conditions

Frequency Constraints: windows on first, second and third collective and cyclic flapping; windows on first, second and third collective and cyclic inplane; and window on first torsional

Autorotation constraint: yes

Stress constraint: yes

References: Third Semi-Annual Report pp.12-13, Thesis, pp. 58-60

Case 14. Teetering rotor (similar to Case 13, except that box-beam dimensions are fixed)

Rotating: yes

Objective function: weighted sum of squares of differences in frequencies

Design variables: lumped weights, stiffness of torsional spring at root

Boundary condition(s) at root: a) flapping -- one analysis performed with pinned conditions, another analysis perfomed

10

with fixed conditions; b) inplane -- one analysis performed

with pinned conditions, another analysis perfomed with fixed

conditions; c) torsion -- fixed conditions

Frequency Constraints: windows on first, second and third

collective and cyclic flapping; windows on first, second and

third collective and cyclic inplane; and window on first

torsional

Autorotation constraint: yes

Stress constraint: yes

References: Third Semi-Annual Report pp.13-14, Thesis, pp. 60-61

Case 15. Teetering rotor (similar to Case 14, except that

stiffness of blade cross-section at root is a design

variable)

Rotating: yes

Objective function: weighted sum of squares of differences in

frequencies

Design variables: lumped weights, stiffness of torsional spring

at root, variable root-stiffness (but except at root, all

other dimensions of the box cross-section are fixed)

Boundary condition(s) at root: a) flapping -- one analysis

performed with pinned conditions, another analysis perfomed

with fixed conditions; b) inplane -- one analysis performed

with pinned conditions, another analysis perfomed with fixed

conditions; c) torsion -- fixed conditions

Frequency Constraints: windows on first, second and third

collective and cyclic flapping; windows on first, second and

third collective and cyclic inplane; and window on first
torsional

Autorotation constraint: yes

Stress constraint: yes

References: Third Semi-Annual Report pp.14, Thesis, pp. 61

Case 16. Teetering rotor (similar to Case 13, except that blade
pretwist is included.

Rotating: yes

Pretwisted Blade: yes

Objective function: initially the weighted sum of squares of
differences in frequencies; after a feasible design is
found, the objective is changed to the weight.

Design variables: flange thicknesses, wall thicknesses of both
sides of box cross-section, lumped weights, stiffness of
torsional spring at root

Boundary condition(s) at root: a) flapping -- one analysis
performed with pinned conditions, another analysis performed
with fixed conditions; b) inplane -- one analysis performed
with pinned conditions, another analysis performed with
fixed conditions; c) torsion -- fixed conditions

Frequency Constraints: windows on first, second and third
collective and cyclic flapping; windows on first, second and
third collective and cyclic inplane; window on first
torsional

Autorotation constraint: yes

Stress constraint: yes

References: Thesis, p. 61, 64

Case **17.** Teetering rotor (similar to Case 14, except that blade
   pretwist is included

Rotating: yes

Pretwisted Blade: yes

Objective function: weighted sum of squares of differences in
   frequencies

Design variables: lumped weights, stiffness of torsional spring
   at root

Boundary condition(s) at root: a) flapping -- one analysis
   performed with pinned conditions, another analysis performed
   with fixed conditions; b) inplane -- one anlaysis performed
   with pinned conditions, another analysis performed with
   fixed conditions; c) torsion -- fixed conditions

Frequency constraints: windows on first, second and third
   collective and cyclic flapping; windows on first, second and
   third collective and cyclic inplane; window on first
   torsional

Autorotation constraint: yes

Stress constraint: yes

References: Thesis, p. 61, 64

Case **18.** Articulated rotor

Rotating: yes

Pretwisted Blade: yes

Objective function: initially the weighted sum of squares of
   differences in frequencies; after a feasible design is
   found, the objective is changed to the weight.

Design variables: flange thicknesses, wall thicknesses of

both sides of box cross-section, lumped weights, stiffness
of torsional spring at root

Boundary condition(s) at root: a) flapping -- pinned; b) inplane
-- pinned at same radial location as in the case of
flapping; c) torsion -- fixed conditions

Frequency Constraints: windows on first, second and third
flapping; windows on first, second and third inplane; and
window on first torsional

Autorotation constraint: yes

Stress constraint: yes

References: Fifth Semi-annual Status Report pp. 8-9,
          Thesis, pp. 67-69

Case 19. Articulated rotor (similar to Case 18, except that box-
beam dimensions are fixed)

Rotating: yes

Pretwisted blade: yes

Objective function: initially the weighted sum of squares of
differences in frequencies; after a feasible design is
found, the objective is changed to the weight.

Design variables: lumped weights, stiffness of torsional spring
at root

Boundary condition(s) at root: a) flapping -- pinned; b) inplane
-- pinned at same radial location as in the case of
flapping; c) torsion -- fixed conditions

Frequency Constraints: windows on first, second and third
flapping; windows on first, second and third inplane; and
window on first torsional

14

Autorotation constraint: yes

Stress constraint: yes

References: Fifth Semi-Annual Status Report, pp. 9-10
Thesis, pp. 67-70

Case 20. Articulated rotor (articulation at different stations for flapping and inplane motion)

Rotating: yes

Pretwisted Blade: yes

Objective function: initially the weighted sum of squares of difference in frequencies; after a feasible design is found, the objective is changed to the weight.

Design variables: lumped weights, stiffness of torsional spring at root.

Boundary conditions(s) at root:

a) Flapping -- pinned;

b) Inplane -- pinned, but pin location is another few feet away from root

Frequency constraints: windows on all first, second and third frequencies (flapping, inplane, torsion)

Autorotation constraint: yes

Stress constraint: yes

References: Sixth Semi-Annual Status Report, pp. 3-4

Case 21. Articulated rotor (similar to case 20 except that box beam dimensions are also design variables)

Rotating: yes

Pretwisted Blade: yes

Objective function: initially the weighted sum of squares of differ-
ences in frequencies; after a feasible design is found, the
objective is changed to the weight.

Design variables: flange thicknesses, wall thicknesses of both sides
of box cross-section, lumped weights, stiffness of torsional
spring at root.

Boundary conditions(s) at root:

a)   Flapping -- pinned;

b)   inplane -- pinned, but pin location is another few feet away
from root

Frequency constraints: windows on all first, second and third fre-
quencies (flapping, inplane, torsion)

Auto rotation constraint; yes

Stress constraint: yes

References: Sixth Semi-Annual Status Reports, p. 5

3.2 FINDINGS RELATED TO OPTIMIZATION OF ROTOR BLADES

The most important general finding of the project is that it
is possible to use an optimization routine such as CONMIN to
tailor blade mass and stiffness distributions in an optimal
manner. Furthermore, formulating the optimization problem in
terms of frequency placement (that is, restricting the natural
frequencies of the blade to lie within narrow intervals located
away from certain integer multiples of the rotor speed) has been
shown to be a useful approach for reducing vibrations.

In addition to these general findings, the project estab-

16

lished a number of specific results, knowledge of which would be useful to anyone intending to apply or extend the optimization approach developed during the project. A list of these results follows.

1. In applying CONMIN to rotor-blade design, gradients of the objective and constraint functions should be calculated by analytical formulas rather than by finite differences. However, finite differences serve as a useful check on the possibility of errors in the computer implementation of the analytical formulas.
   Reference: Second Semi-Annual Status Report, pp. 9-10; Thesis, pp. 23.

2. Frequency constraints may be formulated directly in terms of the frequency in Hz, rather than in terms of eigenvalues (i.e., the square of the circular frequency). If eigenvalues are used, then scaling should be employed in the constraint equations to ensure well-behaved gradients for use in CONMIN.
   Reference: Second Semi-Annual Status Report, pp. 10-12; Thesis, pp. 25

3. The following values of CONMIN parameters were adequate for most of the optimization studies:

   ITMAX = 40-80

   ITRM = 3

   DELFUN = 0.0001 (for cantilever beams)

   = 0.00001 (for rotor blades)

17

DABFUN = 0.0025 (for cantilever beams)

= 0.00001 (for rotor blades)

THETA = 1.0

PHI = 5.0

Reference: Second Semi-Annual Status Report, pp. 13-16;

4. More efficient designs can be achieved if lumped weights are included as design variables (along with dimensions of the cross-section of the blade).

Reference: Second Semi-Annual Status Report, pp. 18-21; Thesis, pp. 27.

5. Because of the stiffening effect of the centrifugal forces in a rotating blade, frequency placement is much less dependent on stiffness and mass distributions than in a non-rotating blade. Thus, the rotational speed has a strong influence on what can be achieved in the optimization process.

Reference: Second Semi-Annual Status Report, pp. 23-24;

6. Use of <u>ten</u> finite-elements appears adequate to model a rotor-blade for optimization studies, although if many frequencies must be calculated, more elements must be used. Empirical rules which have been suggested are a) Use 4n degrees-of-freedom; and b) use n^2 degrees, where n is the number of frequencies to be found.

Reference: Second Semi-Annual Status Report, pp. 25-29;

7. An accurate eigenvalue routine should be used in optimization studies, since errors in eigenvalue calculations can appreciably affect the optimal design.

   Reference: Second Semi-Annual Status Report, pp. 29-31;

8. The natural frequencies of a rotor blade are not greatly affected by small changes in dimensions of the blade cross-section.

   Reference: Second Semi-Annual Status Report, pp. 31-32;

9. For tight frequency-constraint windows, CONMIN is often unable to find a feasible design. In such cases, an objective function consisting of the weighted sum of squares of the differences in frequencies (actual frequency minus desired value) may be used initially. In the process of minimizing this objective function, CONMIN is often able to find a design which satisfies the frequency constraints. If this occurs, the objective function may then be switched to the weight of the blade.

   Reference: Third Semi-Annual Status Report, pp. 5-9;
   Thesis, p. 44, 48, 50, 52, 58

10. The natural frequencies of a blade which has already been built can be modified in a rational (rather than trial-and-error) manner by using CONMIN to specify where lumped mass should be added. It appears best to either raise all undesirable frequencies or lower all undesirable frequencies (a mixture of raised and

19

lowered frequencies is much more difficult to attain).
References: Third Semi-Annual Status Report, pp. 13-14;
Thesis, pp. 60-61; Sixth Semi-Annual Status Report,
p. 4.

11. The _forced_ response of a rotor blade can be adequately
controlled through the approach of frequency placement.
Reference: Fourth Semi-Annual Status Report, pp. 2-10;
Thesis, pp. 71-95.

12. Aerodynamic damping substantially reduces resonant
peaks, but even in the presence of damping, frequency
placement is a powerful driver of loads, and, as a
result, frequency placement can be justifiably con-
sidered an important part of blade optimization in the
presence of damping.
Reference: Fourth Semi-Annual Status Report, pp. 5-7;
Thesis, pp. 75-82.

13. Finite-element modelling errors caused by neglecting
secondary structural items such as shear deformation,
restraint of warping during twist, and filler stiffness
are small. However, accurate filler properties, dimen-
sions and locations are required in order to model the
mass distribution properly.
Reference: Fourth Semi-Annual Status Report, pp. 11-12;

14. Since calculating eigenvalues is the major computa-
tional burden in rotor-blade optimization, an _efficient_
eigenvalue routine should be used. For example, determ-

inant search or subspace iteration can be used to calculate only the needed first few frequencies.

Reference: Fifth Semi-Annual Status Report, pp. 2-5

4. REFERENCES

1. Niebank, C. and Girvin, W., "Sikorsky S-76 Analysis, Design and Development for Successful Dynamic Characteristics", Proceedings of the 34th Annual National Forum of the American Helicopter Society, May 1978, pp. 78-23-1 through 78-23-17.

2. Hirsh, Harold, Dutton, Robert E., and Rasumoff, Abner, "Effect of Spanwise and Chordwise Mass Distribution on Rotor Blade Cyclic Stresses, " Journal of the American Helicopter Society, Vol. 1, No. 2, April 1956.

3. Ellis, C.W. et al., " Design, Development, and Testing of the Boeing Vertol/Army YUH-61A, "Proceedings of the 32nd Annual National Forum of the American Helicopter Society, Preprint 1010, May 1976.

4. Fenanghty, Ronald, R. and Noehren, William L., "Composite Bearingless Tailor Rotor for UTTAS," Journal of the American Helicopter Society, Vol. 22, No. 3, July 1977, pp. 19-26.

5. Hanson, H.W. and Calapodas, M.J., "Evaluation of the Practical Aspects of Vibration Reduction Using Structural Optimzation Techniques," Proceedings of the 35th Annual National Forum of the American Helicopter Society, May 1979, pp. 79-21-1 through 79-21-12.

6. Vanderplaats, G.N., CONMIN - A Fortran Program for Constrained Function Minimization. User's Manual, NASA TMX-62.282, August, 1973.

APPENDIX 1

Thesis of Timothy Ko

SEVER INSTITUTE OF TECHNOLOGY

Doctor of Science Degree

DISSERTATION ACCEPTANCE

(To be submitted by the graduation approval deadline)

DATE: 20 August 1984

STUDENT'S NAME: Timothy Wai Hung Ko

E.R.S. CODE: _____

This student's dissertation, entitled "Design of Helicopter Rotor Blades for Optimum Dynamic Characteristics"

has been examined by the undersigned committee of three faculty members and has received full approval for acceptance in partial fulfillment of the requirements for the degree Doctor of Science.

Signatures: _____ Chairman

_____

_____

_____

Distribution:

5 - Dissertation copies
1 - Candidate
1 - Department
1 - Dean's Office
1 - Registrar

WASHINGTON UNIVERSITY

SEVER INSTITUTE OF TECHNOLOGY

———————————

DESIGN OF HELICOPTER ROTOR BLAD   R

OPTIMUM DYNAMIC CHARACTERISTI..

by

Timothy W H Ko

Prepared under the direction of Professor D. Peters

———————————

A thesis presented to the Sever Institute of
Washington University in Partial fulfillment
of the requirements for the degree of

DOCTOR OF SCIENCE

December, 1984

Saint Louis, Missouri

WASHINGTON UNIVERSITY
SEVER INSTITUTE OF TECHNOLOGY

ABSTRACT

DESIGN OF HELICOPTER ROTOR BLADES FOR

OPTIMUM DYNAMIC CHARACTERISTICS

by Timothy W H Ko

ADVISOR :   Professor D. Peters

December, 1984

Saint Louis, Missouri

The mass and stiffness distributions for helicopter
rotor blades are to be tailored in such a way to give a
predetermined placement of blade natural frequencies. The
optimial design is pursued with respect of minimum weight,
sufficient inertia, and resonable dynamic characteristics.
Finite element technique will be used as a tool. Rotor
types include hingeless, articulated, and teetering.

TABLE OF CONTENTS

TABLE OF CONTENTS
(continued)

LIST OF TABLES

LIST OF TABLES
(continued)

LIST OF FIGURES

LIST OF FIGURES
(continued)

DESIGN OF HELICOPTER ROTOR BLADES FOR
OPTIMUM DYNAMIC CHARACTERISTICS

1. INTRODUCTION

1.1 HELICOPTER DESIGN

The design of helicopter rotor blades involves not only considerations of strength, survivability, fatigue, and cost, but also requires that blade natural frequencies be significantly separated from the fundamental aerodynamic forcing frequencies (e.g. Ref. 1). A proper placement of blade frequencies is a difficult task for several reasons. First, there are many forcing frequencies (at all integer—multiples of the rotor RPM) which occur at rather closely-spaced intervals. For example, 5/rev and 6/rev are less than 20 % apart. Second, the rotor RPM may vary over a significant range through the flight envelope, thus reducing even further the area of acceptable natural frequencies. Third, the natural modes of the rotor blade are often coupled because of pitch angle, blade twist, offset between the mass center and elastic axis, and large aerodynamic damping. These couplings complicate the calculation of natural frequencies. In fact, the dependence on pitch angle makes frequencies a function of loading condition, since loading affects collective pitch. Fourth, the centrifugal stiffness often dominates the lower modes, making it difficult to alter frequencies by simple changes in stiffness or mass.

In the early stages of the development of the helicopter, it was

believed that helicopter vibrations could be reduced (and even elimina-ed) by the correct choice of structural coupling and mass stiffness distribution. However, it is easy to imagine how difficult it is to find just the proper parameters such that the desired natural frequencies can be obtained. The difficulties in placement of natural frequencies have led, in many cases, to preliminary designs which ignore frequency place-ment. Then, after the structure is 'finalized' (either on paper or in a prototype blade), the frequencies are calculated (or measured) and final adjustments made. Reference [2] describes the development of the XH-17 helicopter in which a 300-lb weight was added to each blade in order to change the spanwise and chordwise mass distribution and therby move the first flapwise frequency away from 3/rev. The authors were con-fident that similar adjustments to the mass distribution (and thus to the frequencies and modes of the blades) could greatly reduce rotor vibration on other rotors. An analytic study in Reference [3] predicts that chordwise mass distribution could also be used to lower overall helicopter vibrations. In particular, a forward shift of mass is shown to be useful because it places torsion in resonance with a particular harmonic. The torsion loads can then be tuned to cancel undesirable blade loads. The study also shows, however, that such mass changes may have an adverse effect on stability; and thus stability and vibration must be studied together. Similar benefits of inertia pitch-flap coupl-ing are also observed in shaker tests in Reference [4].

These positive results, and other like them, were at least partial-ly responsible for the optimistic outlook so aptly presented in Ref [5]. In that reference, six helicopter pioneers express their belief that helicopter vibrations can be reduced through proper blade and fuselage

design. This optimism of the 50's was somewhat eroded in the 60's and 70's as the true complications of rotary-wing dynamics became better known. Nevertheless, the belief is still held by most dynamicists that simple concepts (such as frequency placement) can go a long way toward improving rotor design. For example, in Reference [6] six helicopter pioneers (some of the authors of Ref. 4), reminisce on the early days of rotary wing and the recent advances in our understanding of helicopter. Yet, they still contend that much can be learned from simple principles.

Presently, helicopter blades are not tailored to give a set of desired natural frequencies. Instead, blades are designed based on other considerations (including the desired aerodynamic characteristics and the cumulative experience of the designers). Then, after the design is analyzed (either by computer program or by fabrication and testing), the designer checks for frequencies that are poorly placed. These are then adjusted by judicious application of lumped inertias at crucial spanwise locations. These after-the-fact alterations, however, can be detrimental to blade weight, blade cost, and the development time of the aircraft. Sometimes, the problems are unsolvable, and a helicopter is left with a noticeable resonance problem.

The state-of-the-art in helicopter technology is now to the point, however, that it should be possible to correctly place rotor frequencies during preliminary design stages. There are several reasons for this. First, helicopter rotor blades for both main rotors and tail rotors are now being fabricated from composite materials (Refs. 7 and 8). This implies that the designer can choose, with limited restrictions, the exact EI distribution desired. Furthermore, the lightness of composite blades for the main rotor usually necessitates the addition of weight to

give sufficient autorotational blade inertia. Thus, there is a considerable amount of flexibility as to how this weight may be distributed. Second, the methods of structural optimization and parameter identification are now refined to the point where they can be efficiently applied to the blade structure. Some elementary techniques have already been used for the design of rotor fuselages (Ref. 9). It follows that the time is right for the use of structural optimization in helicopter blade design. Some work on this is already under development, and, although not published, some companies are already experiment with the optimum way to add weight to an existing blade in order to improve vibrations.

1.2 PREVIOUS WORK

In this light, we would like to mention a few recent attempts at application of optimization techniques to rotor blade design. In Ref [10], an optimization procedure is applied in order to reduce blade loads consistent with aeroelastic stability. The procedure is not completely automated, however, and the designer must make the design increment at each iteration based on numerical sensitivity parameters. The biggest needs (as identified in this work) are the complete automation of the optimization and the formulation of realistic design constraints. In Reference [11], an optimization package is applied to an aeroelastic response program. The results mirror the earlier conclusions of Reference 2-4. In particular, minimization of vibrations tends to drive some natural frequencies close to integers in order to cancel loads. (The rotor becomes an isolator.) Although this turns out to be a good mathematical solution, stability analyses in Reference [11], as in References [2-4], show that the coalescence of frequencies to suppress vibration tends to introduce aeroelastic instabilities. Thus, flutter margins tend

to become the dominant constraints. Furthermore, minimization of loads at one flight condition may not at all minimize loads at others.

Another investigation into vibration reduction by alteration of mass and stiffness distribution is given in Reference [12]. In that reference, a tip weight is used to change the mode shape. It is hypothesized that changing the mode shape such that it is orthogonal to the forcing function is a way to lower vibrations. However, the conclusions are uncertain since the frequencies also are changed by this added weight (e.g. the second flap mode moves away from 5.06 to 5.19 per rev). One also notices that the loading distribution changes with flight condition so that modal shaping may help one condition but hurt others. Other related previous work is found in Reference [13]. That paper shows that design to minimum loads can result in a disjoint solution. Fortunately, in helicopter problems we generally begin with an adequate (but not perfect) blade design. Thus, many questions such as this (i.e. disjoint in the design space) are automatically avoided. We already have a good first guess and merely wish to refine it.

1.3 SCOPE

In this paper we undertake a much less ambitious aim than the minimization of hub loads. Instead we look at the problem of using optimization techniques in order to place natural frequencies. Even within this reduced problem there are varying levels of complexity. For example, one could consider the retrofit problem:

' Given a blade design find the amount and location of added
  masses required to move frequencies away from integer
  resonances.'

One could also consider the basic design problem in which both stiffness

and mass distributions may be chosen. In this paper, we treat this latter design problem in the form of three uncoupled problems: flap, in-plane, and torsion.

The scope of this present work is not just to find a mass and stiffness distribution to give desired frequencies. It is also to determine meaningful constraints and objective functions that will result in realistic designs. In this area, several items are noteworthy. First, there is the airfoil envelop. Whatever the structural engineer designs must lie within the airfoil cross-section. Second, there is mass balancing. The center of mass of each section should be forward of the one-quarter chord. Third, there is the autorotational constraint. The blade must have sufficient mass moment-of-inertia to insure a safe autorotational capability. Fourth, there is strength. The blade must be strong enough to endure the centrifugal loads as well as the oscillatory bend-ing loads. This last criteria is the most elusive of the four. Designers know how to make a very soft section (hinge or flexure) which neverthe-less can withstand high centrifugal and bending loads. Such flexures generally do not fall within an airfoil envelope, however, and are placed near the root. Therefore, in the work to follow, we first obtain 'optimum' designs and then check to see if the required EI distribution has unrealistically soft spots. Similarly, we check the final designs for axial stresses.

In summary, we work with simple (but realistic) rotor-blade designs and simply experiment with constraints and objective functions in order to determine the feasibility of designing to a desired set of frequen-cies.

1.4 OVERVIEW OF OPTIMAL STRUCTURAL DESIGN

Most approaches to optimal structural structural design may be classified into three categories. (For recent review articles see Refs. 14 and 15.) One such category is 'variational methods.' These generally rely on techniques from the mathematical theory of the calculus of variations, and, when applicable, often provide useful physical insight into the nature of an optimal design. Unfortunately, only relatively simple problems can be solved by this approach, since the mathematics becomes intractable when complex engineering structures are considered.

A second category of structural optimization techniques consists of the application of mathematical programming methods together with the discretization of the structure by finite element techniques. This approach to optimization was founded in 1960 (Ref. 16) with the hope that more complex structures could be analyzed than were possible when using the analytical techniques of the calculus of variations. However, in the late 60's it became apparent that mathematical programming method had limitations of their own, namely, unacceptably long computation times occurring when the number of design variables become large (over 20-100, depending on the type of structure). Fortunately, several improvements developed over the last few years appear to have significantly extended the capability of the mathematical programming approach, and, as a result, it is this approach we intend to draw upon for solution techniques in this research.

A third category of structural optimization approaches is the 'optimality criterion' approach in which an equation expressing some necessary condition of optimality is used as the basis for constructing an iterative (successive re-design) procedure. Originally developed

because of dissatisfaction with mathematical programming techniques, the optimality-criterion approach initially relied on intuitive optimality criterion such as constant stress-ratio and uniform strain-energy density conditions. More recently, optimality criterion (and associated re-design equations) have been derived from the Kuhn-Tucker conditions (see, e.g. Ref. 17) for a constrained minimization problem.

The optimality criterion approach seems especially well-suited to problems with a large number of design variables. Since our design problem will have a moderate number of variables and since deriving efficient re-design equations for our problem is not immediately straightforward, we initially prefer the mathematical programming approach over the optimality-criterion approach.

A structural optimization computer program, called CONMIN (Ref. 27), is available from NASA. It is this program that is used in our present work. CONMIN is based on the mathematical nonlinear programming method of feasible directions.

2. BACKGROUND

2.1 FORMULATION OF PROBLEM

Because numerically-based optimization is best carried out with discrete variables, the finite element technique stands as the most logical choices for the blade model. A recent research project (Ref. 18) has resulted in a finite-element computer program that is ideally suited to the work here. The program allows for tapered, twisted finite elements in a rotating environment. The existing code can calculate natural frequencies, (with and without aerodynamic terms) and force response.

Another important aspect of the rotor blade optimization problem is the selection of the optimality criteria and constraints to be imposed. Our design problem has certain features which are unusual compared to typical problems occurring in the structural optimization literature. There are basically three catagories of criteria. In the first class, one would minimize weight given constraints on the natural frequencies (i.e. frequency 'windows'). In this case, a constraint on rotary inertia is also implied since a rotor must have sufficient inertia to autorotate. The advantage of this approach is that it is directly related to the physical realities of design. The disadvantage, however, is that the first guess will probably not be feasible (that is will not have frequencies that fall in the 'windows'). This can be a stumbling block to convergence. A second type of criteria is one in which the objective is to minimize the discrepancies between desired frequencies and actual frequencies. The constraint then becomes a window on autorotational inertia. Although this avoids unfeasible solutions, it does not directly minimize weight (although weight is limited by the autorotational

constraint). An objective function can be constructed that combined combined blade mass and frequency placement, but the relative weightings of the two components is not obvious. The third category of constraint is to minimize vibrations directly without regard to frequency placement. Although this appears on the surface to be the perfec* solution, there are problems. First, calculation of vibrations is an order-of-magnitude more difficult than the calculation of frequencies. Second, past efforts at this have resulted in strange designs, incompatible with standard helicopter practice. Third, there is still the problem of the weight-vibration trade-off. In this work, we intend to concentrate on the first two categories with some attention to the third.

Another type of constraint involved in the problem is the limitation on structural properties. The blade planform, airfoil, and twist are chosen by the aerodynamicist on the basis of performance. The structural engineer must choose his design to *it in the aerodynamic envelope given. There are five structural parameters to be chosen: 1) flapping stiffness, 2)inplane stiffness, 3) torsional stiffness, 4) mass, and 5) torsional moment of inertia. In practice, these cannot be chosen completely independently. Figure 1 shows the envelope of a typical blade section. All stiffness is assumed to reside in a box-beam of dimension b x h with thicknesses t,d1,d2. This beam is placed as far forward as possible (to keep the elastic axis near the 1/4 chord). Mass properties are due to the box-beam, skin, honeycomb, and two lumped masses. The lumped mass in the tip is typical of rotor blades and is used to keep the mass center forward of the aerodynamic center. A second mass is included to allow independent choice of mass and mass-moment. The constraints of this construction are clear and are listed on the

GENERIC BLADE SECTION CONSTRAINTS
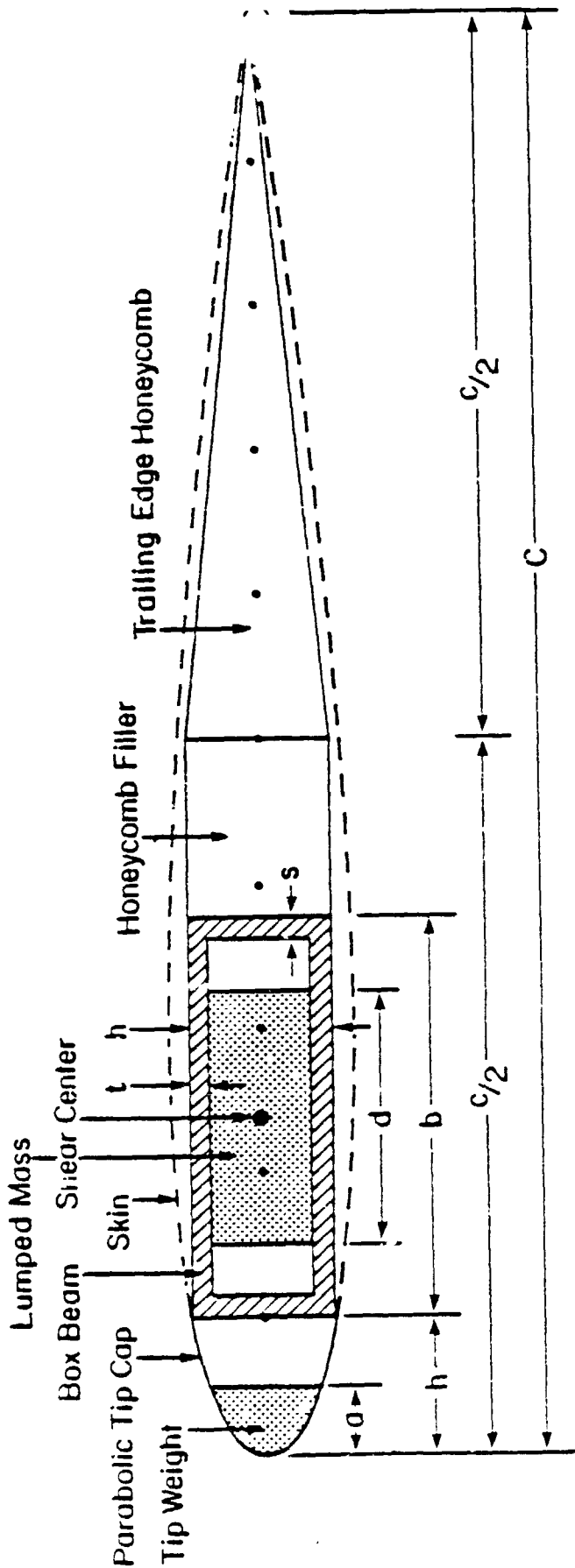
Given: c, h

Variable: a, b, d, s, t

Densities: τ – Tip Weight & Lumped Mass

β – Box Beam

η – Honeycomb

σ – Skin (kg/m)

$\Big\}$ kg/m³

Constraints:

$0 \le a \le h$

$0 \le b \le c/2 - h$

$0 \le d \le b - 2s$

$0 \le s \le b/2$

$0 \le t \le h/2$

Figure 1. Typical Blade Cross Section

figure.

In addition, there are minimum constraints on t,d1,d2 to hold centrifugal loads and to remain within manufacturable limits. For example a simple minimum constraint on area could come from the centrifugal constraint (not considering bending stress). Thus, if σ_m is the maximum stress and if f is a safety factor, then

$$(\sigma_m) \geq f \left[\sum_{i=j+1}^{n} (M_i)\Omega^2 r_i \right]/A_j \tag{1a}$$

$$A_j \geq \frac{f\left[\sum_{i=j+1}^{n} M_i \Omega^2 r_i \right]}{(\sigma_m)} \tag{1b}$$

Of course, when we enter the vibratory-response phase of the work, bending stresses will be included.

Our work will nevertheless include flutter criteria in a simplified manner. First, we can choose frequency placement such that no coalescence occurs between flap-lag, flap-torsion, or lag-torsion. Second, we can constrain the five parameters in Figure 1 such that the mass center is always forward of the 1/4-chord, a common design practice to prevent torsion-flutter in rotor blades.

2.2 Finite-Element Mode

Although tapered, twisted elements are within our capabilities, we introduce here a simple case which is also of value. The stiffnesses GJ, EI_{zz}, EI_{yy} are assumed to be constant along the length of the element.

The lumped mass weight is assumed to be evenly distributed on the two nodes.

Let the deflection of an element in the y a.' z directions at a distance x be denoted as w(x) and v(x), for which the displacement models are assumed to be polynomials of third degree. The expressions are given as

$$w(x) = \frac{u_1}{l^3} (2x^3 - 3lx^2 + l^3) + \frac{u_6}{l^3} (3lx^2 - 2x^3)$$

$$- \frac{u_3}{l^2} (x^3 - 2lx^2 + l^2x) - \frac{u_8}{l^2} (x^3 - lx^2) \qquad (2a)$$

$$v(x) = \frac{u_2}{l^3} (2x^3 - 3lx^2 + l^3) + \frac{u_7}{l^3} (3lx^2 - 2x^3)$$

$$+ \frac{u_4}{l^2} (x^3 - 2lx^2 + l^2x) + \frac{u_9}{l^2} (x^3 - lx^2) \qquad (2b)$$

where v_1, v_3, v_6 and v_8 represent the bending degrees of freedom in the zx plane and u_2, u_7, u_4 and u_9 represent the degrees of freedom in the yx plane

i) The strain energy due to bending deformation can be expressed as

$$U = \int_0^l \left\{ \frac{EI_{yy}}{2} \left(\frac{\partial^2 w}{\partial x^2}\right)^2 + EI_{yz} \frac{\partial^2 w}{\partial x^2} \frac{\partial^2 v}{\partial x^2} + \frac{EI_{zz}}{2} \left(\frac{\partial^2 v}{\partial x^2}\right)^2 \right\} dx \tag{3}$$

ii) The potential energy in tension from the centrifugal force field, which is equivalent to the negative of kinetic energy due to radial displacement, is given by

$$- T_K = U = \int_0^l \frac{T}{2} \left[\left(\frac{\partial w}{\partial x}\right)^2 + \left(\frac{\partial v}{\partial x}\right)^2 \right] dx \tag{4}$$

where T, tension force, is assumed to be constant along each element.

iii) The kinetic energy due to inplane displacement is given by

$$T_K = -\frac{1}{2} \int_0^l m \, v^2 \Omega^2 \, dx \tag{5}$$

which is equivalent to u = T
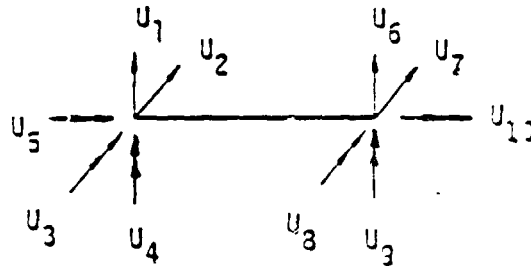
Degrees of Freedom of an Element

Meanwhile, the pretwist angle $\phi(x)$, and the torsional deformation $\theta(x)$ are assumed to be polynomials of first degree, and can be expressed as

$$\phi(x) = \phi_1 \left(1 - \frac{x}{l} \right) - \phi_2 \left(\frac{x}{l} \right) \tag{6a}$$

$$\theta(x) = U_5 \left(1 - \frac{x}{l} \right) + U_{10} \left(\frac{x}{l} \right) \tag{6b}$$

where ϕ_1, ϕ_2 represent the pretwist angle at node 1 and 2, and u_5, u_{10} represent the elastic torsional degree of freedom at each end.

iv)   The torsional energy, due to elastic deformations and centrifugal terms, can be expressed as

$$U = \int_0^l \left\{ \frac{1}{2} ka_1^2 \frac{I}{A} (\phi' + \theta')^2 + \frac{1}{2} ka_2^2 \frac{I}{A} (\phi' - \theta')^2 + \frac{1}{2} GJ\theta'^2 \right\} dx \quad (7a)$$

where $ka_1^2 = \iint z^2 \, dy \, dz = I_{yy}$ (7b)

$$ka_2^2 = \iint y^2 \, dydz = I_{zz} \qquad (7c)$$

v)   The 'torsion-rotation' energy under the effect of rotation is given by

$$T_k = -\int_0^l \frac{\Omega^2}{2} (km_1^2 - km_2^2)(\phi + \theta)^2 \, dx \qquad (8a)$$

where $km_1{}^2$, $km_2{}^2$ are mass moment of inertia which can be expressed as

$$km_1^2 = \iint \rho z^2 \, dy \, dz = \rho I_{yy} \qquad (8b)$$

$$km_2^2 = \iint \rho y^2 \, dy \, dz = \rho I_{zz} \qquad (8c)$$

Total displacement energy now can be used to form the stiffness matrix from

$$\bar{U} = \frac{1}{2} u^T [\kappa] u \qquad (9)$$

where u is the vector of nodal displacements, in the order as u_1, u_6, u_3, u_8, u_2, u_7, u_4, u_9 , u_5 , u_{10} ; [K] is the elemental stiffness matrix of order 10.

vi)   The mass matrix will be obtained by the kinetic energy of an element, which is given by

$$T_\kappa = \int_o^\ell \{\frac{\bar{\bar{m}}}{2} (\frac{\partial v}{\partial t})^2 + \frac{\bar{\bar{m}}}{2} (\frac{\partial w}{\partial t})^2 + \frac{\rho}{2} I_{22} (\frac{\partial^2 v}{\partial t \partial x})^2$$

$$+ \frac{\rho}{2} I_{yy} (\frac{\partial^2 w}{\partial t \partial x})^2 + \frac{1}{2} (km_1^2 + km_2^2)\theta'^2\}dx \tag{10}$$

Written in matrix form, the kinetic energy can be expressed as

$$\bar{T} = \frac{1}{2} u^T [M]\bar{u} \tag{11}$$

where [M] is the mass matrix.

3. ILLUSTRATIVE EXAMPLES OF STRUCTURAL OPTIMIZATION

3.1 CANTILEVER BEAM WITH GIVEN FREQUENCY

Some simple examples will be examined and discussed before the utilization of the program CONMIN. In each case the results will be compared with those obtained by previous researches, if it is available.

The first limiting example is the problem of determining the optimal design of an elastic cantilever beam, such that with a specific natural frequency, the weight of the structure attains the minimum value.

We start with a uniform beam, modeled by ten elements, with a given length of 10 inches, $E = 1.0$ lb-in^2, $EI = 10$ lb-in^2, density $= 0.042$ lb/in^3, and a specified first lowest natural frequency $= 0.6489$ rad/sec. We obtain the final stiffness profile shown in Figure 2. Figure 2 is the present result with ten elements.

A related problem has also been treated by Olhoff [19]. He seeks the design of a cantilever beam that yields a maximum value of a particular higher natural frequency w_n (i.e. of specified order, n) with the volume and length of the beam specified. His work is the dual problem of the example shown in Figure 2. Optimization with respect to the frequency under the constraint of volume is similar to the one of minimizing weight (or volume) under the constraint of specified natural frequency. Figure 3 gives the profile of the optimal cantilever for n = 1 by Olhoff. One can see that the shapes in Figure [2] and [3] are very similiar in that they give a nonlinear taper.

3.2 CANTILEVER WITH TIP MASS

Another example problem is to minimize the weight of a cantilever carrying a mass at the tip, subject to the constraint that the fundamental natural frequency must be greater than or equal to a specified
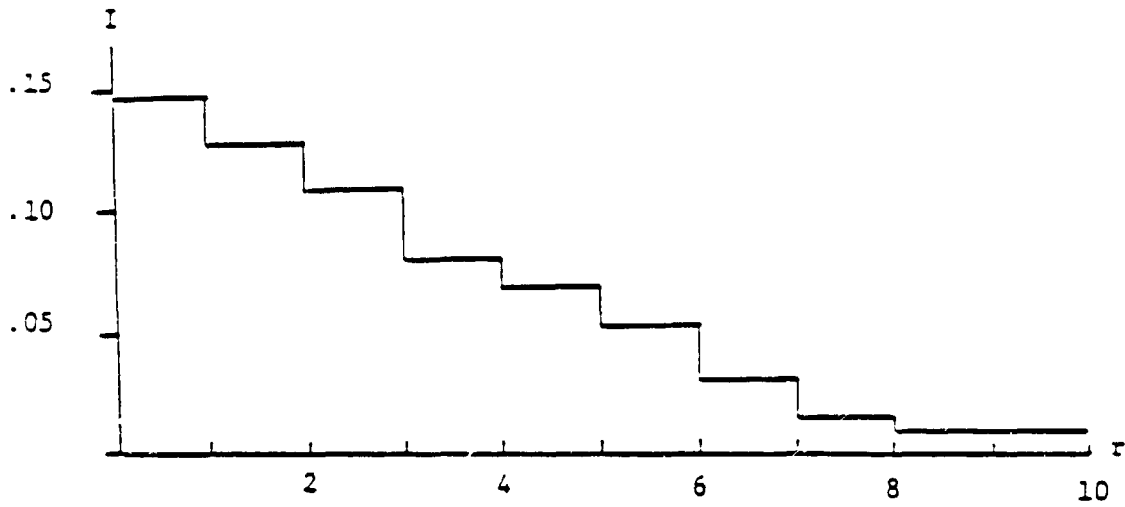
Figure 2.   Area Moment of Inertia for Optimum Beam in
             Present Work.

Figure 3.   Area Moment of Inertia for Optimum Beam
             from Reference 11.

value. The problem was originally formulated by Turner [20]. Kahn and Willmert [21] used an optimality criterion method to solve Turner's problem. In this example, four finite elements are used, with the areas of each as the design variables, as illustrated in Figure 4. The specified natural frequency is 17.752 rad/sec. The other initial data are

$$
\begin{array}{ll}
\text{Modulus of elasticity} & = 10.3 \times 10 \quad \text{psi} \\
\text{Mass density} & = 2.5 \times 10 \quad \text{lb-s}^2/\text{in} \\
\text{Radius of gyration } (A_1) & = 2.0 \quad \text{in} \\
\text{Radius of gyration } (A_2) & = 1.5 \quad \text{in} \\
\text{Radius of gyration } (A_3) & = 1 \quad \text{in} \\
\text{Radius of gyration } (A_4) & = 0.5 \quad \text{in} \\
\text{Concentrated mass} & = 1 \quad \text{lb-s}^2/\text{in} \\
\text{Length of each element} & = 60 \quad \text{in}
\end{array}
$$

where $I = \text{Area} * (\text{radius of gyration})^2$.
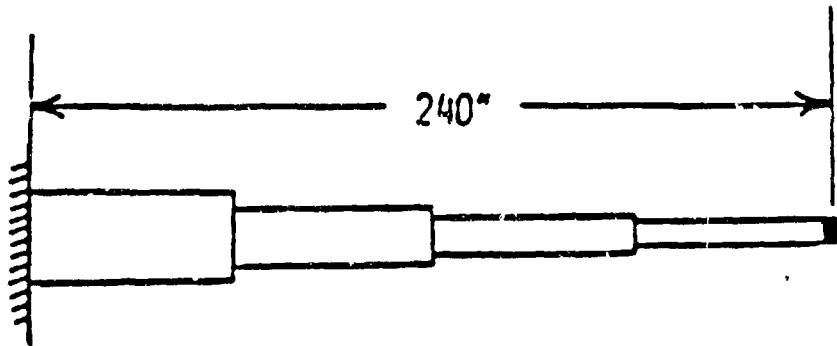
Figure 4   Cantilever beam with concentrated mass

The results of the optimization are shown in Table 1. The feasible starting design is described by A_1 = 200, A_2 × 150, A_3 = 60 and A_4 = 35.

Table 1

Comparison of Cantilever Beam with Concentrated mass

	Ref.[12]	Ref.[13]	This Paper
Iteration	-	23	19
A_1 (in$_2$)	136.81	136.63	134.60
A_2 (in$_2$)	113.73	118.70	116.
A_3 (in$_2$)	83.59	83.58	82.73
A_4 (in$_2$)	34.43	34.61	34.89
Weight (lb)	2243.0	2242.9	2214.4

It can be seen that excellent results have been obtained using the present CONMIN optimization program.

4. NUMERICAL EXPERIMENTS

4.1 DESIGN VARIABLE

Despite the strong documentation and intensive development that has gone into optimization programs, it is always advisable to do some experimentation with these programs for the particular class of problems to which they are to be applied. This has been done in detail for the representative box beam shown in Figure 5. The parameters (see Fig 1) for this car are: h = 2.5 in, s = 0.1 in, s = 0.1 in. b = 4 in, t variable. This beam has been analyzed for various values of the CONMIN parameters and for various combinations of constraints. The first studies are performed for vertical vibrations. a nonrotating beam, no lumped mass, and with two frequency constraints. Each of the CONMIN options is then exercised, and several conclusions drawn.

First, we find that the use of analytic gradients (the derivative of objective function and constraints in closed form) is greatly to be desired. For the particular case in Figure 5, area, weight, and moment of inertia can be expressed in terms of the single variables, t

$$A_i = 0.50 + .60 \, t_i \tag{12a}$$

$$W_i = 1.20 + 18.24 \, t_i \tag{12b}$$

$$I_i = 25/90 + t_i * (285 - 228 \, t_i + 60.8 \, t_i^2) * 124 \tag{12c}$$

Therefore, analytic derivatives are straightforward. Where analytic gradients are not available, however, we find that finite difference gradients still work albeit at a higher computational cost. Second, we
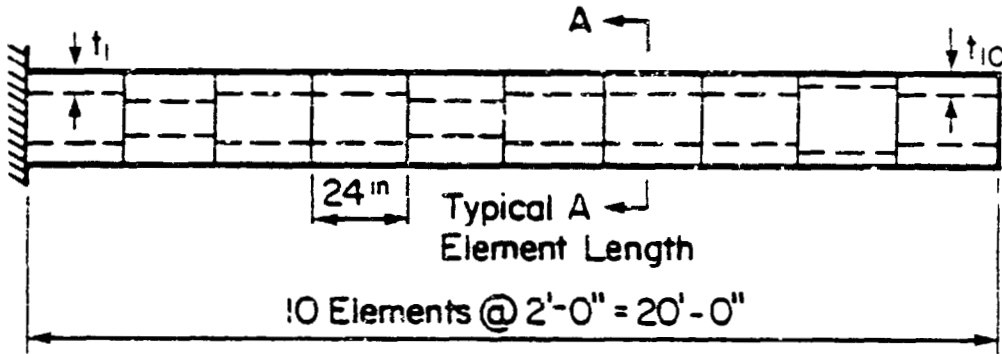
ELEVATION
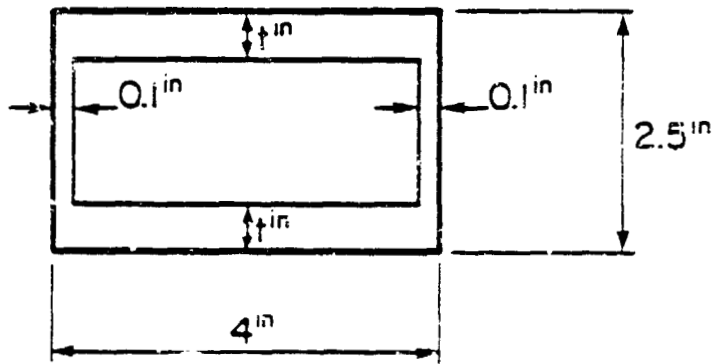
SECTION A-A

Figure 5   Box Beam Cross-Section

find that the optimization is best behaved when frequency constraints are provided in Hz. A constraint (if not scaled) on eigenvalues (w^2) is more difficult for the program when default values are used. Third, we find that initial designs outside of the desired constraints (infeasible) sometimes can lead to convergence. Since this is not always the case, however, alternative strategies are necessary. Fourth, we find that the default values for the CONMIN program worked reasonably well (although they are not always the most efficient values). An example is the number of iterations. Sometimes 40 iterations were required for convergence, although the default value is 10.

In terms of various modes of application, we also have come to several conclusions. First, we could find optimum designs no matter how tightly we closed the windows on frequency (i.e. the frequency constraints). Thus, we are able to essentially 'zero' an objective function based on frequencies (for vertical vibrations alone). Second, we can handle a large number of simultaneous frequency constraints. (We have successfully gone from 2 up to 5 constraints.) The optimization also remains well-behaved when we add blade rotation, lumped mass, and the autorotational constraint.

4.2 CONVERGENCE

We have studied the convergence of the final design as a function of the number of elements used in the finite-element frequency calculation. To study how the optimal design changes as the number of elements increases, a cantilever beam with 'n' elements and with lumped weights added at the nodes but otherwise similar to the beam in Figure 1 is considered. The density, and the constraints on the natural frequency, lumped weights, and moments of inertia are

$$\beta = 0.05 \; lbf/in^3$$

$$1.0 \leq f_1 \leq 1.3 \; (Hz) \tag{13a}$$

$$10.0 \leq f_2 \leq 11.2 \; (Hz) \tag{13b}$$

$$0.0 \leq W_1 \leq 100.0 \quad (lbf) \tag{13c}$$

$$3.83073 \leq I_1 \leq 5.2083 \quad (in^4) \tag{13d}$$

and the initial value of OBJ (the total weight) is 30.2249 lbf.

Results of the study are shown in Figures [6-11]. In all cases, the active frequency constraints were found to be

$$f_1 = 1.3 \; (Hz)$$

$$f_2 = 11.2 \; (Hz)$$

Figure [6] demonstrates, as one would expect, that the optimum weight does in fact decrease as more elements are added to the mesh. The change in optimum weight is quite small (note that the scale of the vertical axis begins at 20.0).

Figure [7] and [8] show the variation of the lumped weight and the moment of inertia (of the cross-sectional area) at the free end versus the total number of elements in the mesh. It appears that these quantities do not converge. The result can be explained, however, by referring to Figure [9], in which the upper curve represents the total weight at the free end. ($m(n)$ is the non-structural,or, lumped weight $s(n)$ is the structural weight associated with the mass distributed throughout

element 'n'). It can be seen from the figure that the total weight appears to converge smoothly as the mesh is refined. The explanation for the apparent non-convergence shown in Figures [7] and [8] and for the convergence shown in the top curve of Figure [9] is that the 'structural weight' at the free end of the cantilever is not really structural, since there is no portion of the beam beyond the free end which needs to be supported. Thus, the optimization routine is indifferent to whether structural or non-structural weight is present at the free end — the only thing that counts is the total weight at that end.

Figure [9] also shows the variation of the lumped weight slightly beyond the middle of the beam. (All optimal designs have non-zero lumped weights there and at the free end of the beam.) The weight can be decrease smoothly as the mesh is refined, although no asymptote appears to be present. The explanation for this behavior is that, as the mesh is refined, the weight in the middle is being place more efficiently - and thus less is needed.

The various sketches in Figure 10a show the distribution of mass and stiffness along the beam for increasing numbers of elements. It is interesting to observe that the optimization routine finds it most efficient to meet the constraints on frequency by varying the lumped weight rather than by varying the stiffness (moment of inertia), since this latter quantity is at its lower bound every re except near the end of the beam. Another interesting aspect of Figure 10 is the manner in which the lumped mass at the center alternates between: 1) being all on one element, and 2) being split between two elements. This phenomenon is a result of the fact that the minimum weight structure would have all the mass at a single point (node or antinode). When this single point lies
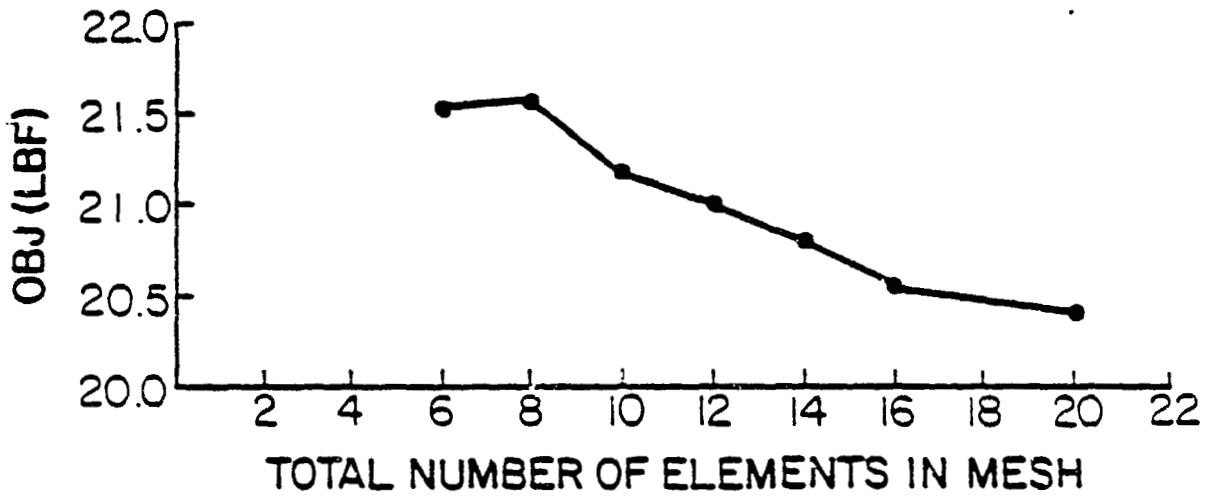
Figure 6   Convergence of Weight of Objective Function
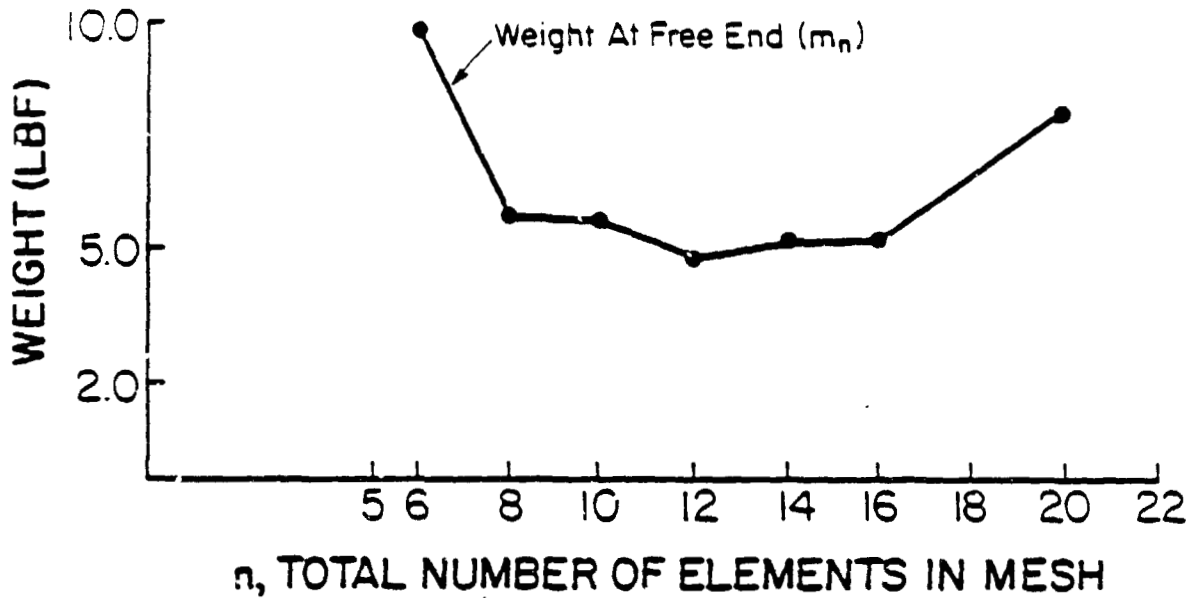
Figure 7   Weight Objective Function Versus Number of Elements
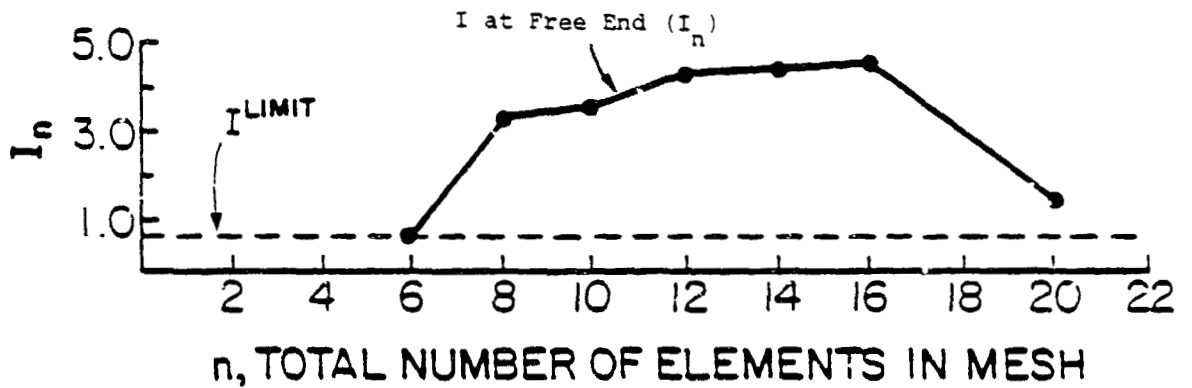
Figure 8   Area Moment of Inertia Versus Number of Elements
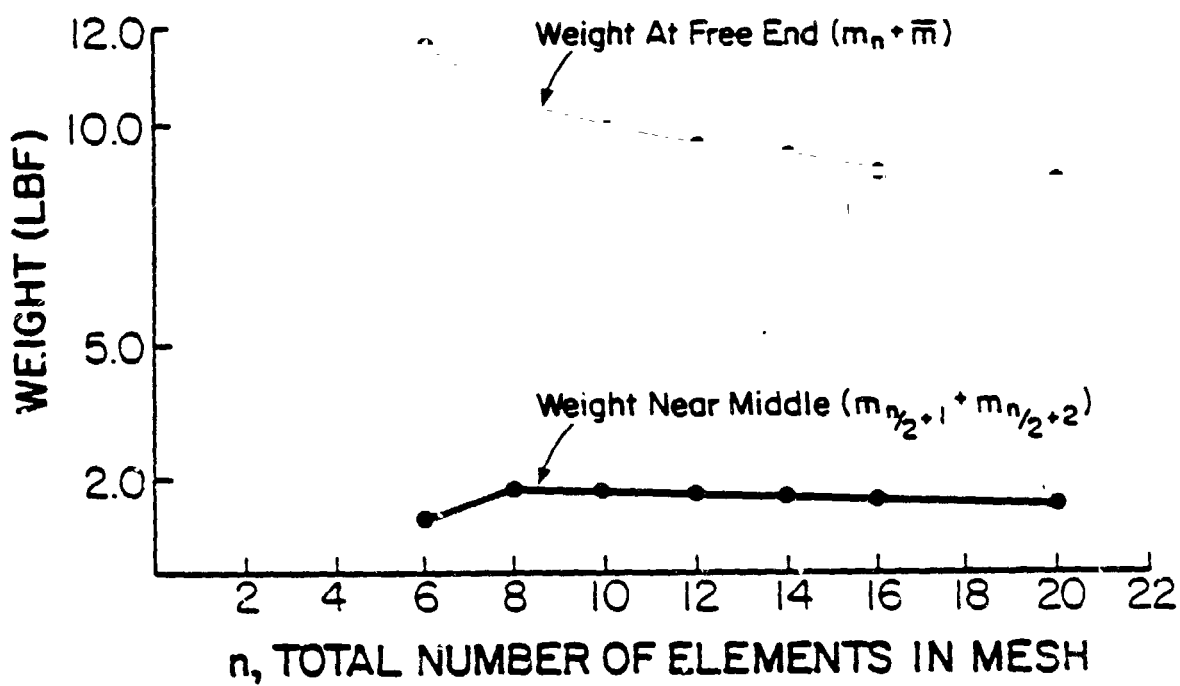
Figure 9   Weight Versus Number of Elements

Figure 10a   Optimal Distribution for Various Meshes

$n = 10$

$m_{10} = 8.7873$

$OBJ = 21.1457$
(Note: $OBJ <$
 Previous OBJ_{10})

$m_6 = 1.6810$

$I_{10} = 0.98311$

I^{LIMIT}
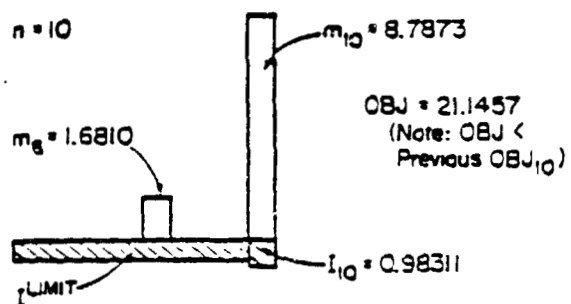
Figure 10b   Alternative Optimum

near a structural node the mass is placed there. On the other hand, when the mesh causes the point to be between nodes, the mass is accordingly divided between the two closest nodes.

As was pointed out previously in reference to Figures [7] and [8], the optimization algorithm appears to treat the structural and non-structural mass at the end of the beam as interchangable. To test this hypothesis further, the optimal design problem statement was altered slightly by decreasing the upper bound constraint on the moment of inertia from 5.2083 to 2.0. The resulting optimum design is shown in Figure [10b], and should be compared with the design (for n = 10) shown in Figure [10a]. Note that the constraint on the moment of inertia for element 10 is not active in the optimal design of Figure [10b] (the constraint was active during the CONMIN iterations leading to this optimal design). Thus, the effect of the constraint is to lead the optimization algorithm along a different path than that followed when the constraint value was 5.2083. The design found, however, has about the same total weight at the free end (= 9.9705 lbf) as the previous ten-element optimum (= 9.9222 lbf). This result confirms the hypothesis that CONMIN increases the moment of inertia at the free end only as a means of increasing the mass there. Once that option is closed (that is, the upper bound constraint is reduced to a value of 2.0), CONMIN simply increases the lumped weight at the beam tip. This finding suggests that, in future optimization studies, a tight constraint be imposed on the moment of inertia at the free end, since little structural capability is needed there, and necessary end mass can be adequately represented by the lumped weight design variables.

5. PRELIMINARY CALCULATION FOR ROTORS

5.1 WIND TURBINE BLADE

The first example in this section is the optimization of a wind turbine rotor blade at 30 rpm. Initial data is taken from Ref.[22]. A ten-element model is used. Only the flapping is considered. The area moment of inertia, I, and the lumped weight of each element are taken as the design variables (see Fig 1 for blade area cross-section). Young's Modulus, $E = 0.2 \times 10^6$ lb-in^2, and density $= 0.0334$ lb/in^3 are assumed to be constant. Blade radius, $R = 750$ inches. Table 2 shows the profile of moment of inertia and the distribution of added weight for the initial and final configurations. The final profile of the area moment of inertia along the blade is similar as the one in the previous example. The optimization procedure has removed material from the inboard sections and placed it more outboard. The lumped mass is concentrated at the tip of the blade as might be expected. We also note that most of the originally-postulated lumped mass is removed so that only the mass inherent in the stiffness elements or necessary for the autorotational constraint is maintained. (Although wind turbine have no autorotational constraint, a certain moment of inertia is still useful to smooth out wind vibration.

An important aspect of the optimization problem is the existence (or lack of it) of a feasible solution. A 'feasible solution' is defined as any set of design variables that satisfy the constraints (whether or not that particular solution is an optimum). It is possible that, if the problem is poorly formulated, no feasible solution exists. What is more often the case, however, is that there are feasible solutions but

that the optimization scheme may not be able to find them. Thus, it is advantageous to have a feasible initial guess so that one is assured that at least a local optimum is possible.

For example, Table 2 illustrates that the first guess is feasible ($w_1 >$ 2.82 no./rev). Here we found that CONMIN was able to move from this first guess through the space of feasible solutions. In other cases, however, when the first guess is not feasible we have found that CONMIN is not able to reach a solution. In such cases, one must add or remove some weight (or add or remove EI) from the first guess to move from into the feasible space; or, alternatively, we must begin with frequency-placement as the objective function and then switch to weight when the frequencies are within tolerance.

For example, Table 3 represents data for the same wind turbine as in Table 2, but the constraint on the first natural frequency has been lowered to remove it from the dangerous 3/rev range. This implies that the first guess in Table 2 is no longer feasible. In order to overcome this, a lumped mass is added to station 9 (225.4 vs 49.50). This lowers w_1 below 2.621 rev but also lowers w_2 to 8.25/rev. This could be alleviated in one of two ways: 1) move the mass to the node of the second mode, or 2) simply widen the w_2 window. We have done the latter. It is interesting that the added weight is ultimately rearranged to other places and other weight removed such that the new design is no heavier than the optimum in Table 2. Furthermore, w_2 is raised to 8.57 so that the 'widened window' had no effect on the solution.

Table 2. Optimization of Wind Turbine Blade

FIRST NATURAL FREQUENCY: FROM 1.65 TO 1.85 Hz

SECOND NATURAL FREQUENCY: FROM 2.82 Per/Rev / 4.85 Hz TO 3.17 Per/Rev / 5.05 Hz

MASS MOMENT OF INERTIA: 8.31 / $\geq 2.5 \times 10^8$ lb-in^2 TO 8.65 Per/Rev

ROTATING SPEED: 30 RPM
Young's Modulus: 0.2×10^6 lb-in^2
DENSITY: 0.86×10^{-4} slugs/in^3

Data:
a = 0   b = 2.5
n = 0   s = 0.1
o = 0   t = variable
b = 4.0

ELEMENT No.	1	2	3	4	5	6	7	8	9	10
LENGTH Inches	30	30	75	75	75	75	75	75	75	75
MOMENT OF INERTIA In^4 I	1012.5	620.0	460.0	302.5	195.0	117.5	55.00	17.50	10.25	10.50
F	440.00	437.6	390.9	409.6	383.7	309.1	239.1	27.55	10.9	10.01
AREA In^2 I	65.83	57.4	52.8	47.2	42.0	36.89	30.51	22.866	19.56	19.715
F	52.23	52.15	50.58	51.22	50.32	47.49	44.34	25.7	19.39	19.19
DISTRIBUTED MASS lbs I	65.61	57.17	131.64	117.5	104.66	61.8	75.9	56.93	48.69	49.08
F	52.02	51.94	125.93	127.5	125.3	118.24	110.41	63.99	48.29	48.29
LUMPED MASS lbs I	66.0	57.5	132.5	110.5	105.5	92.5	76.5	57.00	49.50	49.50
F	0	0	0	0	0	0	0	71.44	0	16.84

	Blade OBJ Weight (lbs)	w_1 Hz	w_2 Hz	w_1/Ω	w_2/Ω	Moment of Inertia
INITIAL(I)	1611.4	1.71	4.933	2.93	8.458	2.5×10^8
FINAL (F)	1119.7	1.65	5.046	2.82	8.65	2.5×10^8

Table 3. Wind Turbine with Added Mass

FIRST NATURAL FREQUENCY	FROM	1.4 TO 2.4	1.53 Hz 2.62 Per/Rev	ROTATING SPEED: 30 RPM
SECOND NATURAL FREQUENCY	FROM	4.8 TO 8.22	5.0 Hz 8.57 Per/Rev	YOUNG'S MODULUS 0.2×10^8 lb-in^2
				DENSITY 0.8678×10^{-4} slugs/in^3

CONSTRAINTS: $a = 0$ $b = 4.0$ $s = 0.1$
$\eta = 0$ $h = 2.5$ $t = $ variable
$\sigma = 0$

MASS MOMENT OF INERTIA $\geq 2.5 \times 10^8$ lb-in^2

ELEMENT NO		1	2	3	4	5	6	7	8	9	10
LENGTH in		30	30	75	75	75	75	75	75	75	75
MOMENT OF INERTIA in^4	I	1012.5	620.0	460.0	302.5	195.0	117.5	55.00	17.50	10.25	10.5
	F	325.6	317.9	302.3	275.7	238.8	192.0	136.6	22.45	10.0	10.0
AREA in^2	I	65.88	57.4	52.8	47.2	42.0	36.89	30.51	22.86	19.56	19.715
	F	48.15	47.84	47.20	46.05	44.33	41.86	38.34	24.40	19.39	19.39
DISTRIBUTED MASS lbs	I	65.61	57.17	131.64	117.5	104.66	91.8	75.9	56.93	48.69	49.08
	F	47.95	47.64	117.5	114.6	110.38	104.2	95.46	60.75	48.29	48.29
LUMPED MASS lbs	I	66.0	57.5	13.25	118.5	105.5	92.5	76.5	57.0	225.4	49.5
	F	0	0	0	0	0	0	0	5.77	0	228.9

(lb)	OBJ(lb)	w_1 Hz	w_1/Ω	w_2 Hz	w_2/Ω	Moment of Inertia
INITIAL	1787.1	1.48	2.55	4.81	8.25	3.21×10^8
FINAL	1037.1	1.48	2.55	5.00	8.57	2.5×10^8

5.2 HELICOPTER BLADE

The design and analysis of a representative helicopter blade is discussed. Similar to Section 3, only flapping is considered and a ten-element model is used. The initial configuration is modeled after the rotor in Reference 23. Density is constant along the blade and equal to 0.17×10^{-3} slugs/in^3. Young's Modulus is equal to 0.49×10^8 lb-in^2 at the root and is equal to 0.585×10^8 lb-in elsewhere. Blade radius is equal to 193 inches. Results are given in Table 4 and 5. In Table 4, w_1 is in the desired range but w_2 is too small. Furthermore, the autorotational inertia is larger than necessary. In this case, the CONMIN program is able to remove mass and stiffness in such a way to raise w_2 and lower w_1. The minimum bending inertia set as a constraint (0.4) is reached at every point except the root. The root remained high to keep $w_1 > 1.05$. The new blade is one-third the original mass. In Table 5, a stiffer initial design is used and the frequency w_1 is forced to be very high. In this case, the program CONMIN would 'like' to decrease EI and m, but any removal of material could lower w_1 beyond its lower bound of 1.24/rev. To counter this, the optimization scheme adds EI near the root (to maintain $w_1 > 1.24$/rev). Furthermore, the lumped mass necessary to maintain autorotational constraint is moved slightly inboard to have less effect on w_1 (keep it high) but more effect on w_2 (keep it low). This example illustrates the physical soundness of this optimization scheme. It does the same things that a designer would do (given appropriate constraints) but in a more systematic manner. Thus, with proper constraints, optimization can prove a valuable tool for frequency placement.

Table 4. Helicopter Blade

CONSTRAINTS			
FIRST NATURAL FREQUENCY	: FROM	7.5 TO	9.5 Hz
		1.05	1.34 Per/Rev
SECOND NATURAL FREQUENCY	: FROM	18.5	20.5 Hz
		2.61	2.89 Per/Rev
MASS MOMENT OF INERTIA		$\geq$ 8.7 x 10^5 lb-in^2	

ROTATING SPEED: 425 RPM

YOUNG'S MODULUS: Element 1: 4.9 x 10^7 lb-in

Rest: 5.85 x 10^7

Density : 0.17 x 10^{-3} slugs/in^3

a = 0 b = 3.75 s = .1
q = 0 h = 2.5   t = variable
σ = 0

ELEMENT NO		1	2	3	4	5	6	7	8	9	10
LENGTH in		5	10	20	15	15	25	30	35	30	13
MOMENT OF INERTIA in^4	I	14.28	3.42	10.25	18.8	10.25	0.512	0.406	0.406	0.406	0.406
	F	0.87	0.4	0.4	0.4	0.4	0.4	0.4	0.4	0.4	0.4
AREA in^2	I	20.6	3.327	18.7	22.19	18.7	0.664	0.59	0.59	0.59	0.59
	F	0.91	0.59	0.59	0.59	0.59	0.59	0.59	0.59	0.59	0.59
DISTRIBUTED MASS lbs	I	7.21	2.32	26.17	23.29	19.63	1.16	1.24	1.04	1.24	0.54
	F	0.318	0.413	0.826	0.619	0.619	1.03	1.24	1.03	1.24	0.54
LUMPED MASS lbs	I	0	3.04	1.67	0	0	7.46	10.75	5.21	6.55	6.6
	F	0	0	0	0	0	0	17.17	0	0	16.08

	OBJ(lb)	w_1 Hz	w_1/Ω	w_2 Hz	w_2/Ω	Moment of Inertia
INITIAL	131.54	8.3	1.17	17.66	2.49	9.76 x 10^5
FINAL	41.137	7.47	1.05	20.48	2.89	8.71 x 10^5

Table 5. Helicopter Blade with Stiff Flapping

CONSTRAINTS	FIRST NATURAL FREQUENCY	: FROM 8.8 TO 10.8 Hz	1.24 TO 1.52 Per/Rev
	SECOND NATURAL FREQUENCY	: FROM 17.7 TO 19.7 Hz	2.49 TO 2.78 Per/Rev
	MASS MOMENT OF INERTIA	$\geq 8.7 \times 10^5$ lb-in^2	

ROTATING SPEED: 425 RPM

YOUNG'S MODULUS: Elemnt 1: 4.9×10^7 Rest: 5.85×10^7

DENSITY: 0.17×10^{-3} slugs/in^3

$a = 0$ $b = 3.75$ $s = .1$
$n = 0$ $h = 2.5$ t = variable

ELEMENT NO		1	2	3	4	5	6	7	8	9	10
LENGTH in		5	10	20	15	15	25	30	35	30	13
MOMENT OF INERTIA in^4	I	14.28	13.42	20.0	25.8	5.28	0.512	0.406	0.406	0.406	0.406
	F	35.73	22.14	9.198	3.176	1.747	0.494	0.4	0.4	0.4	0.4
AREA in^2	I	20.6	20.26	22.55	24.05	13.19	0.664	0.594	0.594	0.594	0.594
	F	26.08	2?	17.32	3.00	1.576	0.652	0.59	0.59	0.59	0.59
DISTRIBUTED MASS lbs	I	7.16	14.08	31.34	25.07	13.74	1.153	1.238	1.44	1.23	0.536
	F	9.06	16.08	24.06	3.13	1.64	1.132	1.23	1.435	1.23	0.5،
LUMPED MASS lbs	I	0	3.04	1.67	0	6.4	7.46	10.78	4.0	4.55	6.6
	F	0	0	0	0	0	0	28.1	10.15	7.04	0

	OBJ	w_1 Hz	w_1/Ω	w_2	w_2/Ω	Mass Moment of Inertia
INITIAL	141.76	8.883	1.25	10.55	2.76	8.88×10^5
FINAL	104.86	8.77	1.24	19.7	2.78	8.71×10^5

We have also examined the designs in Tables 3-5 with respect to axial stress due to centrifugal loads. In each case, the maximum stresses after optimization are equal to or only slightly higher than the original stresses.

6. TEETERING ROTORS

6.1 Definition

In this section we attempt our first optimization of a realistic cross-section (see Figure 11), one which is little different from our first design pattern, (Figure 1). Therefore, it is sufficiently general that both the bending and torsional stiffnesses of some currently existing blades can be matched. Using this generic cross-section and starting from an actural rotor blade design. (Ref.[24]), we have studied the possibility of moving natural frequencies away from resonances while simultaneously satisfying constraints on the following: stress, the size of lumped weights to be added, capability for autorotation, and thickness of the main structural member (the box beam). Because a teetering blade was considered, cyclic and collective modes of vibration were calculated independently by a change in the boundary condition at the blade root. In the initial phase of the study, we considered collective flapping modes first, then cyclic flapping, and finally combined collective and cyclic flapping. The results of these studies were favorable (i.e. we were able to change the frequencies in the desired manner and still satisfy the constraints). Building on these results, in the second phase of this section, we consider a more challenging problem which involves combined modes of collective flapping, cyclic flapping, collective inplane, cyclic inplane and torsional vibrations.

In this section, the primary design variables are: 1) the wall thickness of the box beam and 2) lumped weights, that can be added at specified stations along the beam. In the final problem studied, the

GENERIC BLADE SECTION CONSTRAINTS
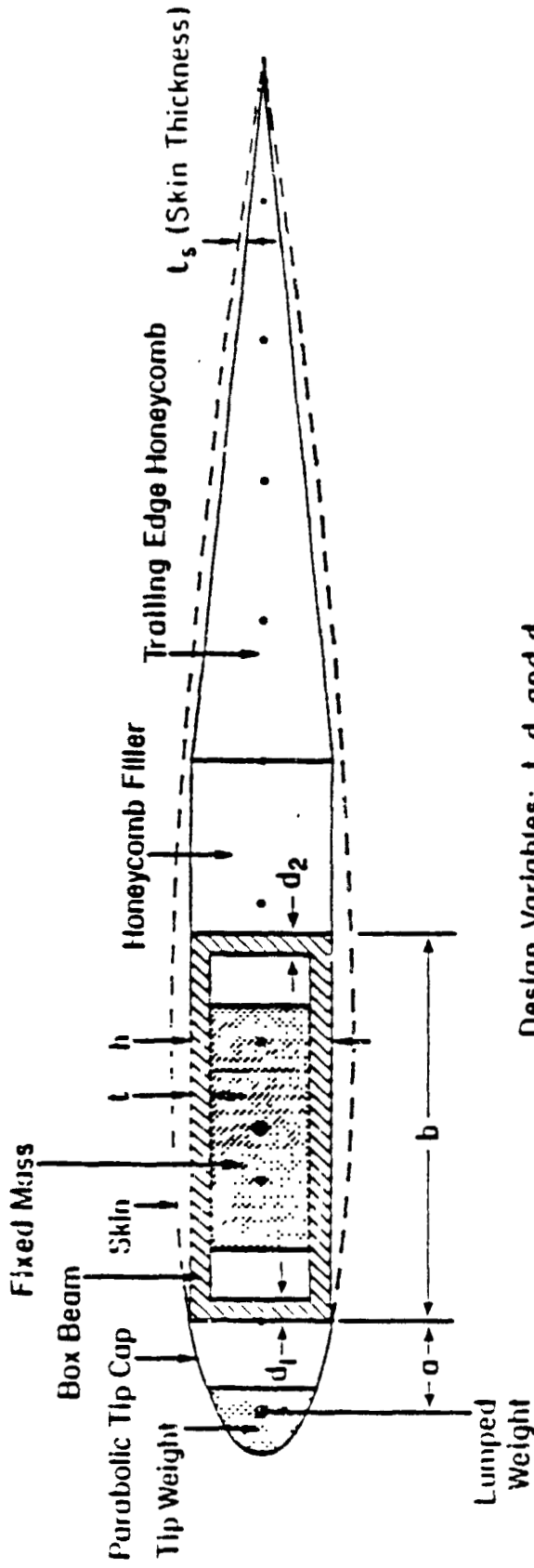
Design Variables: t, d_1 and d_2.

Fixed Parameters: $h = 2.0$ in
$b = 4.65$ in
$t_s = 0.016$ in

Area Of Honeycomb $= 25.2$ in^2

Circumference Of Trailing Edge $= 30.5$ in

Dimension a was taken to be zero for the
computation of mass moment of inertia

Figure 11   Blade cross-section with variable box dimension

wall thicknesses are taken as fixed, and only the lumped weights are allowed to vary. This situation corresponds to that encountered in practice when a blade has actually been designed and manufactured, but then found to have poorly placed frequencies — thus lumped weights are added at various positions along the beam to change the frequencies. We found that our optimization routine was able to handle this problem adequately, although the total weight of the beam could not be used as the objective function, as had been done previously. Instead, a 'frequency placement' objective function was used.

6.2 Flapping Frequencies

The first set of optimization problems in the section is concerned with flapping response only. The starting design for the optimization procedure in each of the three cases studied is a typical metal-bladed teetering rotor with a diameter of approximately 24 feet. Ten finite elements are used to model the rotor; their lengths are given in Table 6. The objective of the optimization is to minimize the total weight of the blade. The design variables are the wall thickness, t_i, of the finite element representation of the box beam (the structural member in the rotor - see Fig. 1) and the lumped weight w_i, associated with each finite element. The lumped weight is the sum of two components, a fixed component (representing the weight of the leading and trailing edge strips, honeycomb, skin and nose weight,) and a variable component (representing additional non-structural mass which may be added at various positions along the length of the rotor) to modify the dynamic behavior in a desired manner. The side conditions on the element thick-nesses are, in units of inches,

$$0.00044 < t_i < 0.730$$

The side conditions on the lumped weights consist of a lower bound only, which represents the **fixed** component of weight for each element and is given in Table 6 under the heading 'w_{min}'. Note that the element thicknesses t_i are not given in Table 6; instead, the area moment of inertia, I, is represented. Using the dimensions given in Fig. 12, we can show that I related to the thickness by the equation

$$I = 2.593t^3 - 7.780t^2 + 7.780t + 0.506^-$$

The moment of inertia is given, rather than the thickness, to facilitate comparison with I_o, the portion of the moment of inertia which is contributed by those parts of the cross-section other than the box beam. (Thus I_o remains fixed as t_i is varied.) Table 6 also contains the values of the box weight, which are calculated by multiplying the weight density of the box beam material by the cross-sectional area of the box. Thus, the box weight is not an independent design variable, but depends on the thickness t_i. The box weight is included in the table to facilitate comparison with the distribution of lumped weight. The constraints for the optimization are both the autorotation constraint,

$$\text{sum } (w_i')r_i^2 \implies 0.5567 \times 10^7 \text{ lb-in}^2$$

(where w_i' is the total weight of element i, and r_i is the distance from the root to the center of the i-th finite element). The frequency constraints will be described in subsequent sections of this thesis.Some
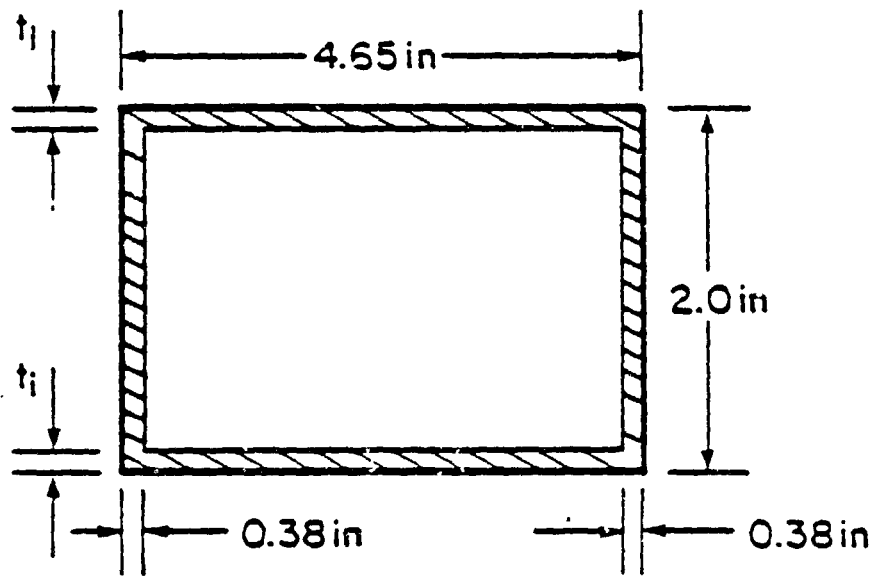
Figure 12   Dimensions and Definition of Design Variable for
             Box Beam Cross-Section

additional data which complete the problem description are the values of the elastic modulus, 0.105×10^8 lb/in^2, the radius, 288.8 in, the rotational speed, 324 rpm, and the mass density of the box beam material, 0.000262 slugs/in^3.

6.2.1 Collective Modes

The initial problem to be considered is the optimization of the blade with respect to collective flapping modes only. Because we are studying a teetering rotor, the collective mode of flapping may be analyzed by imposing a fixed boundary condition at the root of the rotor. The imposed frequency constraints are

$$1.15 < p1 < 1.50 \tag{16a}$$

$$3.40 < p2 < 3.60 \tag{16b}$$

$$6.40 < p3 < 6.60, \tag{16c}$$

in which p1, p2 and p3 are the first three collective flapping mode frequencies non-dimensionalized by dividing by the rotor speed.

The starting design for the optimization algorithm is given in Table 6 under the heading 'initial'. This initial design was chosen to correspond closely with an actual rotor blade; thus, it is not surprising to find that the design is infeasible with respect to the frequency constraints we have imposed. The optimization algorithm used in this study, CONMIN, supposedly permits an infeasible starting point and attempts to proceed from this starting point to a feasible point. However, for our design problems, this feature of CONMIN failed to produce a feasible design after many iterations. As an alternative approach, we

formulated a preliminary optimization problem in which the previous objective function (weight) was replaced by a 'frequency-placement' objective:

$$obj^{fp} = (3.50 - p2)^2 + (6.50 - p3)^2 \qquad (17)$$

The numbers 3.50 and 6.50 are the average of the bounds of the frequency constraint inequalities which are violated by the initial design. The remainder of the optimization problem is the same as the original problem, except that the constraints on those frequencies which appear in the frequency placement objective are omitted. CONMIN was applied to this preliminary problem. In the process of minimizing the preliminary objective, CONMIN was able to drive the frequencies sufficiently close to their bounds that a feasible design (with respect to the original problem) was obtained. At this point, the original objective function was reinstated and CONMIN applied once again.

Table 6 gives the optimized design obtained by this two-stage optimization procedure, with the corresponding frequencies and the total weight. From the point of view of helicopter vibrations, the initial design of this blade is acceptable, since (except for the third mode) the number/rev is far away from even integer values. The third mode is, however, near 6.0/rev. The frequency of the second mode does not satisfy the inequality constraints, but is not near an even integer multiple. Note that the final design moves the third frequency to 6.53, while keeping the other frequencies within the constraints. At the same time, the weight of the blade drops from 344.5 lb to 265.6 lb.

Table 6 Initial and Final design for collective flapping modes (teetering rotor)

Rotating Speed : 324 RPM
Young's Modulus : 0.105 x 10^8 lb/in^2
Axial Stress < 20,000 psi

mass of moment
inertia > 0.5429x10^7 lb-in^2
density of box beam : 0.000261 mugs/in^3

Element No.	1	2	3	4	5	6	7	8	9	10
Length (in)	14.4	14.4	14.4	43.2	28.80	28.80	28.8	28.80	43.2	43.2
Area Moment of Inertia (in^4) Io(unchanged)	48.6	93.38	64.8	5.76	1.76	1.47	1.03	1.03	1.03	1.03
Box Beam Init. I(θ)	1.86	1.86	1.86·	1.86	1.86	1.86	1.86	1.86	1.86	1.86
Final	0.51	0.51	0.51	0.63	0.51	0.51	0.51	0.56	1.72	1.91
Min. lumped weight (lb)	42.72	86.02	3.06	9.19	6.13	6.13	6.13	6.13	9.19	9.19
lumped weight (θ) Init.	42.72	86.02	41.38	20.46	9.23	6.46	6.13	6.40	14.3	20.46
Final	42.72	86.02	3.06	9.19	6.13	6.13	6.13	6.13	9.59	32.54
Box Beam Weight (lb) Init.	1.98	4.68	4.68	14.05	9.36	9.36	9.36	9.36	9.36	9.36
Final	0.94	2.22	2.22	7.19	4.43	4.43	4.43	4.60	13.08	14.46

Note : (θ) -- design variable

Natural Frequencies (No./rev)

Collective Flapping (fixed boundary)
1.15 < p1 < 1.5
3.4 < p2 < 3.6
6.4 < p3 < 6.6

Cyclic Flapping (pinned boundary)

	Blade Weight (lb)	p1	p2	p3
Initial	344.5	1.19	3.26	6.00
Final	265.6	1.17	3.59	6.51

Area moment of inertia : $I = 2.593t^3 - 7.780t^2 + 7.780t + 0.5067$
where t is the top thickness of box beam
$0.07044 < t < 0.7320$

6.2.2 Cyclic Modes

The next problem to be studied is the optimization of the blade with respect to cyclic modes of flapping. The non-dimensionalized frequency constraints are now

$$0.90 < p1 < 1.05$$
$$2.40 < p2 < 2.60$$
$$4.40 < p3 < 4.60,$$

in which p1, p2 and p3 are the first three cyclic non-dimensionalized flapping-mode frequencies. For cyclic flapping modes, the boundary condition at the root corresponds to a pinned support. The frequency-placement objective was again chosen by noting which frequency constraints were violated by the initial design. Noting the initial frequency values given in Table 7, we define

$$obj^{fp} = (2.50 - p2)^2 + (4.50 - p3)^2$$

Table 7 gives the optimal design found by the two-stage optimization procedure with the corresponding frequencies. The final weight of the blade is shown to drop from 344.5 lb to 295.2 lb.

6.2.3 Combined Collective and Cyclic Modes

Next we consider the optimization of the beam with respect to combined collective and cyclic modes. Thus, in each iteration an analysis must be performed to find the frequencies corresponding to a fixed boundary condition; and then another analysis must be performed to find

Table 7 Initial and Final design for cyclic flapping modes (teetering rotor)

Rotating Speed : 324 RPM 8
Young's Modulus : 0.105 x 10⁶ lb/in² → 0.105×10^6 lb/in²
Axial Stress ≤ 20,000 psi

Mass of moment inertia $\geq 0.5429 \times 10^?$ lb-in²
density of box beam : 0.000263 sugs/in³

Element No.	1	2	3	4	5	6	7	8	9	10
Length (in)	14.4	14.4	14.4	43.2	28.80	28.86	28.8	28.80	43.2	41.2
Area Moment of Inertia (in⁴) Io(unchanged)	48.6	93.38	64.8	5.76	1.76	1.47	1.03	1.03	1.03	1.03
Box Beam I(#) Init.	1.86	1.86	1.86	1.86	1.86	1.86	1.86	1.86	1.86	1.86
Box Beam I(#) Final	0.55	0.51	0.51	2.04	0.51	0.51	0.51	1.75	0.51	0.51
Min. lumped weight (lb)	42.72	86.02	3.06	9.19	6.13	6.13	6.13	6.13	9.19	9.19
lumped weight (#) Init.	42.72	86.02	41.38	20.46	9.23	6.46	6.13	6.40	14.3	20.46
lumped weight (#) Final	42.72	86.02	3.06	5.19	25.88	10.41	6.13	11.54	12.8	34.8
Box Beam Weight (lb) Init.	1.98	4.68	4.68	14.05	9.36	9.36	9.36	9.36	9.36	9.36
Box Beam Weight (lb) Final	0.96	2.22	2.22	6.65	10.28	4.43	4.43	8.11	6.56	6.56

Note : (#) -- design variable

Natural Frequencies (No./rev)

Collective Flapping (fixed boundary)
—
—
—

Cyclic Flapping (pinned boundary)
$0.9 < p_1 < 1.05$
$2.4 < p_2 < 2.60$
$4.4 < p_3 < 4.60$

	p_1	p_2	p_3
Initial	1.02	2.64	4.67
Final	1.02	2.58	4.50

Blade Weight (lb)	
Initial	344.5
Final	295.2

Area moment of Inertia : $I = 2.593t^3 - 7.780t^2 + 7.780t + 0.5067$
where t is the top thickness of box beam
$0.0044 < t < 0.7320$

the frequencies for a pinned boundary condition. All other aspects of
the design problem remain the same as before. The constraints on the
collective flapping modes are

$$1.15 < p1 < 1.60 \tag{17a}$$

$$3.40 < p2 < 3.60 \tag{17b}$$

$$6.30 < p3 < 6.60 \tag{17c}$$

The constraints on the cyclic modes are

$$0.90 < p1 < 1.10 \tag{18a}$$

$$2.40 < p2 < 2.60 \tag{18b}$$

$$4.40 < p3 < 4.60 \tag{18c}$$

For this problem, weighting factors are introduced into the frequency-
placement objective,

$$obj^{fp} = [2(3.50 - p2)^2 + (6.45 - p3)^2]_{collective} +$$

$$[2(2.50 - p2)^2 + (4.50 - p3)^2]_{cyclic} \tag{19}$$

The results of the optimization are given in Tables 8. The cyclic
modes of the initial design are well-placed in the sense that they are
not near odd integers/rev, but the third collective mode is near 6.0/rev
(the same as in the first example). Note that the final design moves the

Table 8 Initial and Final design for collective and cyclic flapping modes

Rotating Speed : 324 RPM
Young's Modulus : 0.105 x 10^8 lb/in^2
Axial Stress ≤ 20,000 psi

mass of moment Inertia ≥ 0.5429×10^7 lb-in^2
density of box beam : 0.000263 mugs/in^3

Element No.	1	2	3	4	5	6	7	8	9	10
Length (in)	14.4	14.4	14.4	43.2	28.80	28.80	28.8	28.80	43.2	43.2
Area Moment of Inertia (in^4) Io(unchanged)	48.6	93.38	64.8	5.76	1.76	1.47	1.03	1.03	1.03	1.03
Box Beam I (I) Init.	1.86	1.86	1.86	1.86	1.86	1.86	1.86	1.86	1.86	1.86
Final	1.36	0.51	2.17	3.05	0.51	0.51	0.51	2.89	0.786	3.05
Min. lumped weight (lb)	42.72	86.02	3.06	9.19	6.13	6.13	6.13	6.13	9.19	9.19
lumped weight (I) Init.	42.72	86.02	41.38	20.46	9.23	6.46	6.13	6.40	14.3	20.46
Final	42.72	86.02	23.95	31.75	6.13	6.13	6.13	6.13	9.46	9.19
Box Beam Weight (lb) Init.	1.98	4.68	4.68	14.05	9.36	9.36	9.36	9.36	9.36	9.36
Final	1.53	2.21	5.51	31.51	4.43	4.43	4.43	17.34	7.90	31.51

Note: (I) -- design variable

Natural Frequencies (No./rev)

Collective Flapping (fixed boundary)			
$1.15 < p1 < 1.60$			
$3.40 < p2 < 3.60$			
$6.40 < p3 < 6.60$			
	p1	p2	p3
	1.19	3.26	6.06
	1.20	3.40	6.33

Cyclic Flapping (pinned boundary)			
$0.9 < p1 < 1.16$			
$2.4 < p2 < 2.60$			
$4.4 < p3 < 4.60$			
	p1	p2	p3
	1.02	2.64	4.67
	.02	2.64	4.58

Blade Weight (lb)	
Initial	344.5
Final	338.5

Area moment of inertia : $I = 2.593t^3 - 7.780t^2 + 7.780t + 0.5067$
where t is the top thickness of box beam
$0.00044 < t < 0.7320$

third collective frequency to 6.33 while keeping the other frequencies in the 'safe' range. However, the weight of the blade only decreased from 344.5 to 333.5 lb, in contrast to the previous example in which the weight decreased to 265.6. The difference is caused by the larger number of frequency constraints in this example compared to the previous example.

6.3 SIMULTANEOUS FLAPPING INPLANE AND TORSION

The next problem to be studied is that of optimizing a teetering rotor blade subject to the following simultaneous constraints on frequencies (non-dimensionalized by dividing by the rotor rotational speed):

1 collective flapping modes,

$$0.5 < p1 < 1.5$$
$$2.3 < p2 < 3.7$$
$$4.3 < p3 < 5.7$$

2. cyclic flapping modes,

$$0.5 < p1 < 1.5$$
$$1.3 < p2 < 2.7$$
$$3.3 < p3 < 4.7$$

3. collective inplane modes,

$$0.0 < p1 < 1.0$$
$$4.3 < p2 < 5.7$$
$$14.3 < p3 < 15.7$$

4. cyclic inplane modes and

$$0.1 \; < \; p1 \; < \; 1.5 \qquad\qquad (23a)$$

$$5.3 \; < \; p2 \; < \; 6.7 \qquad\qquad (23b)$$

$$17.3 \; < \; p3 \; < \; 18.7 \qquad\qquad (23c)$$

5. torsional mode

$$3.3 \; < \; p1 \; < \; 3.7 \qquad\qquad (24)$$

(The first lower bound for cyclic inplane modes, 0.10, was later repalced by 1.0 in the problem formulations of the following sections). Because we are considering a teetering blade, the collective-flapping and cyclic-inplane modes can be modeled by clamped boundary conditions at the root, while the cyclic-flapping and collective-inplane modes can be modeled by pinned boundary conditions.

The elastic modulus, blade length, speed of rotation, and density of the box-beam material are unchanged from the values used before. In addition to frequency and autorotation constraints, the axial stress is constrained to be less than 20,000 psi. The value of the bound in the autorotational constraint has been changed slightly to 0.5429×10^7 ib-in^2.

In the problem described in section 3., the thicknesses, t_i, d_{1i} and d_{2i}, of both the vertical and horizontal walls of the box beam (see Fig. 2) are allowed to vary - that is, are also design variables, with the following side constraints (in units of inches);

Table 9   Data for Teetering Rotor Blade

Rotating Speed : 324 RPM
Youngs Modulus : 0.105 x 10^8 lb/in^2
Axial Stress ≤ 20,000 psi

mass of moment
inertia ≥ 0.5429x10^7 lb-in^2
density of box beam : 0.000263 mug2/in^3

Element	No.	1	2	3	4	5	6	7	8	9	10
Length	(in)	14.4	14.4	14.4	43.2	28.80	28.80	28.8	28.80	43.2	43.7
Box Beam Dimension	t (in)	0.600	0.600	0.600	0.435	0.318	0.282	0.266	0.266	0.256	0.266
	d1 (in)	0.550	0.550	0.440	0.452	0.464	0.464	0.464	0.464	0.464	0.464
	d2 (in)	0.224	0.224	0.224	0.224	0.175	0.125	0.125	0.125	0.125	0.125
Area and mass moment of inertia of y-axis	Ibx (in4)	2.93	2.94	2.92	2.62	2.24	2.09	2.03	2.03	2.03	2.03
	Iox (in4)	47.54	92.30	64.05	5.38	1.53	1.30	0.85	0.85	0.85	0.85
	Mbx (mug-in)x10^-3	0.760	0.770	0.765	0.685	0.586	0.547	0.532	0.532	0.532	0.532
	Mox (mug-in)x10^-2	0.273	0.273	0.270	0.200	0.080	0.040	0.022	0.022	0.022	0.022
Area and mass moment of inertia of x-axis	Iby (in4)	12.79	12.80	12.50	10.54	8.98	8.57	8.40	8.40	8.40	8.40
	Ioy (in4)	48.11	160.50	312.90	294.22	210.66	167.62	132.50	102.70	84.90	81.88
	Mbx (mug-in)x10^-2	0.335	0.335	0.327	0.276	0.236	0.225	0.225	0.225	0.225	0.225
	Moy (mug-in)x10^-2	0.015	0.015	4.378	8.146	5.690	4.490	3.576	3.280	3.190	2.930
Min. lumped weight (lb)		96.54	55.77	2.69	8.07	5.38	5.38	5.38	5.38	8.07	8.07
w -- lumped weight (lb)		96.54	55.77	6.95	11.63	7.68	5.76	5.38	6.12	11.81	19.98
CJ (lb-in^2 x10^6)		55.0	55.0	53.5	43.0	34.0	32.0	31.0	31.0	31.0	31.0
Rotary inertia (mug-in^2) (w/g,*(b/2)^2)		0.000	0.000	0.097	0.163	0.107	0.081	0.075	0.086	0.165	0.279

$$0.01 < t_i < 1.0$$

$$0.01 < d_{1i} < 2.32$$

$$0.01 < d_{2i} < 2.32, \quad i = 1,2,\ldots,10.$$

(25a,b,c)

The initial values of these variables are given in Table 9. In the problems discussed in section 3.2 and 3.3, the box beam dimensions t_i, d_{1i} and d_{2i} are fixed at these initial values.

Tables 9 also gives data defining both fixed and initial stiffness and inertia values of the blade. In the tables, $'I_{ox}'$ and $'I_{oy}'$ represent the portions of the flapping and inplane area moments of inertia of the blade section which are independent of the design variables. $'I_{Bx}'$ and $'I_{By}'$ are the area moments of inertia of the box beam – thus functions of the (initial) values of the design variables, w_i, d_{1i}, d_{2i}, and t_i. M_{ox} and M_{By} are the rotary inertias of the box beam with respect to flapping and inplane and are calculated simply by multiplying the mass density of the box-beam material by the area moment of inertias. M_{ox} and M_{oy} are the contributions to the rotary inertia of the section which are independent of the design variables. Note that since these contributions come from items with different densities, a single uniform value of density cannot be defined for the M_o terms.

Other initial inertia and stiffness properties are also defined in Table 9. As before, the lumped weights associated with the finite elements are taken as design variables; but, to permit greater latitude in placing torsional frequencies and to match more closely the behavior of a true helicopter blade, a torsional spring is introduced at the blade root; and it stiffness is taken as a design variable. The side

constraints on the lumped weights are given in Table 9 under the heading w_{min}; the side constraint on the torsional stiffness consists of the requirement that the stiffness be non-negative.

Since a torsional mode is involved, special treatment is given to GJ, the torsional rigidity, which is a function of all variables including t, d_1, d_2, the area of the trailing edge, and the lumped mass. The procedure for calculating GJ is described in Appendix A.

Table 9 also contains the contribution of the lumped weight to the rotary inertia, which equals the lumped mass (w_i/g) times $(b/2)^2$. This expression has been chosen to match the behavior of the true blade. It is assumed that the lumped weights cf the first two elements contribute nothing to the rotary inertia.

6.3.1 Variable Box Dimension

As was done with the optimization involving flapping only, a two-step optimization procedure is used, which involves a frequency-placement objective followed by a weight objective. The frequency-placement objective has the general form

$$obj^{fp} = sum \ [wf_i \ (p_{*i} - p_i)^2] \tag{26}$$

in which the sum is taken over those frequencies which are to be changed from their initial values to the desired values p_{*i}. Values of p_{*i} and the weighting factors wf_i are given in Table 10 with the results of the optimization. Examination of the values of lumped weight given in Table 10 shows that weight is concentrated at the tip of the blade because of the autorotational constraint. The stress at the first element is close to the stress constraint value of 20,000 psi. The total weight changes

Table 10 Initial and final design for flapping, inplane, torsional modes of Teetering rotor blade with variable box beam dimension

Element	No.		1	2	3	4	5	6	7	8	9	10
Box Beam t (I) 0.01 < t < 1.0		I	0.600	0.600	0.600	0.435	0.318	0.282	0.266	0.266	0.266	0.266
		F	0.375	0.441	0.471	0.343	0.384	0.335	0.306	0.290	0.153	0.183
Box Beam d1 (I) 0.01 < d1 < 2.32		I	0.550	0.550	0.440	0.452	0.464	0.464	0.464	0.464	0.464	0.464
		F	0.506	0.529	0.429	0.438	0.498	0.516	0.501	0.471	0.416	0.441
Box Beam d2 (I) 0.01 < d2 < 2.32		I	0.224	0.224	0.224	0.224	0.175	0.125	0.125	0.125	0.125	0.125
		F	0.219	0.218	0.219	0.168	0.125	0.127	0.126	0.124	0.120	0.123
lumped weight (I) (lb)	Min.		96.54	55.77	2.69	8.07	5.38	5.38	5.38	5.38	8.07	8.07
		I	96.54	55.77	6.95	11.63	7.68	5.76	5.38	6.12	11.81	19.98
		F	96.54	55.77	5.58	10.61	9.59	7.15	6.40	6.89	8.93	26.87
Stress x 10⁴ (psi)		I	1.40	1.34	1.30	1.61	1.87	1.85	1.73	1.49	1.11	0.44
		F	2.00	1.70	1.60	1.96	1.66	1.63	1.54	1.36	1.60	0.62

$Stress \times 10^4$

Natural Frequencies (No/rev)

<<<<<<< >>>>>>>

	Collective flapping (fix ')			Cyclic inplane (fixed)			Cyclic flapping (hinged)			Collective inplane (hinged)			Torsion
Constraint	$0.5 < p_1 < 1.5$	$2.3 < p_2 < 3.7$	$4.3 < p_3 < 5.7$	$0.1 < p_1 < 1.5$	$5.3 < p_2 < 6.7$	$17.3 < p_3 < 18.7$	$0.5 < p_1 < 1.5$	$1.3 < p_2 < 2.7$	$3.3 < p_3 < 4.7$	$0.0 < p_1 < 1.0$	$4.3 < p_2 < 5.7$	$14.3 < p_3 < 15.7$	$3.3 < p_1 < 3.7$
	p_1	p_2	p_3	p_1	p_2	p_3	p_1	p_2	p_3	p_1	p_2	p_3	p_1
I	1.18	3.22	5.89	1.22	7.05	18.50	1.00	2.58	4.65	0.00	5.71	15.63	3.87
F	1.18	3.09	5.67	1.19	6.70	18.40	1.00	2.51	4.63	0.00	5.50	15.69	3.40

	Total mass Weight (lb)	Root-Spring Stiffness(I) (in-lb/rad.)
I	345.0	6.5×10^5
F	339.0	4.10×10^5

	Collective flapping			Cyclic inplane			Cyclic flapping			Collective inplane			Torsion
Weighting Factor	*	*	2.60	*	*	3.30	*	*	*	*	*	*	4.10
Desired Frequency	*	*	5.00	*	*	6.00	*	*	*	*	*	*	3.50

Note : (I) -- Design Variable   (*) -- Zero

insignificantly, from 345 to 339 lb. However, the root spring shows a significant effect on the torsional mode. The spring constant changes from 6.5×10^5 to 4.10×10^5 in-lb/radian.

The placement of the frequencies is shown in Table 9,also. Note that the third collective mode of flapping, which was near 6.0/rev, moves to 5.67/rev; and the second cyclic mode of inplane, which was near 7/rev, moves to 6.7/rev. Finally, the torsion mode, which was 3.87/rev, moves to 3.4/rev.

6.3.2 Fixed Box Dimensions

We next consider the problem of modifying a blade which has already been constructed, but which has been subsequently found to have inappropriate natural frequencies. Since the blade is already built, the only way its dynamic behavior can be modified is through the addition of lumped mass and also through changing the root spring. Thus, in contrast to the problem of section 3.1, here the box-beam weight, the flapping and inplane-bending inertia, and the torsional rigidity are constant. All starting values and fixed parameters are the same for this problem as in the previous section. Finding a starting design which satisfies all of the frequency constraints is a difficult task for this problem, and thus the frequency-placement objective is the only objective function used; the second phase (with weight as the objective function) is never reached. Values of the weighting factors and frequency bounds which appear in the objective function are given in Table 11.

The final values of the lumped weights and axial stresses are shown in same Table 11, with frequencies, root-spring stiffness, and total weight. The most significant frequencies are the third collective flapping mode and the second cyclic inplane mode, which are seen to move far

away from the undesirable integer/rev values. However, the first cyclic inplane frequency is near 1/rev.

6.3.3 Variable Root Bending Stiffness

The problem formulated in the previous section presented computational difficulties in that it was found difficult to find a design which satisfied all the frequency constraints simultaneously when only lumped mass and the root spring were used as the design variables. This difficulty may be caused by the dominating influence of the root bending inertias. Thus, it seems reasonable to include the values of $'I_{oy}'$ at the root as one of the design variables. The frequency-placement objective is used throughout the optimization (the weight is not used as the objective), and all starting data and fixed parameters are given the same values as in Section 3.2. Values of the weighting factors and frequency bounds which appear in the objective function are given in Table 12 with the results of the optimization.

The results of Tables 12 differ from those of Tables 10 and 11. The lumped weight changes at the first, fourth, and fifth elements. The stiffness of the root spring moves from 6.5×10^5 to 4.32×10^5 in-lb/radian. However, the most significant effect is the change of I_{oy} (the bending moment of inertia at the root from 48.11 to 290.29 in^4. Table 12 shows that all frequencies are placed in the safe range.

6.4 Effect of Pretwist

In this section, we will do the optimization of a beam which is pretwisted. (Pretwisted blade implies that the mot' .is of flapping and inplane are coupled). The procedure of analysis will be the same as in section 6.3. Data are identical to those of section 6.3 save that the

Table 11 Initial and final design for flapping, inplane and torsional modes
of Teetering rotor blade with box beam dimension fixed

Element	No.		1	2	3	4	5	6	7	8	9	10
Box Beam t		I	--	--	--	--	--	--	--	--	--	--
$0.01 < t < 1.0$		F	--	--	--	--	--	--	--	--	--	--
Box Beam d1		I	--	--	--	--	--	--	--	--	--	--
$0.01 < d1 < 2.32$		F	--	--	--	--	--	--	--	--	--	--
Box Beam d2		I	--	--	--	--	--	--	--	--	--	--
$0.01 < d2 < 2.32$		F	--	--	--	--	--	--	--	--	--	--
lumped weight (ℓ) (lb)	Min.		96.54	55.77	2.69	8.07	5.38	5.38	5.38	5.38	8.07	8.07
		I	96.54	55.77	6.95	11.63	7.68	5.76	5.38	6.12	11.81	19.98
		F	96.54	55.77	6.95	14.72	14.52	11.52	8.77	6.78	11.86	26.69
Stress x 10^4 (psi)		I	1.40	1.34	1.30	1.61	1.87	1.85	1.73	1.49	1.11	0.44
		F	2.00	1.70	1.60	1.96	1.65	1.63	1.53	1.36	1.60	0.63

Natural Frequencies (No/rev)

	Collective flapping (fixed)			Cyclic inplane (fixed)			Cyclic flapping (hinged)			Collective inplane (hinged)			Torsion
	$0.5 < p1 < 1.5$	$2.3 < p2 < 3.7$	$4.3 < p3 < 5.7$	$0.1 < p1 < 1.5$	$5.3 < p2 < 6.7$	$17.3 < p3 < 18.7$	$0.5 < p1 < 1.5$	$1.3 < p2 < 2.7$	$3.3 < p3 < 4.7$	$0.0 < p1 < 1.0$	$4.3 < p2 < 5.7$	$14.3 < p3 < 15.7$	$3.3 < p1 < 3.7$
	p1	p2	p3	p1	p2	p3	p1	p2	p3	p1	p2	p3	p1
I	1.18	3.21	5.07	1.22	7.05	18.50	1.00	2.58	4.63	0.00	5.76	15.63	3.07
F	1.18	3.10	5.56	1.09	6.38	17.32	1.00	2.51	4.58	0.00	5.25	14.92	3.49

		Total mass Weight (lb)	Root-Spring Stiffness (θ) (in-lb/rad.)
I	345.0		6.5×10^3
F	371.5		4.38×10^5

	Weighting Factor	Desired Frequency
	*	*
	*	*
	3.30	3.30
	5.00	6.00
Torsion	4.20	3.50

Note : (θ) -- Design Variable ; (-) -- Box Beam Dimension is fixed ; (*) -- Zero

Table 12 Initial and final design for flapping, inplane, and torsional modes of teetering rotor blade with box beam dimension fixed except root stiffness

Element	No.	1	2	3	4	5	6	7	8	9	10
Box Beam t 0.01 < t < 1.0	I	—	—	—	—	—	—	—	—	—	—
	F	—	—	—	—	—	—	—	—	—	—
Box Beam d1 0.01 < d1 < 2.32	I	—	—	—	—	—	—	—	—	—	—
	F	—	—	—	—	—	—	—	—	—	—
Box Beam d2 0.01 < d2 < 2.32	I	—	—	—	—	—	—	—	—	—	—
	F	—	—	—	—	—	—	—	—	—	—
	Min.	96.54	55.77	2.69	8.07	5.38	5.38	5.38	5.38	8.07	8.07
lumped weight (β) (lb)	I	96.54	55.77	6.95	11.63	7.68	5.76	5.38	6.12	11.81	19.98
	F	96.54	55.91	6.95	18.14	18.21	5.76	5.33	6.12	11.81	19.88
Stress x 10^4 (psi)	I	1.40	1.34	3.30	1.61	1.87	1.85	1.73	1.49	1.11	0.44
	F	1.48	1.41	1.18	1.70	1.91	1.85	1.73	1.49	1.11	0.44

<<<<<<< Natural Frequencies (No/rev) >>>>>>>

	Collective flapping (fixed)			Cyclic inplane (fixed)			Cyclic flapping (hinge-4)			Collective inplane (hinged)			Torsion
Root Ioy (in^4) —(β)	0.5 < p1 < 1.5			1.0 < p1 < 2.0			0.5 < p1 < 1.5			0.0 < p1 < 1.0			3.3
I 48.11	2.3 < p2 < 3.7			7.3 < p2 < 8.7			1.3 < p2 < 2.7			4.3 < p2 < 5.7			< p1 <
F 290.29	4.3 < p3 < 5.7			18.3 < p3 < 19.7			3.3 < p3 < 4.7			14.3 < p3 < 15.7			3.7
	p1	p2	p3	p1	p2	p3	p1	p2	p3	p1	p2	p3	p1
Total mass / Root-Spring Weight Stiffness(β)													
(lb) (in-lb/rad.)													
I 345.0 6.5x10^5	1.18	3.21	5.87	1.22	7.05	18.50	1.00	2.58	4.63	0.00	5.71	15.63	3.87
F 329.0 3.32x10^5	1.18	3.14	5.55	1.53	7.71	19.16	1.00	2.47	4.50	0.00	5.45	15.39	3.51
Weighting Factor	*	*	3.31	6.67	3.30	*	*	*	*	*	*	*	4.20
Desired Frequency	*	*	5.00	1.50	8.00	*	*	*	*	*	*	*	3.50

Note : (β) -- Design Variable (-) -- Box Beam Dimension is fixed (*) -- Zero

pretwisted angle is now included.

6.4.1 Variable Box Dimension

A two-step optimization procedure is still used. The box beam dimensions and lumped weights as (well as the root spring) are considered as design variables. The results are shown in Table 13. In a similar fashion as results in section 6.3, the weight is concentrated at the tip of the blade because of the autorotational constraint. Root stress is close to the stress constraint which is 20,000 psi. The total weight does not decrease. Instead, it increases from 3.4 lb to 354 lb. The spring constant changes from 6.5×10^5 to 4.2×10^{5} in-lb/rad. The second collective mode of flapping moves from 5.89 to 5.67 no/rev while second cyclic mode of inplane moves from 7.08 to 6.54 no/rev.

6.4.2. Fixed Box Dimensions

For a blade of existing construction, only the lumped weights are considered as design variables. The results of optimization are shown in Table 14. The total weight increases from 345 lb to 372 lb. The third collective mode of flapping and the second cyclic mode of inplane move into the safe range.

Table 13 Initial and final design for flapping, inplane, torsional modes
of Teetering rotor (with pretist) blade with variable box beam dimension

Element	No.	1	2	3	4	5	6	7	8	9	10
pretwist(rad) x10^-1		0.000	-0.087	-0.209	-0.384	-0.663	-0.855	-1.029	-1.221	-1.483	-1.797
Box Beam t (#) 0.01 < t < 1.0	I	0.600	0.600	0.600	0.435	0.318	0.282	0.266	0.266	0.266	0.266
	F	0.436	0.457	0.468	0.322	0.391	0.381	0.324	0.271	0.191	0.256
Box Beam d1 (#) 0.01 < d1 < 2.32	I	0.550	0.550	0.440	0.452	0.464	0.464	0.464	0.464	0.464	0.464
	F	0.526	0.533	0.429	0.438	0.492	0.509	0.494	0.467	0.427	0.465
Box Beam d2 (#) 0.01 < d2 < 2.32	I	0.224	0.224	0.224	0.224	0.175	0.125	0.125	0.125	0.125	0.125
	F	0.217	0.218	0.219	0.167	0.124	0.126	0.126	0.124	0.121	0.125
lumped weight (#) (lb)	Min.	96.54	55.77	2.69	8.07	5.38	5.38	5.38	5.38	8.07	8.07
	I	96.54	55.77	6.95	11.63	7.68	5.76	5.38	6.12	11.81	19.98
	F	96.54	55.77	5.54	10.26	9.85	7.68	6.56	6.45	9.04	35.57
Stress x 10^4 (psi)	I	1.40	1.34	1.30	1.61	1.87	1.85	1.73	1.49	1.11	0.44
	F	2.00	1.87	1.81	2.00	1.88	1.73	1.74	1.72	1.76	0.65

Natural Frequencies (No/rev)

<<<<<<<   >>>>>>>

	collective flapping			Cyclic inplane (fixed)			Cyclic flapping (hinged)			Collective inplane (hinged)			Torsion
	$0.5 < p1 < 1.5$	$2.3 < p2 < 3.7$	$4.3 < p3 < 5.7$	$0.1 < p1 < 1.5$	$5.3 < p2 < 6.7$	$17.3 < p3 < 18.7$	$0.5 < p1 < 1.5$	$1.3 < p2 < 2.7$	$3.3 < p3 < 4.7$	$0.0 < p1 < 1.0$	$4.3 < p2 < 5.7$	$14.3 < p3 < 15.7$	$3.3 < p1 < 3.7$
	p1	p2	p3	p1	p2	p3	p1	p2	p3	p1	p2	p3	p1
I	1.18	3.22	5.84	1.21	7.08	18.50	1.00	2.58	4.61	0.00	5.76	15.65	3.87
F	1.17	3.19	5.67	1.10	6.54	17.80	1.00	2.59	4.69	0.00	5.38	15.32	3.41

	Total mass Weight (lb)	Root Spring Stiffness(#) (in-lb/rad.)
I	345.0	6.5×10^5
F	454.0	4.24×10^5

	collective flapping			Cyclic inplane			Cyclic flapping			Collective inplane			Torsion
Weighting Factor	*	*	1.00	*	*	1.08	*	*	*	*	*	*	1.68
Desired Frequency	*	*	5.00	*	*	6.00	*	*	*	*	*	*	3.50

Note : (#) - Design Variable   (*) -- Zero

Table 14 Initial and final design for flapping, inplane and torsional modes
of Teetering rotor (with pretwist) blade with box beam dimension fixed

Element	No.	1	2	3	4	5	6	7	8	9	10
Pretwist (rad) x10^{-1}		0.000	-0.087	-0.209	-0.384	-0.663	-0.855	-1.029	-1.221	-1.483	-1.797
Box Beam t 0.01 < t < 1.0	I	–	–	–	–	–	–	–	–	–	–
	F										
Box Beam d1 0.01 < d1 < 2.32	I	–	–	–	–	–	–	–	–	–	–
	F										
Box Beam d2 0.01 < d2 < 2.32	I	–	–	–	–	–	–	–	–	–	–
	F										
lumped Weight (lb)	Min.	96.54									
	I	96.54	55.77	2.69	8.07	5.38	5.38	5.38	5.38	8.07	8.07
				6.95	11.63	7.68	5.76	5.38	6.12	11.81	19.98
	F	98.10	59.33	7.13	14.57	10.53	7.51	6.38	6.84	12.93	31.31
Stress x 10^4 (psi)	I	1.40	1.34	1.30	1.61	1.87	1.85	1.73	1.49	1.11	0.44
	F	1.61	1.55	1.51	1.88	2.20	2.10	2.15	1.79	1.39	0.59

Natural Frequencies (No/rev)

	collective flapping			Cyclic Inplane (fixed)			Cyclic flapping (hinged)			Collective Inplane (hinged)			Torsion
	0.5 < p1 < 1.5			0.1 < p1 < 1.5			0.5 < p1 < 1.5			0.0 < p1 < 1.0			3.7 <
	2.3 < p2 < 3.7			5.3 < p2 < 6.7			1.3 < p2 < 2.7			4.3 < p2 < 5.7			< p1 <
	4.3 < p3 < 5.7			17.3 < p3 < 18.7			3.3 < p3 < 4.7			14.3 < p3 < 15.7			3.7
	p1	p2	p3	p1	p2	p3	p1	p2	p3	p1	p2	p3	p1
I	1.18	3.21	5.87	1.22	7.05	18.50	1.00	2.58	4.63	0.00	5.71	15.63	3.87
F	1.18	3.21	5.57	1.11	6.64	17.31	1.00	2.60	4.58	0.00	5.41	14.79	3.50

	Total mass (lb)	Root-Spring Stiffness(#) (in-lb/rad.)
I	345.0	6.5x10^5
F	372.0	4.39x10^5

	Weighting Factor	Desired Frequency
collective flapping	1.24	5.00
Cyclic Inplane	1.00	6.00
Torsion	205.80	3.50

Note : (#) -- Design Variable ; (-) -- Box Beam Dimension is fixed ; (*) -- Zero

7. ARTICULATED ROTORS

7.1 Definition

Articulated rotor blade will be the subject of design blade in this section. Ref[25] The primary design variables are same as before: the wall thickness of box beam and lumped weights. Because the blade is articulated with a rigid hub, there is no distinction between collective or cyclic modes for flapping and inplane. The blade is pretwisted. The boundary condition for flapping is a hinge at the root. There is root spring for torsional motions and an offset for inplane. Table 15 gives data for both the initial (and minimum) blade stiffnesses and inertias as well as for the initial variables such as box beam dimensions, lumped weights,etc.

7.2.1 Variable Box Dimension

Box beam dimensions, lumped weights and root spring are taken as design variables. Tables 16 shows the intial and final results of the optimization procedure. The inplane frequency moves from 4.84 to 4.69 no/rev while the torsional mode moves from 4.25 to 4.45. The total weight drops slightly from 96.55 to 95.48 lb. The root spring changes from 2.41×10^6 to 2.89×10^6.

7.3. Fixed Box Beam Dimensions

Box beam dimensions will be considered to be fixed in this section. Only lumped weights and the root spring are taken as design variables. The final results are shown in Table 17.

Table 15   Data for Articulated Rotor Blade

Rotating Speed : 293 RPM
Young's Modulus : 0.160 x 10^6 lb/in^2
Axial Stress : < 30,000 psi

mass of moment inertia > 0.2000x10^7 lb-in^2
density of box beam : 0.000417 mugs/in^3

Element	No.	1	2	3	4	5	6	7	8	9	10
Length	(in)	16.4	26.4	26.4	26.4	26.4	26.4	26.4	26.4	26.4	26.4
Box Beam Dimension	t (in)	0.140	0.120	0.090	0.072	0.060	0.060	0.060	0.060	0.060	0.060
	d1 (in)	0.345	0.530	0.390	0.068	0.055	0.042	0.048	0.055	0.042	0.025
	d2 (in)	0.100	0.120	0.090	0.060	0.060	0.060	0.060	0.060	0.060	0.060
Area and mass moment of inertia of y-axis	Ibx (in4)	0.671	0.631	0.502	0.376	0.319	0.317	0.318	0.319	0.317	0.166
	Iox (in4)	0.388	0.480	0.154	0.067	0.036	0.020	0.025	0.036	0.020	0.021
	Mbx (mug-in)x10^-3	0.280	0.263	0.210	0.160	0.133	0.132	0.132	0.133	0.132	0.069
	Mox (mug-in)x10^-2	0.211	0.319	0.278	4.769	0.395	0.281	0.296	0.341	0.311	0.293
Area and mass moment of inertia of x-axis	Iby (in4)	0.000	8.333	6.555	3.278	2.820	2.700	2.754	2.820	2.700	1.355
	Ioy (in4)	3.750	1.770	7.630	11.10	11.24	11.23	11.75	12.61	11.05	6.33
	Mby (mug-in)x10^-2	0.000	0.347	0.273	0.136	0.117	0.112	0.114	0.117	0.112	0.056
	Moy (mug-in)x10^-2	0.211	0.319	0.278	4.769	0.395	0.281	0.296	0.341	0.311	0.293
Min. lumped weight (lb)		0.89	1.435	1.435	1.435	1.435	1.435	1.435	1.435	1.435	1.435
w - lumped weight (lb)		6.718	9.088	1.978	1.435	2.352	5.852	6.342	6.573	6.372	5.962
GJ (lb-in x10^6)		16.00	14.60	11.20	8.40	7.20	7.00	7.10	7.20	7.00	4.00
Pretwist Angle (rad)		0.00	0.072	3.849	6.980	5.06	3.49	1.745	-1.745	-1.920	-3.66
Rotary inertia (mug-in) 10^-2 (w/g)A(b/2)^2		0.0	0.687	0.149	0.109	0.178	0.444	0.479	0.497	0.482	0.451

Table 16 Initial and final design for flapping, inplane, torsional modes of Articulated rotor blade with variable box beam dimension

Element	No.		1	2	3	4	5	6	7	8	9	10
Box Beam t (#) 0.01 < t < 0.7		I	0.140	0.120	0.090	0.072	0.060	0.060	0.060	0.060	0.060	0.030
		F	0.159	0.114	0.094	0.093	0.079	0.071	0.055	0.046	0.047	0.047
Box Beam d1 (#) 0.01 < d1 < 2.75		I	0.345	0.530	0.390	0.068	0.055	0.042	0.048	0.055	0.042	0.025
		F	0.384	0.580	0.422	0.071	0.057	0.043	0.049	0.055	0.042	0.024
Box Beam d2 (#) 0.01 < d2 < 2.75		I	0.100	0.120	0.090	0.060	0.060	0.060	0.060	0.060	0.060	0.024
		F	0.104	0.126	0.093	0.062	0.062	0.062	0.061	0.060	0.059	0.024
lumped weight (#) (lb)		Min.	0.890	1.435	1.435	1.435	1.435	1.435	1.435	1.435	1.435	1.435
		I	6.718	9.088	1.978	1.435	2.352	5.852	6.342	6.573	6.372	5.962
		F	5.459	5.575	1.936	1.617	3.098	8.457	6.276	4.696	4.866	7.044
Stress x 10^4 (psi)		I	1.39	1.32	1.64	2.54	2.84	2.60	2.12	1.55	0.94	0.61
		F	1.27	1.31	1.56	2.04	2.19	2.11	2.01	1.71	1.15	0.71

$<<<<<<<$ Natural Frequencies (No/rev) $>>>>>>$

			Flapping (hinged)			Inplane (offset)			Torsion (spring)	
Root-Spring Stiffness(#) (in-lb/rad.)			0.01 < p1 < 1.50	2.23 < p2 < 2.63	4.26 < p3 < 4.67	0.01 < p1 < 1.50	4.30 < p2 < 4.70	12.30 < p3 < 12.70	4.3 < p1 < 4.7	
			p1	p2	p3	p1	p2	p3	p1	
Total mass Weight (lb)	96.55	I 2.41x10^6	1.03	2.70	4.51	0.24	4.84	12.30	4.25	
	95.48	F 2.89x10^6	1.03	2.54	4.43	0.24	4.69	12.44	4.45	
Weighting Factor			*	*		*	1.99	*	1.00	
Desired Frequency			*	*		*	4.50	*	4.50	

Note : (#) -- Design Variable   (*) -- Zero

Table 17 Initial and final design for flapping, inplane and torsional modes
of Articulated rotor blade with box beam dimension fixed

Element	No.	1	2	3	4	5	6	7	8	9	10
Box Beam t 0.01 < t < 0.7	I	—	—	—	—	—	—	—	—	—	—
	F	—	—	—	—	—	—	—	—	—	—
Box Beam d1 0.01 < d1 < 2.75	I	—	—	—	—	—	—	—	—	—	—
	F	—	—	—	—	—	—	—	—	—	—
Box Beam d2 0.01 < d2 < 2.75	I	—	—	—	—	—	—	—	—	—	—
	F	—	—	—	—	—	—	—	—	—	—
lumped weight (#) (lb)	Min.	0.89	1.435	1.435	1.435	1.435	1.435	1.435	1.435	1.435	1.435
	I	6.718	9.088	1.978	1.435	2.352	5.852	6.342	6.513	6.372	5.962
	F	6.015	8.164	2.401	1.981	3.779	8.745	4.288	4.067	4.525	7.595
Stress x 10^4 (psi)	I	1.39	1.32	1.64	2.54	2.84	2.60	2.12	1.55	0.94	0.61
	F	1.37	1.30	1.61	2.49	2.74	2.41	1.91	1.47	1.00	0.75

<<<<<<< Natural Frequencies (No/rev) >>>>>>>

	Flapping (hinged)			Inplane (offset)			Torsion (spring)
	0.01 < p1 < 1.50	2.23 < p2 < 2.63	4.26 < p3 < 4.67	0.01 < p1 < 1.50	4.30 < p2 < 4.70	12.30 < p3 < 12.70	4.3 < p1 < 4.7
	p1	p2	p3	p1	p2	p3	p1
I	1.03	2.70	4.51	0.24	4.84	12.30	4.25
F	1.03	2.57	4.67	0.24	4.43	12.30	4.39
Weighting Factor	*	*	*	*	*	*	1.00
Desired Frequency	*	*	*	*	*	*	4.50

	Root-Spring Stiffness(#) (in-lb/rad.)	Total mass Weight (lb)
I	2.41x10^6	96.55
F	2.78x10^6	94.89

Note : (#) -- Design Variable   (*) -- Zero

8. RELATION BETWEEN VIBRATION AND FREQUENCY PLACEMENT

8.1 FORMULATION

In this section, we would like to show whether or not the forced response of the blade can be adequately controlled, as we have assumed, by our approach of 'frequency placement', that is, of restricting the natural frequencies of the blade to lie within narrow intervals located away from certain integer multiples of the rotor speed. Also we would examine whether or not aerodynamic damping substantially reduces the resonant peaks, in which case concern about avoiding resonances through proper selection of frequency windows would be unnecessary. Finally, the sensitivity of the optimal design to the choice of frequency window will be studied.

This investigation is carried out through two, somewhat overlapping, problems. First, the forced response of an initial (i.e., non-optimized) design is compar . to the response of a final design; cases with and without aerodynamic damping are considered. Next, the response of initial and final designs are evaluated as a single natural frequency is varied (the others being held fixed). In each case, a forcing function containing harmonics of the rotor speed is applied. Again, cases with and without aerodynamic damping were considered. The general finding from these studies is that frequency placement is a viable means of reducing vibration, although it is by no means the only method and should be used in conjunction with others.

8.2 RESPONSE VERSUS FREQUENCY

The equations of motion for the finite-element representation of a rotor blade, subjected to an external excitation, may be written in

matrix form as

$$[M]\{\ddot{X}(t)\} + [c]\{\dot{X}(t)\} + [K]\{X(t)\} = \{F(t)\}, \tag{27}$$

where

[M] = mass matrix,

{X(t)} = column vector of nodal displacement,

[C] = damping matrix,

[K] = stiffness matrix, and

{F(t)} = forcing function column vector.

The forcing function may in turn be expressed as

$$\{F(t)\} = \{V_o\} e^{iwt}, \tag{28}$$

where

w = forcing frequency, and

V_o = forcing amplitude.

After some calculation, it can be shown that the amplitude of the response — written as {X}, independent of t — can be given as

$$\{X\} = [K + iwC - w^2 M]^{-1}\{V_o\} \tag{29}$$

In this section, the response of both the initial and final (optimal) designs to an external forcing function is studied as the frequency of the forcing function is varied. Blades both with and without aerodynamic damping are considered. To formulate these problems, consider the forced behavior of a rotor-blade. Only the flapping response is considered. The inplane response is inferred from the results

without damping, since there is little aerodynamic damping in the in-plane direction.

Fig. [13] shows a plot of the forcing amplitude V_o [Ref. 25] used in the study. Given the forcing amplitude, we can calculate the response of each node of the finite-element representation of the blade as the value of the forcing frequency, w, is varied. The tip (finite-element node farthest from the hub) response is of special interest. Before the results obtained from this study are presented, it is useful to examine the frequency placement results which are described in Chapter 6 (see Table 10). The results for the frequencies (in units of cycles/rev) are, for flapping mode only,

MODE	INITIAL DESIGN	FINAL DESIGN
1st	1.18	1.18
2nd	3.22	3.09
3rd	5.89	5.67

Blade dimensions are given in Table 9.

The frequencies in the above table correspond to the symmetric modes of a teetering rotor. Thus, only _even_ harmonics of the rotor speed have been considered as forcing frequencies. As a result, the optimized blade (Final design) finds the third mode moved away from the critical 6.0/rev (from 5.89 to 5.67). Similarly, the movement of the second mode to 3.09/rev removes it from 2.0 and 4.0/rev. In the comparison study to follow, however, we will apply the entire spectrum of frequencies to this blade (not just even harmonics). Thus, the 'Final Design' can no longer be considered optimum. A comparison of the two blades, however,
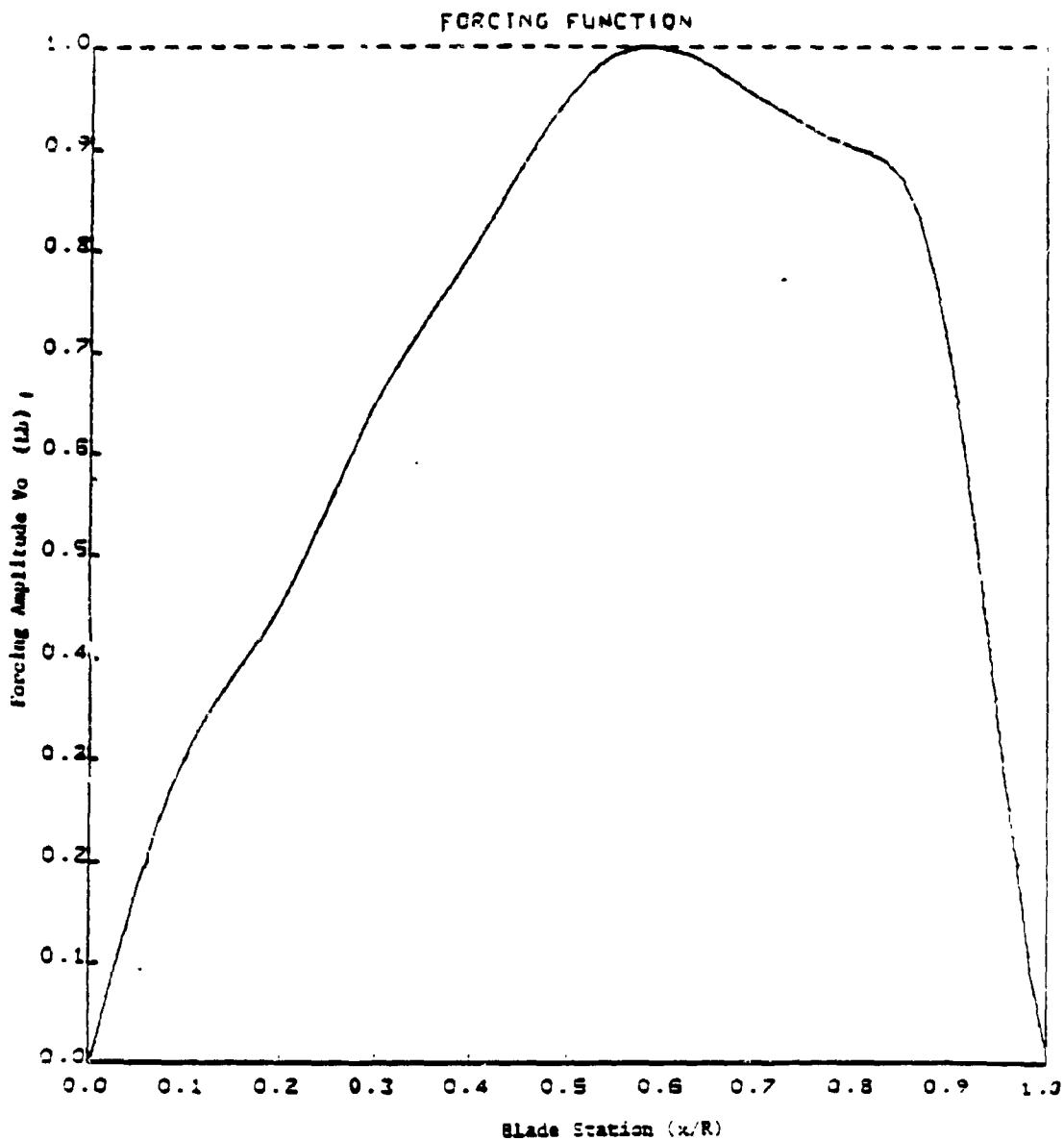
Figure 13   Radial Variation of Forcing Function

does indicate the strong effect of resonance because each case has a distinct resonance (6 and 3/rev).

We shall now consider the results of the present study. Fig. 14 shows the tip responses of both the initial design and final (i.e., optimized) design as functions of the forcing frequency. Aerodynamic damping has been neglected (Alternatively, the results can be interpreted as giving the inplane response). It can be seen that near 1.18 cycles/rev, the responses of the two designs are very similar. However, the responses corresponding to the second and third modes differ significantly. For example, in the second mode, the peak of 3.22 cycles/rev (initial design) moves to 3.09 cycles/rev (final design)/ Similarly, the peak of the third mode moves from 5.89 cycles/rev to 5.67 cycle/rev, which is especially important since it is highly desirable to keep the frequency away from the integer frequency of 6 cycles/rev. We conclude from these results that the frequency placement approach does have a significant effect on the forced tip response when damping is not considered.

Next, the effect of aerodynamic damping is considered. The presence of the damping implies that results to be presented correspond to flapping. Mathematical details of the damping formulation are available [Ref.18]. The effect of aerodynamic damping on reducing the resonant peaks of the tip response of the initial blades is shown in Fig. 15. Fig. 16 shows the damped responses of both the initial and optimized blades so that the effect of frequency placement can be studied. It is interesting to observe here that when damping is included, no apparent advantage is gained by optimizing the blade, at least in terms of reducing the tip response, except in the range of 3-4/rev, in which a
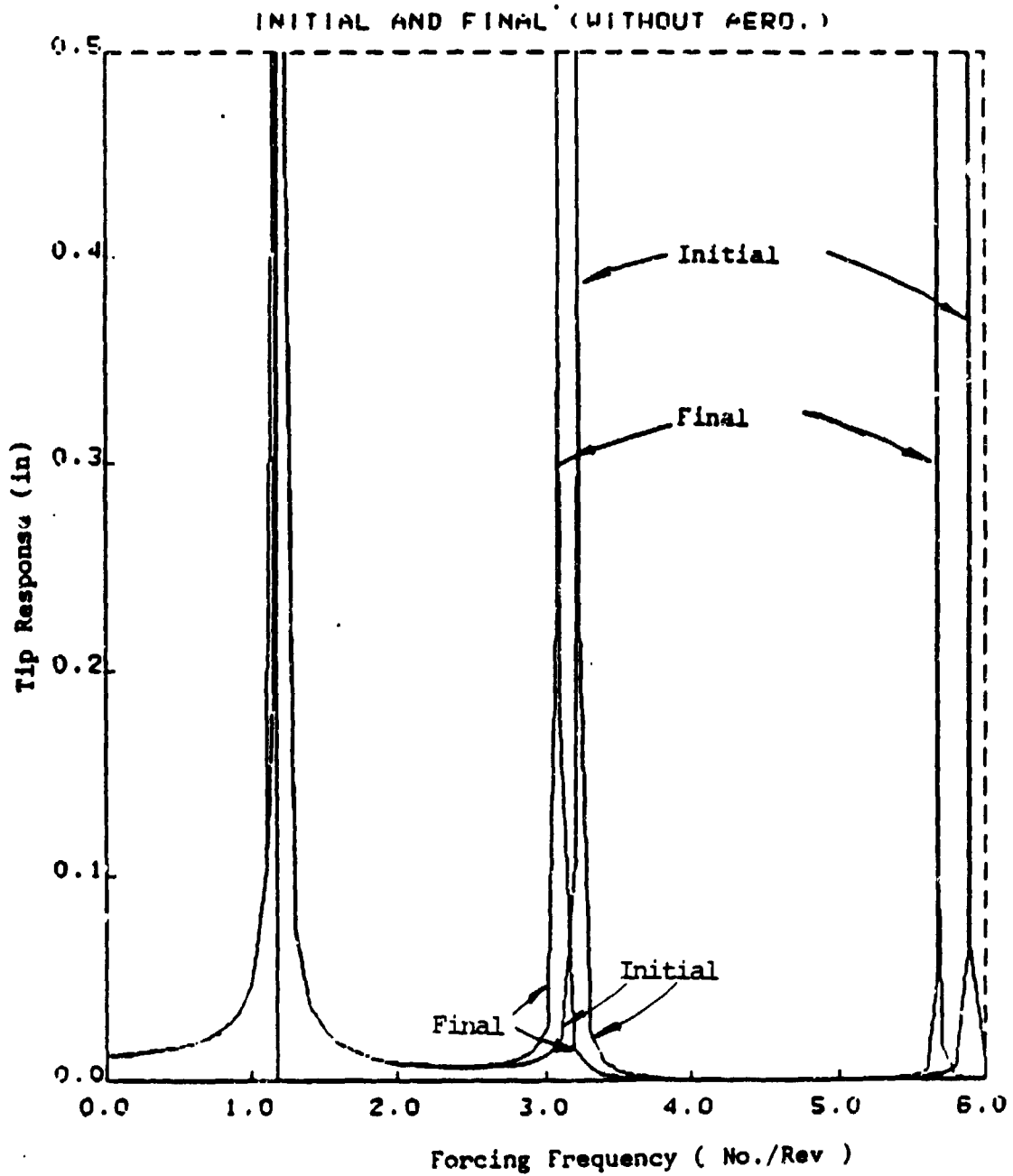
Figure 14   Tip Response Versus Forcing Frequency for both
Initial and Final Designs Without Damping
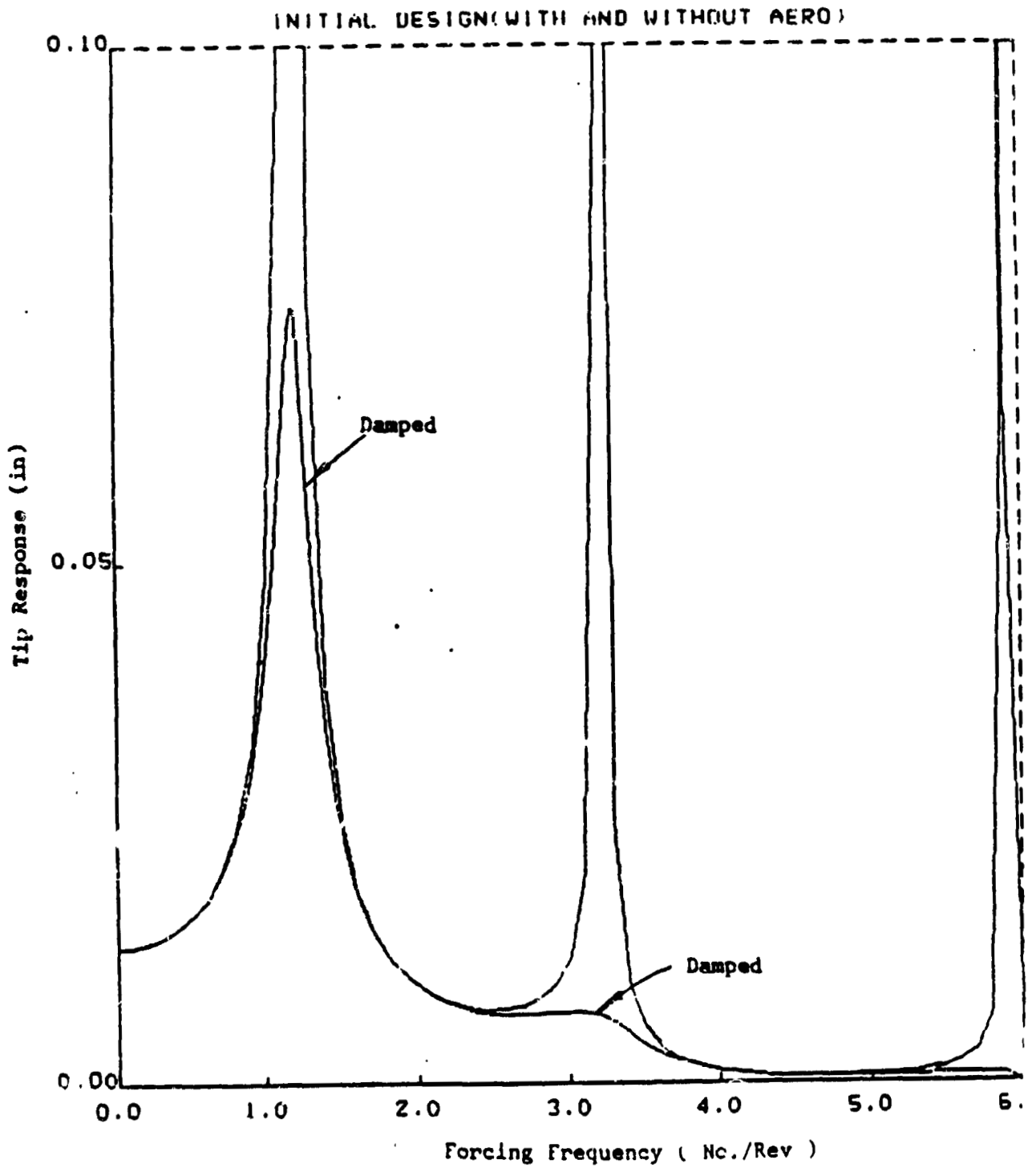
Figure 15   Tip Response Versus Forcing Frequency for Initial
Design Both With and Without Damping
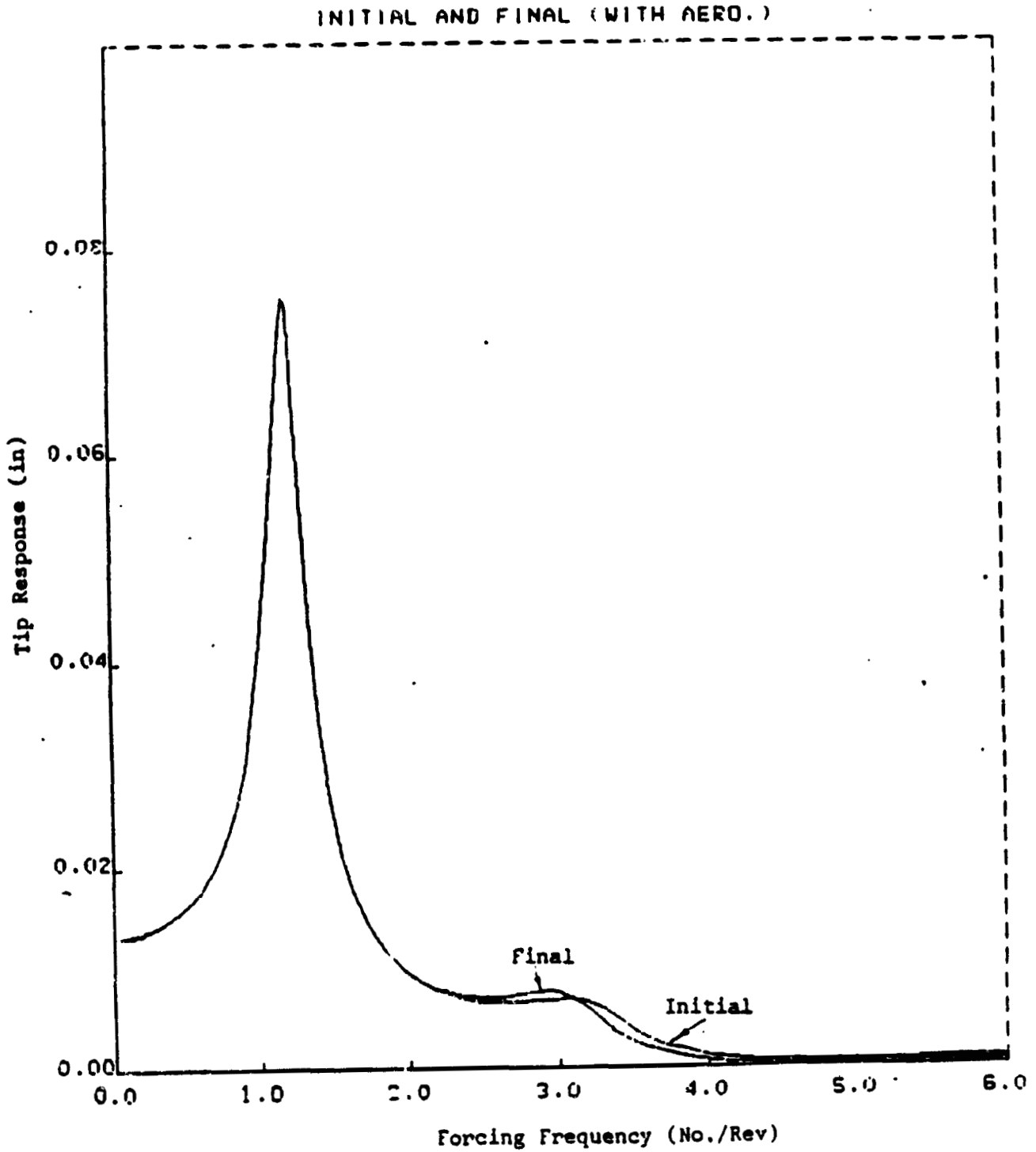
Figure 16   Tip Response Versus Forcing Frequency for Both
Initial and Final Design With Damping

which a thirty-five percent reduction occurs. However, we must also examine the effect of optimization when the response is measured by the average shear force existing in the blade.

Consequently, the shearing force in the blade is considered next. As a measure of the average shear in the rotor, we consider the sum of the squares of the shear force (abbreviated SSS),

$$SSS = Y_1^2 + Y_2^2 + \ldots + Y_{10}^2 \tag{30}$$

In this section, Y_i represents the shear force at node i in the (ten-element) finite-element model. Note that the root shear is necessarily included as one of the terms on the right-hand side of the equation, so that a large value of root shear will cause SSS to also be large.

Fig. 17 shows the variation of SSS with respect to the forcing frequency for the initial design with and without aerodynamic damping. Fig. 18 shows the same quantities for the final (optimized) design. Fig. 19 compares the quantity SSS corresponding to initial and final designs when aerodynamics is considered. Inspection of these figures shows that, in contrast to behavior of the tip response, the shear response is significantly affected by changing blade frequency, even when aerodynamic damping is included. The 3/rev loads are increased by fifty percent due to the movement of w_2 from 3.22 to 3.09/rev. Similarly, the 6/rev loads are reduced by seventy percent due to the movement of w_3 from 5.89 to 5.67/rev. Thus, even with damping, frequency placement is a powerful driver of loads. It follows that frequency placement can be justifiably considered an important part of blade optimization.
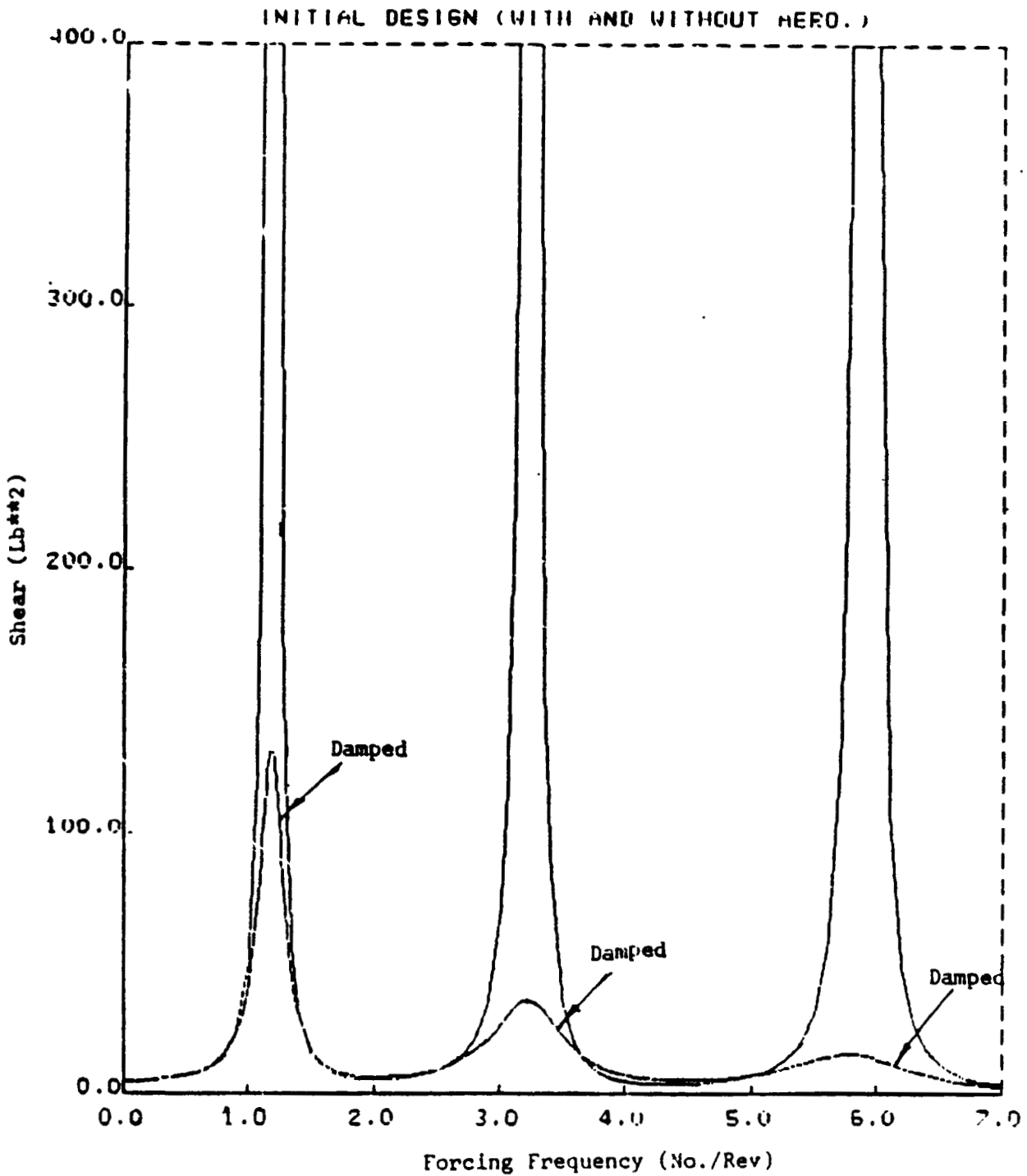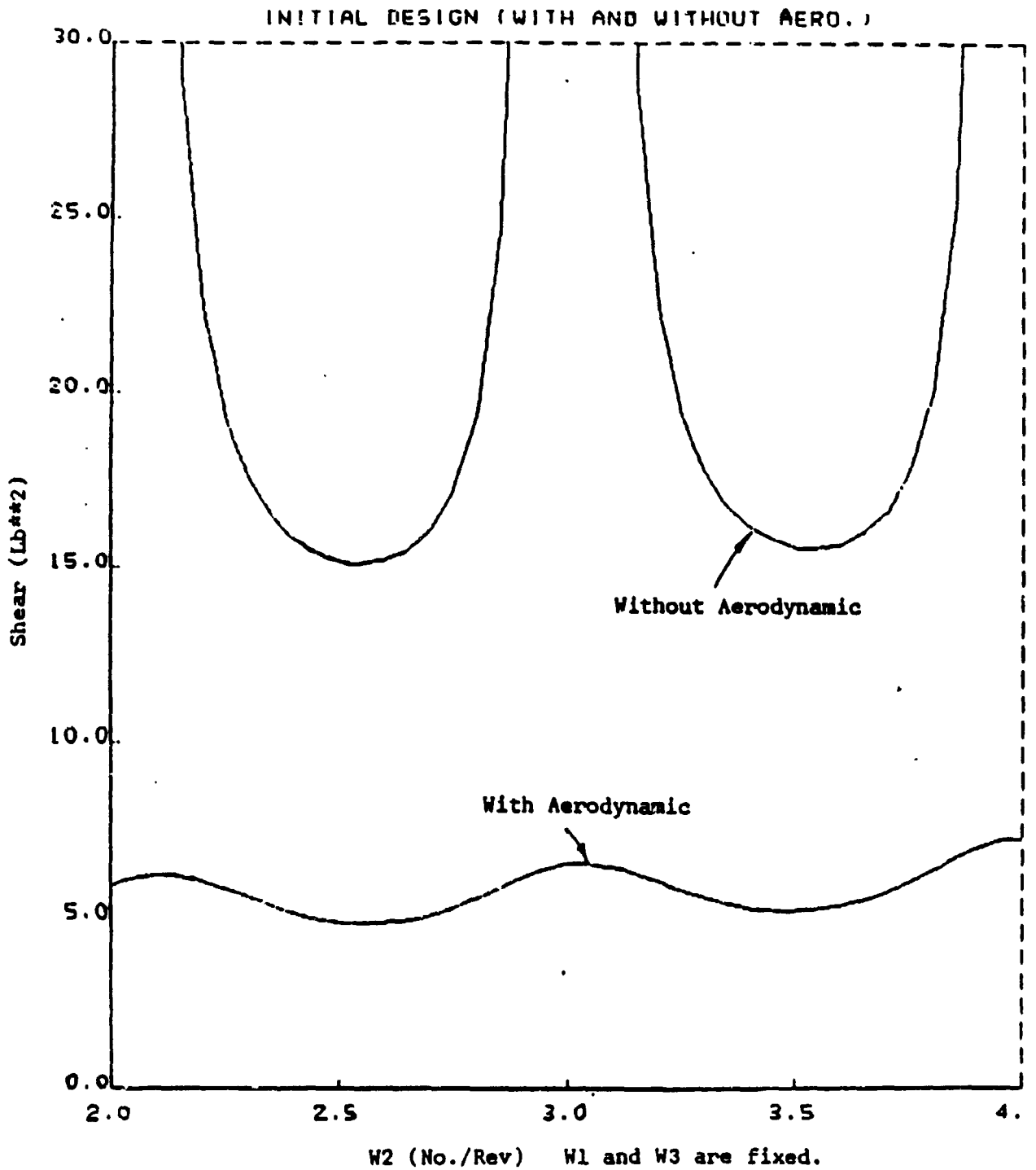
Figure 17   Sum of Squares of Shears Versus Forcing Frequency
for Initial Design Both With and Without Damping
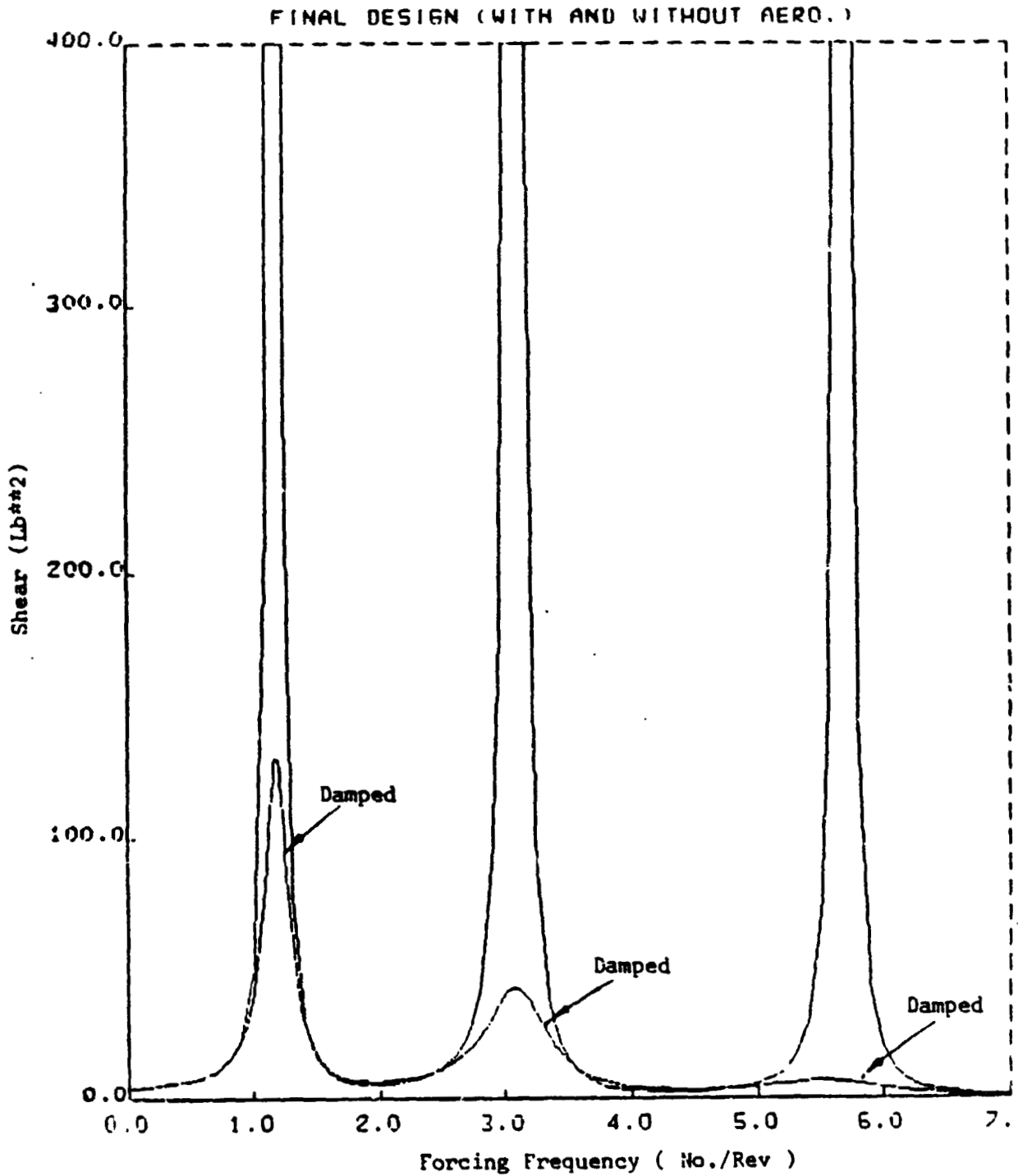
Figure 18 Sum of Squares of Shears Versus Forcing
Frequency for Final Design Both With and
Without Damping

INTIAL AND FINAL DESIGN (WITH AERO.)
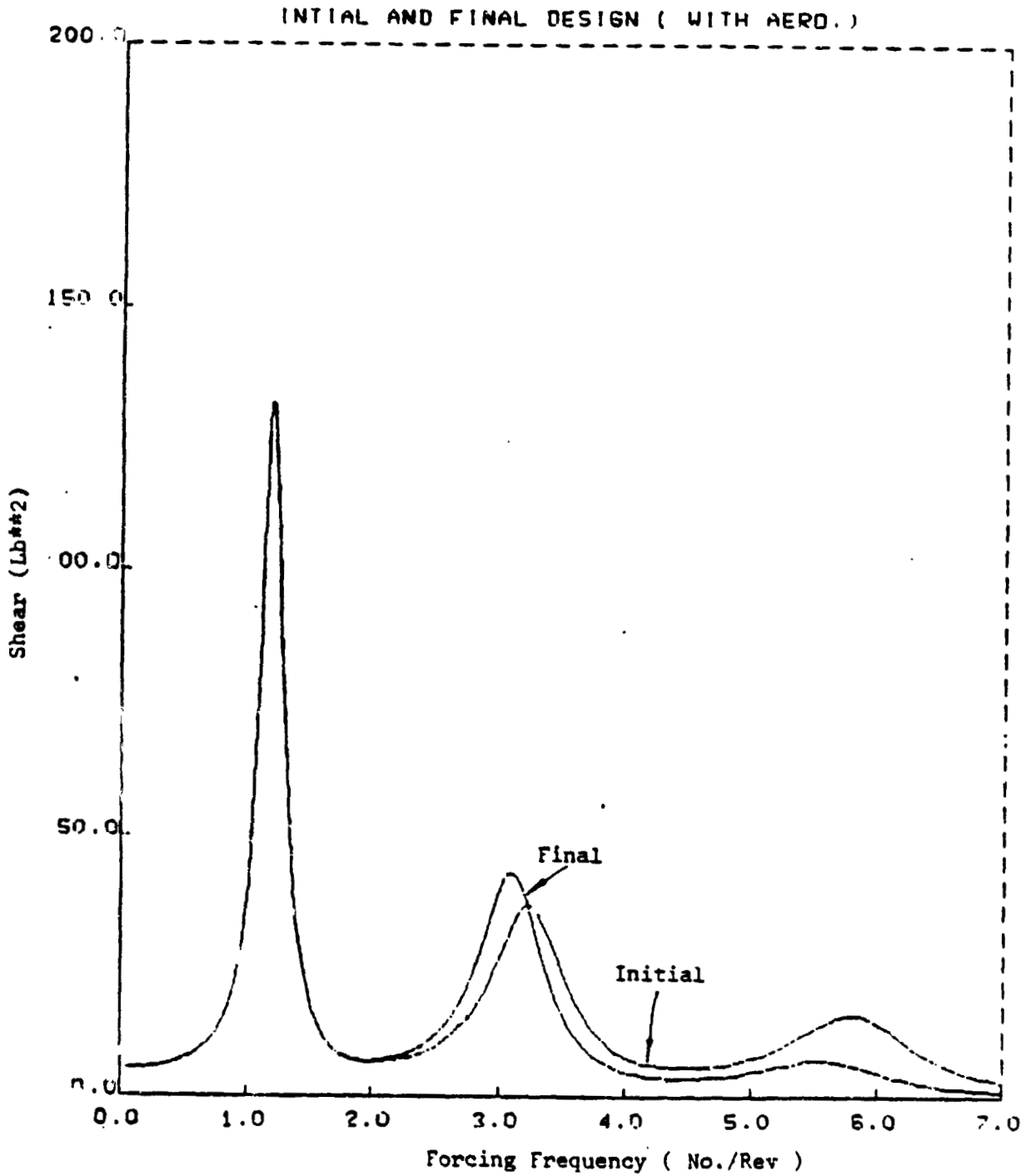
Figure 19   Sum of Squares of Shears Versus Forcing Frequency
for Both Initial and Final Designs With Damping

8.3 RESPONSE VERSUS PLACEMENT

In the study just described, the response of the blade to changes in the forcing frequency was considered. Now we consider a different approach. In effect, we examine how the blade responds to a forcing function 'during the optimization procedure' — in the sense that during optimization, the optimization algorithm varies the natural frequency of the blade (to force it to satisfy the frequency constraints). In obtaining the results to be presented next, we simulated the optimization procedure by varying the natural frequency. Thus we can observe what happens to the forced response during frequency placement.

The formulation of the approach is as follows. Through appropriate transformations (described in Appendix 11.3), the system mass matrix can be written as

$$[M] = [U]^{-T}[U]^{-1} \tag{31}$$

and the system stiffness matrix as

$$[K] = [M][U] \, \text{diag}[\, (w_i^2) \,] [U]^T [M] \tag{32}$$

were w_i are the natural frequencies of the system, $[U]$ is a matrix whose columns are eigenvectors, and the notation 'diag' indicates a diagonal matrix (all off-diagonal terms vanish). From examination of these expressions, it can be seen that the stiffness and mass matrices can be considered functions of the natural frequencies. Thus it becomes possible to fix all frequencies but one, and then study the response of the system as that one frequency is varied with mode shapes also held fixed. In particular, the response to the following forcing function will be studied:

$${F(t)} = {V_1}e^{iwt} + {V_2}e^{i2wt} + \ldots + {V_n}e^{inwt} \tag{33}$$

where

$$w = \text{the rotor speed, and}$$

$${V_n} = (1/n){V_o}, \tag{34}$$

where ${V_o}$ was defined previously in Fig. 13. Since the arguments of the exponentials are integer multiples of w, resonance will occur at harmonics of the rotor speed. The particular forcing function given above is known from empirical observation to provide an approximate, but physically realistic representation of the radial and harmonic variation of the amplitude of the load on a real blade. As mentioned in this section, the blade response will be defined by the tip displacement and the sum of the squares of the shears except that, here, the n = 1 term has been omitted from the expressions for calculating tip displacement and shears because this term represents a tip-path plane tilt that is controlled by the pilot for trimming purposes. It is not part of the true vibratory loads we are considering.

Results for the problem just formulated are shown in Fig. 20, where the sum of the squares of the shears is plotted as a function of w_2, the second natural frequency, with the other natural frequencies being fixed. This figure corresponds to the initial blade design (blade dimensions are given in Table 9. Fig. 21 shows the same quantity for the case where the third natural frequency is varied. It is interesting to note that the response curve for the damped case in Fig. 21 lacks resonant peaks — apparently the damped response is so completely dominated by the resonance of the second natural frequency, which is fixed near 3/rev, that the (damped) resonant peaks for the third frequency are negligible by comparison. It should be noted that the

Figure 20   Sum of Squares of Snears Versus Second Natural Frequency
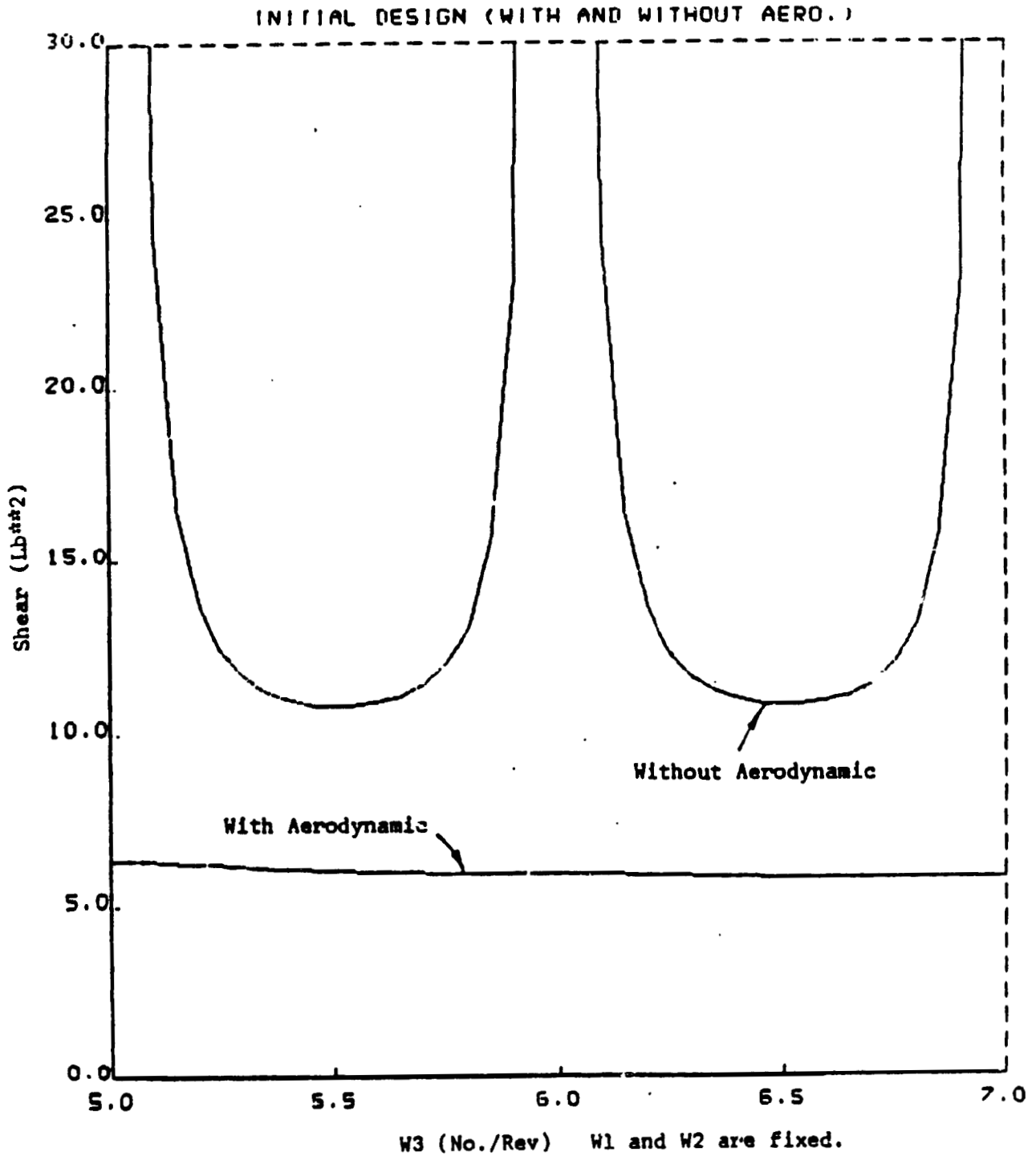for Initial Design Both With and Without Damping

Figure 21   Sum of Squares of Shears Versus Third Natural Frequency
for Initial Design Both With and Without Damping

response of the original design is respresented by only one point on Figure 20 or Figure 21. This value can be found by taking w_2 = 3.22 or w_3 = 5.89 on those figures, since these are the initial design values (Table 10).

For the _final_ (optimal) design, the analogous quantities are plotted in Figs. 22 and 23. Again, no resonant peaks are present in the damped response when the third natural frequency is varied. Comparison of magnitudes of ordinates in Figs. 20 and 22 (no damping) shows that the overall shear measure is reduced in the final design in the regions away from resonance. Also, the choice of scale on the vertical axis in Fig. 22 highlights the effect of frequency placement. Note that by inspection of Figs. 20-23. a designer may select the design frequency which minimizes the average shear as measured by the SSS.

One of the most interesting results of Fig. 22 is information about the width of valleys and peaks, since this gives design information. First, let us examine the non-damping curve (inplane response). Here, the minimum points are nearly at the centers of the regions (2.55/rev) and (3.5'/rev). The frequency windows to maintain no more than thirty percent increase in loads are 2.40 - 2.70/rev and 3.40 - 3.70/rev (plus or minus 0.15/rev) — a fairly narrow window. For the damped curves (flapping response), mimima are also near the one-half points, but the window for thirty-percent increases are much wider: 2.20 to 2.90/rev and 3.20 to 3.80/rev (plus or minus 0.30/rev). Stated another way, inplane frequencies should be no closer than a 0.4/rev from integers, but flapping frequencies may be as close as 0.2 from an integer. It should be emphasized that these observations apply to this particular example and may not be generalized for other frequency constraints.
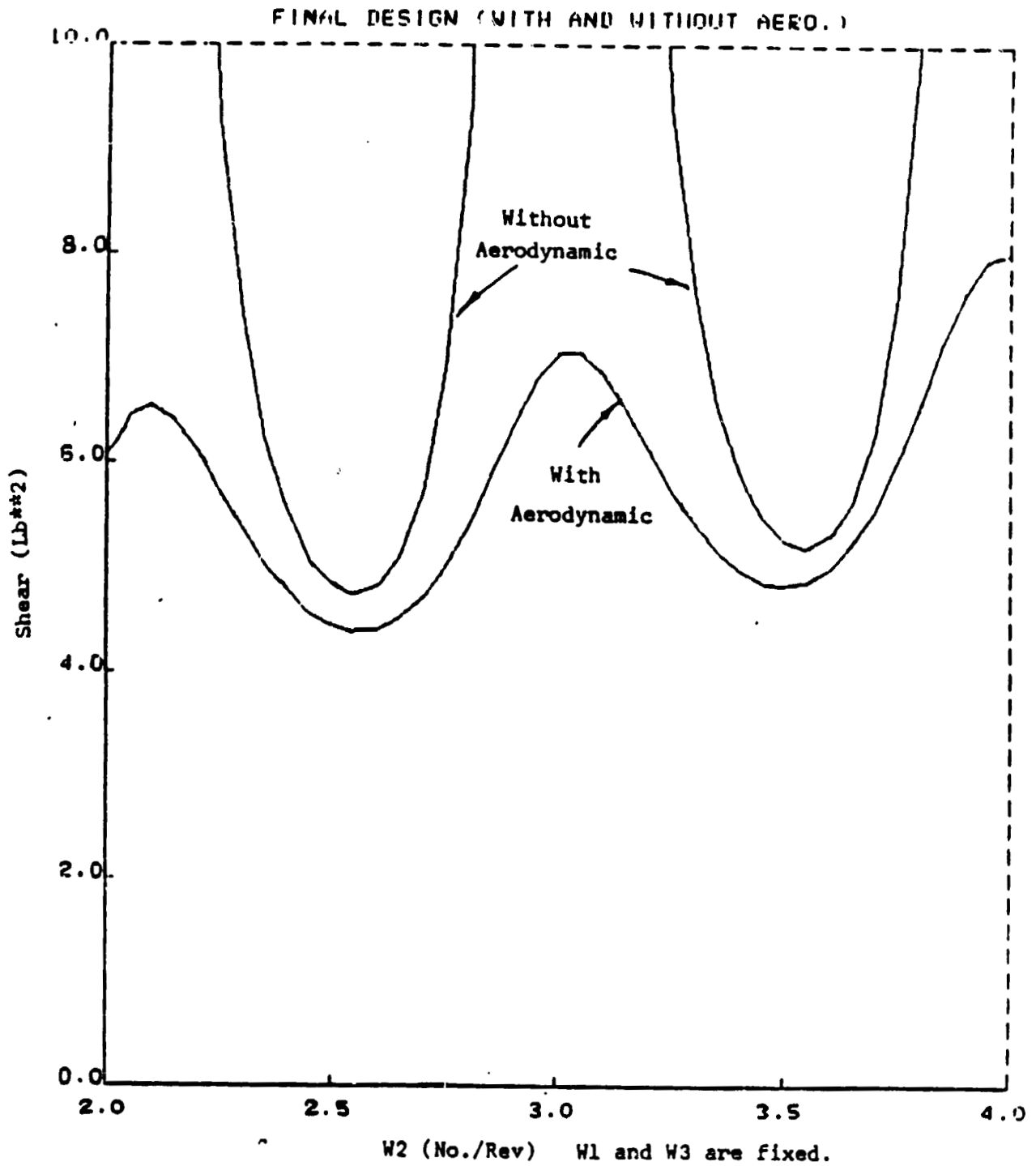
Figure 22   Sum of Squares of Snears Versus Second Natural Frequency
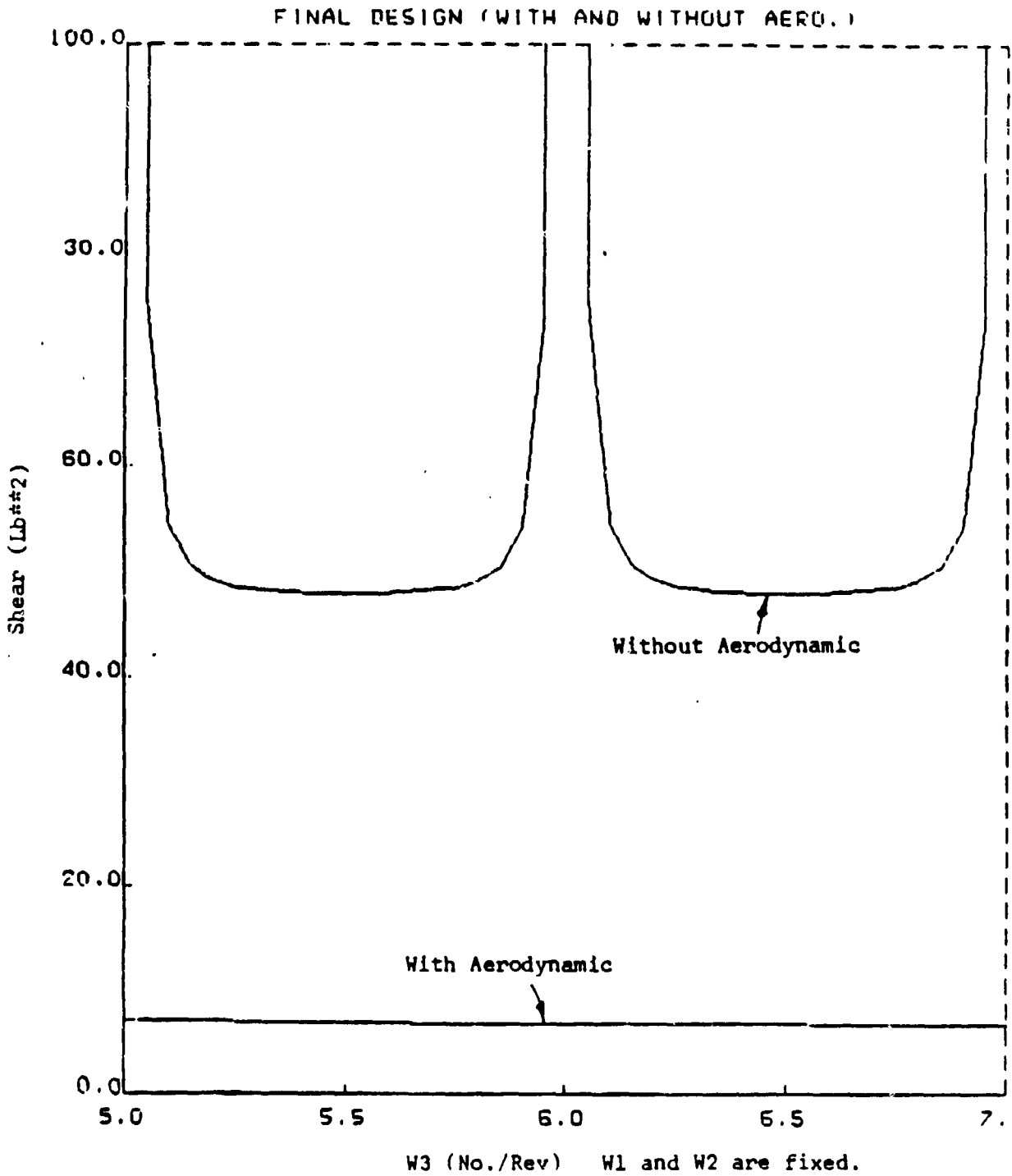for Final Design Both With and Without Damping

Figure 23 Sum of Squares of Shears Versus Third Natural for Final Design Both With and Without Damping

Another conclusion to be drawn from the above results is that the undamped response curve has very flat-bottomed 'valley' when one of the fixed frequencies is near an integer value (cf. Figs. 22 and 23).

8.4 RESPONSE DUE TO EVEN-INTEGER HARMONICS

In this section, we still study the response of the blade due to the change of forcing frequency. However, the forcing frequency will be a little different from the one in section 8.3.1. We will consider only the even integer forcing frequencies for which the collective m   are optimized. Thus, the forcing function may be written as

$$\{F(t)\} = V_2 e^{i2wt} + V_4 e^{i4wt} + V_6 e^{i6wt} + V_8 e^{i8wt}$$

where

$$w = \text{rotor speed}$$

$$V_n = 1/n \cdot V_o$$

Since the arguments of the exponentials are even integer multiples of w only, the resonance will expectedly occur at an even integer of harmonics of the rotor speed. The response of shear stress will be studied in this section.

Results for this case are shown in Fig 24, where the sum of the squares of the shear harmonics is plotted as a function of w_2 (w_1 and w_3 are fixed; w_1 = 1.18 and w_3 = 5.89). The figure corresponds to the initial blade design. Resonance peaks occur at 2 and 4/rev. Thus, for the shear response, a second frequencies around 3.0 would be the suitable choice for w_2 as design frequncy. Fig 25 is a similar comparison for a variable value of w_3 (w_1 = 1.18 and w_2 = 3.22 are fixed). Here, the resonance is at 6.0/rev, and w_3 = 5 or w_3 = 7 would be ideal.
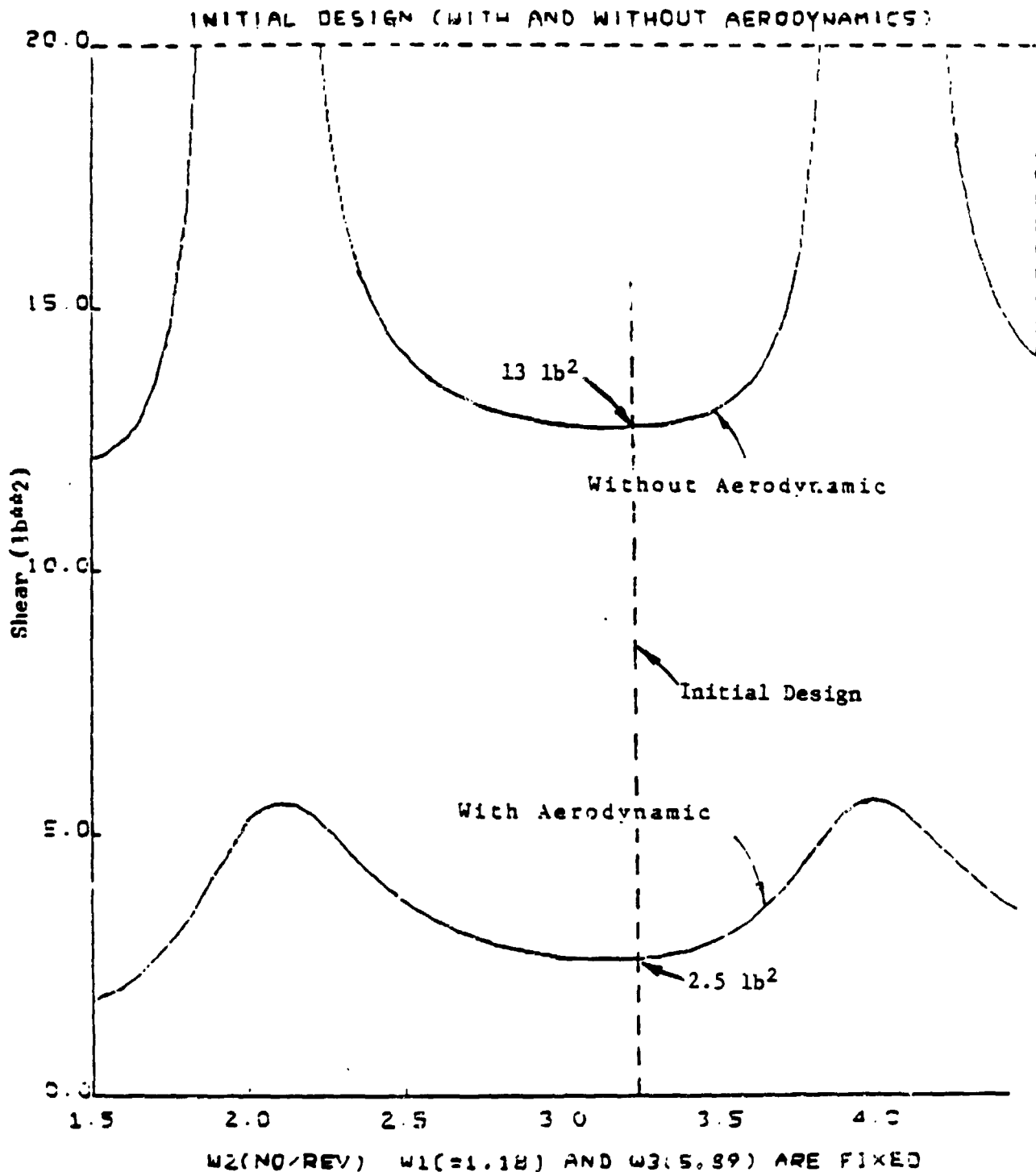
Figure 24   Sum of Squares of Shears Versus Second Natural Frequen·
for Initial Design Both With and Without Damping
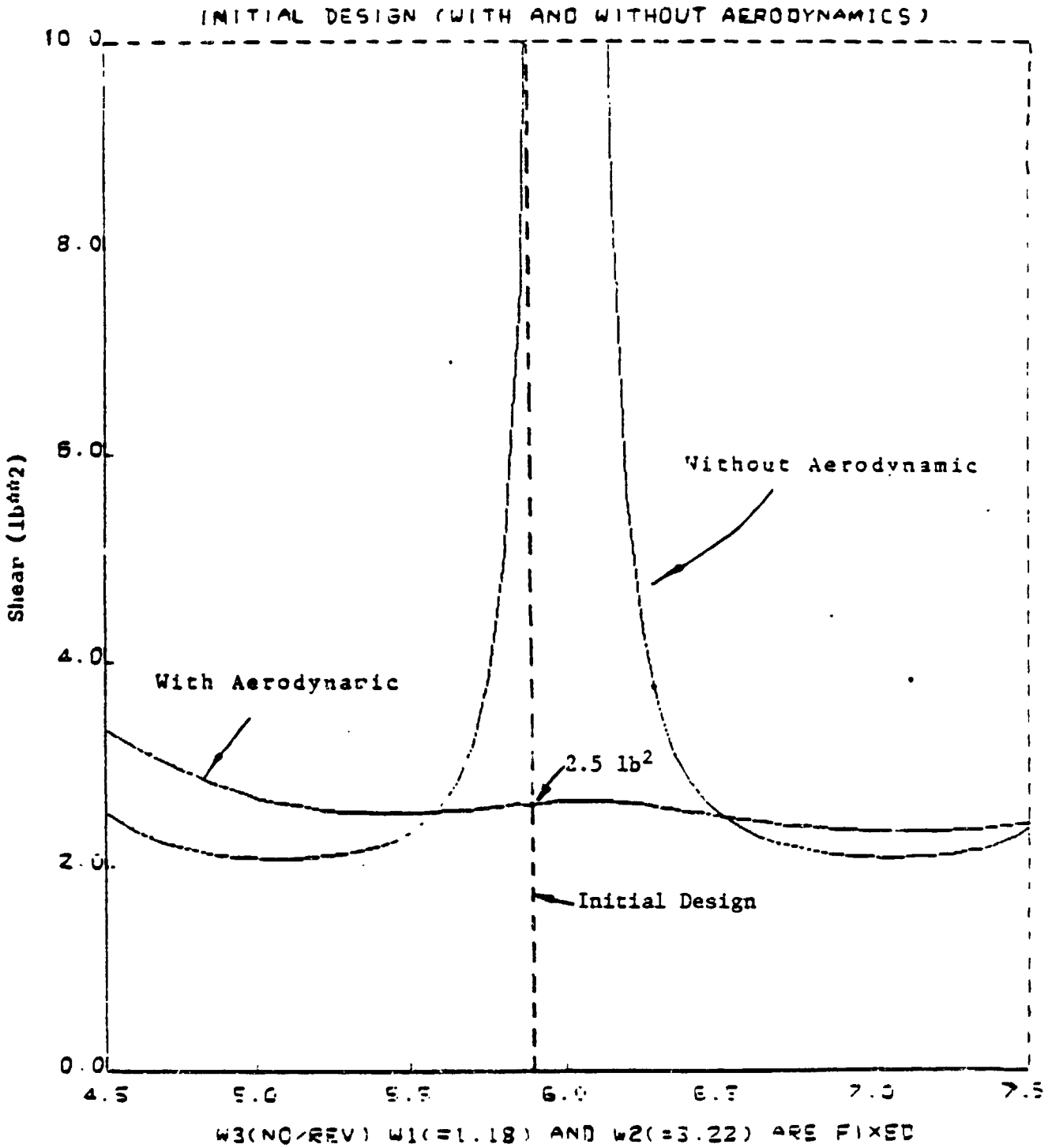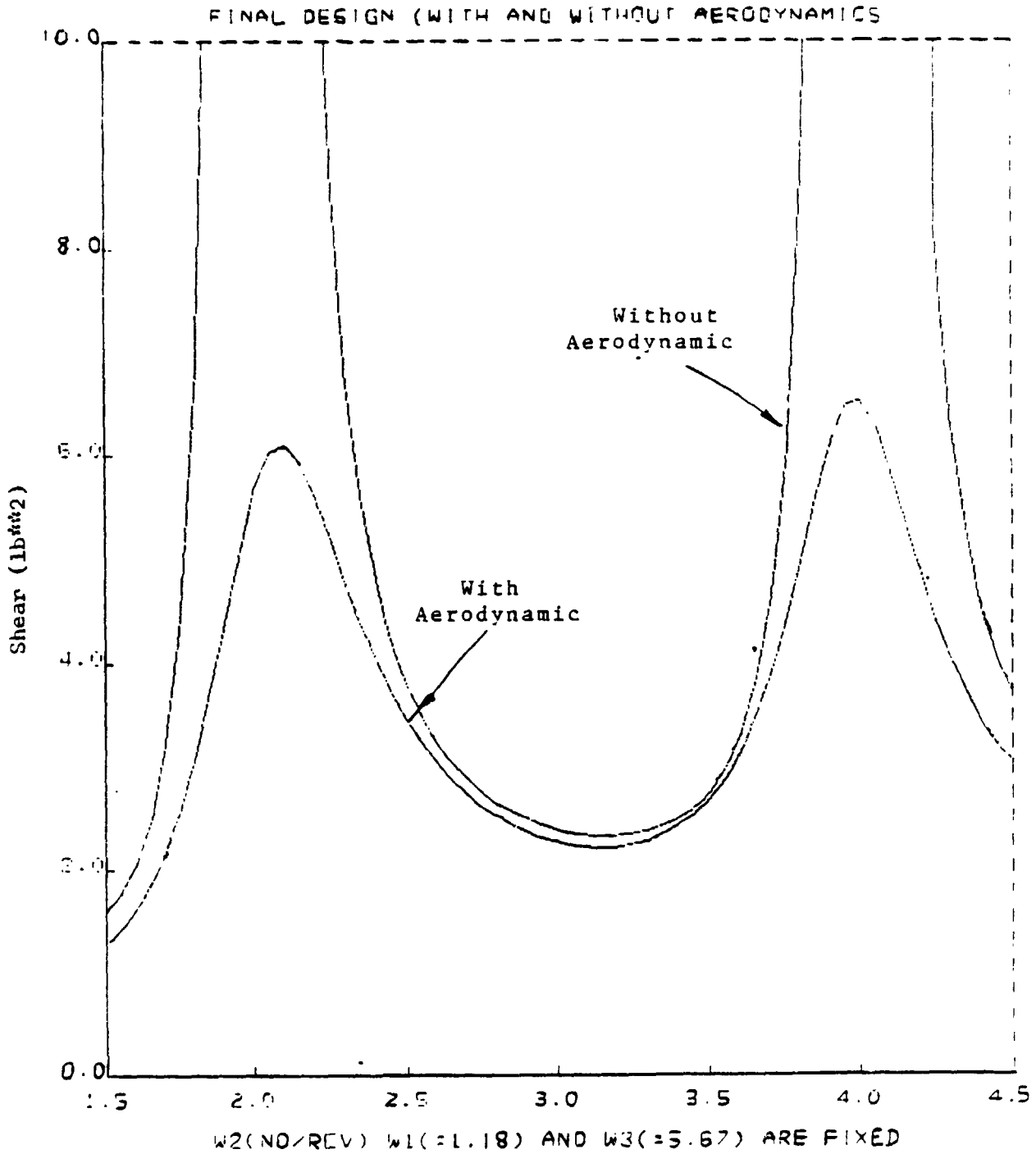(where Forcing Function is Even Integer Multiple)

Figure 25 Sum of Squares of Shears Versus Third Natural Frequency
for Initial Des' Both with and without Damping
(where Forcing   action is Even Integer Multiple)

ideal.

Results are shown in Fig 26 and 27 for the final design blade. Again, it is noted that the resonance peaks appear at even integers. A comparison of Fig 24 and 25 with Fig 26 and 27 shows the relatively lower vibrations of the final design. In either case, however, we see the sensitivity of vibrations to frequency, even with aerodynamics.

Figure 26   Sum of Squares of Shears Versus Second Natural Frquency
for Final Design Both with and without Damping
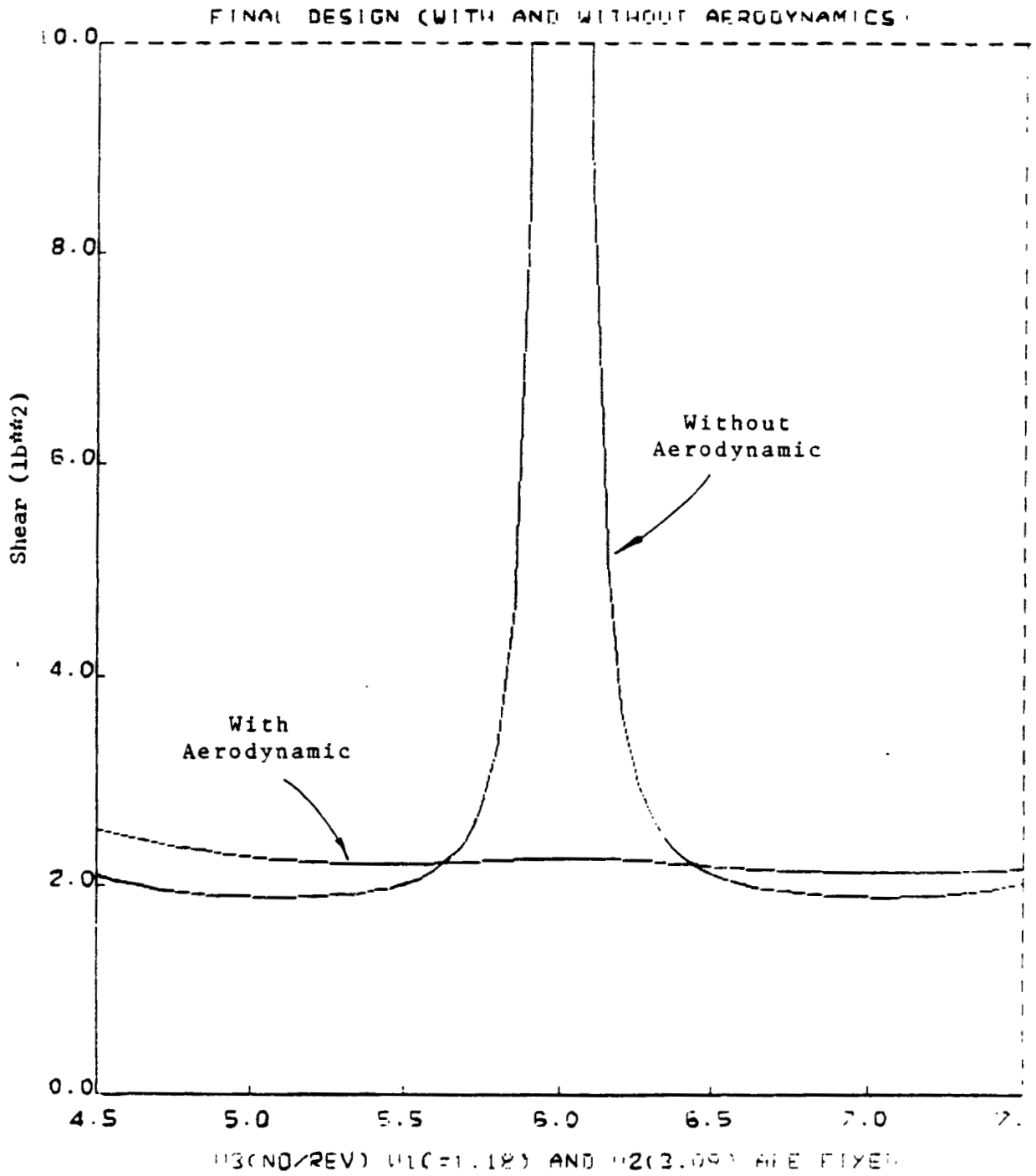(where Forcing Function is Even Integer Multiple)

Figure 27   Sum of Squares of Shears Versus Third Natural Frequency
for Final Design Both With and Without Damping
(where Forcing Function is Even Integer multiple)

9. SUMMARY AND CONCLUSION

The optimization technique works very successfully on the design of rotor blades even when there are as many as 55 constraints. The most efficient optimization procedure involves 2 steps. In the first step, the objective function is based on frequency placement with appropriate structural constraints. In the second step, the objective function is weight with frequency windows as constraints.

As far as the optimization of helicopter blades is concerned, the appropriate constraints include autorotational inertia, axial stress, geometric limitations of the cross-section, and the placement of mass center forward of the quarter chord.

Proper choice of input data can ensure the optimization runs smoothly and converges faster. Although we have up to 15 full constraints and 40 side constraints at one time, the program works very well. The reason may be due to the fact that the input data are practical enough to meet (or to be close to) most of the constraints even before the optimization starts. However, if we start the optimization with random input data, the results may not be as good as expected.

The forced response of the blade can be adequately controlled, as expected, by the approach of 'frequency placement'.

The optimization techniques results in realistic designs by placement mass at antinodes or nodes, by adding stiffness at antinodes or nodes, and by placing mass near the tip to achieve autorotational inertia at minimum weight.

10. ACKNOWLEDGEMENTS

11. APPENDICES

APPENDIX 11.1

Nomenclature

a	size of tip mass
A	area of cross-section of box beam
b	width of box beam
c	blade chord
[C]	damping matrix
d	width of lumped mass
d_1, d_2	wall thickness of box beam
e	weighting function
EI_{yy}	flapping stiffness
EI_{zz}	inplane stiffness
f	safety factor
F	final design
F(t)	forcing function
g	gravity
GJ	torsional stiffness
h	height of box beam
I	initial design
I_{Bx}, I_{By}	area moment of inertia of box beam
I_{ox}, I_{oy}	constant area moment of inertia of blade
M_{Bx}, M_{By}	mass moment of inertia of box beam
M_{ox}, M_{oy}	constant mass moment of inertia of blade
[K]	stiffness matrix
ka_1, ka_2	area moment of inertia
km_1, km_2	mass moment of inertia

l	length of an element
[M]	mass matrix
$p1, p2, p3$	blade first three frequencies (no/rev)
r	distance from rotation axis
R	length of the blade
s	box beam thickness
SSS	sum of squares of shear force
t	box beam thickness
T	tension force
T_k	kinetic energy
U	total energy
$U_1 .. U_{10}$	displacement of degree of freedom of element
[U]	unit matrix
$V_0, V_1 .. V_n$	forcing amplitude
v	displacement in yx plane
w	displacement in zx plane
w_1, w_n	blade frequencies
wf	weighting factor
x	coordinate axis and length parameter
θ	blade twist
ϕ	pretwist angle
ρ	mass density of the blade
ϵ	small parameter
ψ	Ωt
Ω	rotating speed
σ_m	maximum stress
σ	mass of skin

τ, β, η density of lumped mass, box beam, honeycomb

APPENDIX 11.2

Calculation of Torsional Stiffness, GJ

The blade cross section is shown in Fig. 1 and is idealized into a two cell torsion box in Fig.28. Although the bending and torsional inertias include the contribution of all masses (including the filler elements), the torsional stiffness is based only on the structural box and thin-skin elements. The torsional stiffness, GJ, is based on classical thin-walled closed section theory.(Ref.26) The effects of warping re and distortion of the cross section are neglected. The equations are briefly summarized as follows:

Considered cell i, having an enclosed area of A_1, and thickness t. The length along the circumference is measured by c, and the shear stress is denoted by s.. The torsion constant is

$$J = [2A_1 / \int_i (s\ dc)] T \qquad (37)$$

where $\int_i dc$ is the line integral along the entire closed box, and T represents the total torque applied to the entire system. We also have

$$2TA_1/J = \int_i (s\ dc) = \int_i (q\ dc/t) \qquad (38)$$

where c is the constant shear flow in the i-th box. Denoting the single adajcent box as k, there will be a common wall, ik, between the two boxes. The shear flow in the common wall will be the difference of shear flows q_i and q_k. Thus, for the i-th box,

$$q_i \int_i (dc/t) - q_k \int_{ik} (dc/t) = 2TA_i/J \qquad (39)$$

and for the k-th box

$$-q_i \int_{ik} (dc/t) + q_k \int_k (dc/t) = 2TA_k/J \qquad (40)$$

Defining $q_j = Q_j(2T/J)$ and $n_{jm} = \int_{jm} (dc/t)$, we can reform Eqs.3 to read

$$n_{ii}Q_i - n_{ik}Q_k = A_i \qquad (41a)$$

$$-n_{ik}Q_i + n_{kk}Q_k = A_k \qquad (41b)$$

Furthermore,

$$T = 2(q_iA_i + q_kA_k) = (4T/J)(Q_iA_i + Q_kA_k) \qquad (42)$$

Thus, the torsional constant, J, is given by

$$= 4(Q_iA_i + Q_kA_k) \qquad (43)$$

Specifically, for the two cell box shown in Fig.28, cal box 1 the box beam and box 2 the equivalent trailing edge. Denote the circumference of box 2 by C. The areas, A_1 and A_2 are given.

Then, from the other dimensions,

$$n_{11} = n/d_1 + 2(b/t_1) + h/d_2 \qquad (44a)$$

$$n_{12} = n/d_2 \qquad (44b)$$
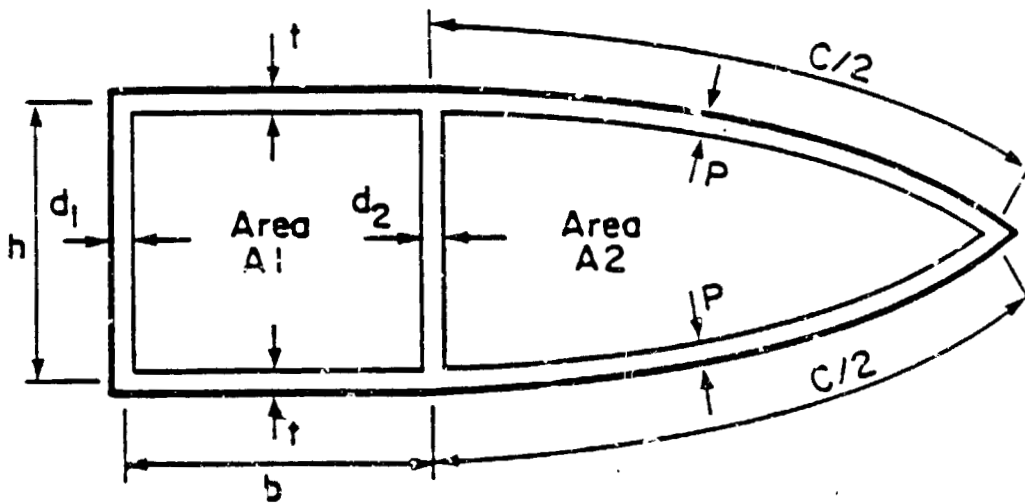
$$n_{22} = C/p + h/d_2 \qquad (44c)$$

Then, solving Eqs. 4a and 4b gives

$$Q_1 = (A_1 n_{22} + A_2 n_{12})/D \qquad (45a)$$

$$Q_2 = (A_2 n_{11} + A_1 n_{12})/D \qquad (45b)$$

$$D = n_{11}n_{22} - (n_{12})^2 \qquad (45c)$$

Thus, all quantities in Eq.6 are known and the torsional constant, J, can be evaluated.

Cell 1: Constant thicknesses for sides of box beam
represent weighted effects of variable
thickness elements.

Cell 2: This cell represents configuration of
skin and trailing edge.

Fig. 28   Idealized two-cell model for calculation of torsional stiffness.

APPENDIX 11.3

Derivation of Mass and Stiffness Matrices
as Functions of Natural Frequencies

Define

$$[K^*] = [M]^{-1/2}[K][M]^{-1/2}, \tag{46}$$

and construct a square matrix $[U^*]$ by using the eigenvectors of $[K^*]$ as columns. If the eigenvectors are normalized to the identity matrix, that is, if

$$[U^*]^T[U^*] = [I], \tag{47}$$

it then follows that

$$[U^*]^T[K^*][U^*] = \text{diag} \, [\, (w_i^2) \,], \tag{48}$$

where w_i^2 are the eigenvalues of $[K^*]$.

Next, let

$$[U] = [M]^{-1/2}[U^*], \tag{49}$$

from which it follows that

$$[U]^T = [U^*]^T[M]^{-1/2}, \tag{50}$$

$$[U]^{-1} = [U^*]^T[M]^{1/2}, \tag{51}$$

$$[U]^T[K][U] = \text{diag} \, [\, (w_i^2) \,], \tag{52}$$

and

$$[U]^T[M][U] = [I]. \tag{53}$$

Finally, then, the stiffness and mass matrices can be written as functions of the eigenvalues, w_i^2:

$$[M] = [U]^{-T}[U]^{-1}$$

$$= [M]^{1/2}[M]^{1/2}, \tag{54}$$

and

$$[K] = [U]^{-T}\text{diag}[(w_i^2)][U]^{-1}$$

$$= [M]^{1/2}[U^*]\text{diag}[(w_i^2)][U^*]^T[M]^{1/2}$$

$$= [M][U]\text{diag}[(w_i^2)][U]^T[M]. \tag{55}$$

Note that the eigenvectors, $[U]$, and eigenvalues, w_i^2, appearing on the right-hand side were originally calculated from the stiffness and mass matrices, $[K]$ and $[M]$. If we consider only relatively small changes in the frequencies, w_i, then the eigenvectors should relatively unchanged. Thus the last two equations for $[M]$ and $[K]$ with $[U]$ held fixed can be considered as expressing the mass and stiffness matrices as explicit functions of the natural frequencies.

12. BIBLIOGRAPH

1. Niebank, C. and Girvin, W., 'Sikorsky S-76 Analysis, Design and Development for Successful Dynamic Characteristics.' Proceedings of the 34th Annual Natural Forum of the American Helicopter Society, May 1978, pp 78-23-1 through 78-23-17.

2. Hirsh, Harold, Dutton, Robert E., and Rasumoff, Abner, 'Effect of Spanwise and Chordwise Mass Distribution on Rotor Blade Cyclic Stresses,' Journal of the American Helicopter Society, Vol. 1, No. 2, April 1956.

3. Miller, Rene H. and Ellis, Charles W., 'Helicopter Blade Vibration and Flutter,' Journal of the American Helicopter Society, Vol. 1, No. 3, July 1956.

4. Daughaday, H., DuWaldt, F., and Gates, C., 'Investigation of Helicopter Blade Flutter and Load Amplification Problems,' Journal of the American Helicopter Society, Vol. 2, No. 3, July 1957.

5. Gerstenberger, et al., 'The Rotary Round Table: How can Helicopter Vibration be Minimized?' Journal of American Helicopter Society, Vol. 2, No.3, July 1957.

6. Alex, et al. 'Pioneers Panel,' AHS 35th Anniversary Forum and Technology Display, Washington, DC, May 21-23, 1979.

7. Ellis, C.W. et al., 'Design, Development, and Testing of the Boein Vertol/Army YUH-61A,' Proceedings of the 32nd Annual National Foru the American Helicopter Society, Preprint 1010, May 1976.

8. Fenanghty, Ronald R. and Noehren, William L., 'Composite Bearingless Tailor Rotor for UTTAS,' Journal of the American Helicopter Society, Vol. 22, No. 3, July 1977, pp 19-26.

9. Hanson, H.W. and Calapodas, M.J., 'Evaluation of the Practical Aspects of Vibration Reduction Using Structural Optimization Techniques,' Proceedings of the 35th Annual National Forum of the American Helicopter Society, May 1979, pp 79-21 through 79-21-12.

10. Bielewa, Richard L., 'Techniques for Stability Analysis and Design Optimization with Dynamic Constraints of Nonconservative Linear Systems,' AIAA/ASME 12th Structures, Structural Dynamics, and Materials Conference, Anaheim, California, April 19-21, 1971. AIAA Paper No. /1-388.

11. Friedmann, Peretz, 'Response Studies of Rotors and Rotor Blades with Application to Aeroelastic Tailoring,' Semi-Annual Progress Report on Grant NSG-1578, December 1981. (Also unplubished U.S.C. Doctoral Thesis, December 1982).

12. Talyor, Robert B., 'Helicopter Vibration Reduction by Rotor Blade Modal Shaping,' Proceedings of the 38th Annual Forum of the American Helicopter Society, Anaheim, CA, May 1982.

13. Johnson, R. J., 'Disjoint Design Spaces in the Optimization of Harmonically Excited Structures,' AIAA Journal, Vol. 14, No. 2, February 1976, pp 259-261.

14. Niordson, F.I. and Pederson, P., 'A Review of Optimal Structural Design,' Proceedings of the 13th International Congress of Theoretical and Applied Mechanics, Springer-Verlag, Moscow (1973).

15. Venkayya, V.B., 'Structural Optimization: A Review and Some Recommendations,' Int. J. for Num. Mech. Engrg., Vol. 13, 1978, pp 203-228.

16. Scnmit, L.A., 'Structural Design by Systematic Synthesis,' Proc. 2nd Nat. Conf. Electronic Computation, AJCE, 105-132 (1960).

17. Fox, R.L., Optimization Methods for Engineering Design, Addison-Wesley, Reading, PA 1971.

18. Ko, Timothy, Use of Tapered, Twisted Finite Elements, M.S. Thesis, Washington University, 1979.

19. Olhoff, Niels, 'Optimization of Vibration Beam with respect to Higher Order Natural Frequencies,' J. Struct. Mech. 4(1), 87-122 (1976).

20. Turner, M.J., 'Design of Minimum Mass Structures with Specified Natural Frequencies.' AIAA J. 5(3), 406-412 (1967).

21. Khan, M.R. and Willmer, K.D., 'An Efficient Optimality Criterion Method for Natural Frequency Constrained Structures,' Computers Structures, Vol. 14, No. 9-6, pp 501-507, 1981.

22. Donham, Robert E. and Schmidt, Jaap, '100-KW Hingeless Metal Wind Turbine Blade: Design, Analysis, and Fabrication,' Preprint No. S-998, Proceedings of the 31th Annual National Forum of the American Helicopter Society, May 13-15, 1975.

23. Robinson, et al., 'Design Variables for a Controllable Twist Rotor,' Preprint No. 914, Proceedings of the 31th Annual National Forum of the American Helicopter Society, May 13-15, 1975.

24. Private information from a Helicopter Company.

25. Private information from a Helicopter Company.

26. Kollbrunner, C.F. and Basler,K.,Torsion in Structures; an Engineering Approach. Springer-Verlag, Berlin, 1969.

27. Vanderplaats, G.N. ' CONMIN - A FORTRAN PROGRAM FOR CONSTRAINED FUNCTION MINIMIZATION'., Ames Research Center and U.S. Army Air Mobility R D Laboratory, Moffett Field, Calif. 94035

13. VITA

Biographical items on the author of the thesis, Mr Timothy W H Ko

1) Born ███████ ███████ in ████ ███.

2) Attended National Cheng Kung University in Taiwan, R O C from
   1973 to 1978. Received Bachelor of Science Degree in Mechanical
   Engineering in May 1977.

3) Attended Washington University in St. Louis, Missouri from
   August, 1978 to present. Recieved Master of Science Degree in
   Mechanical Engineering in May 1980. Working on Docotor of
   Science Degree in Mechaincal Engineering. Awarded a Graduate
   Traineeship and Research Assistantship from September to May
   1984.

4) Member of American Helicopter Society.

December , 1984

Short Title : Optimum Design of Rotor Blades ,   Ko, D.Sc. 1984